

AD-A282 684



0

WL-TR-93-3112

**INTEGRATED PASSIVE  
AND ACTIVE CONTROL  
OF STRUCTURES**



Vernon H. Neubert

Department of Engineering Science and Mechanics  
The Pennsylvania State University  
University Park, Pennsylvania 16802

December 1993

Final Report for Period May 1990 - May 1993

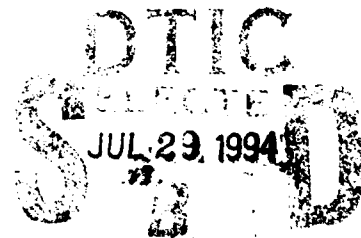
100P 94-23968



Approved for public release; distribution unlimited.

DTIC QUALITY INSPECTED 5

**FLIGHT DYNAMICS DIRECTORATE  
WRIGHT LABORATORY  
AIR FORCE MATERIEL COMMAND  
WRIGHT-PATTERSON AIR FORCE BASE, OHIO 45433-7542**



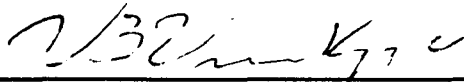
94 7 27 056

NOTICE

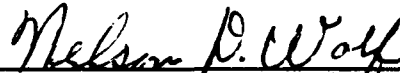
When Government drawings, specifications, or other data are used for any purpose other than in connection with a definitely related Government procurement operation, the United States Government thereby incurs no responsibility or any obligation whatsoever. The fact that the Government may have formulated or in any way supplied the said drawings, specifications, or other data, is not to be regarded by implication, or otherwise as in any manner, as licensing the holder or any other person or corporation; or as conveying any rights or permission to manufacture, use, or sell any patented invention that may in any way be related thereto.

This report is releasable to the National Technical Information Service (NTIS). At NTIS, it will be available to the general public, including foreign nations.

This technical report has been reviewed and is approved for publication.



VIPPERLA B. VENKAYYA  
Project Engineer  
Design & Methods Development Sec.



NELSON D. WOLF, Technical Manager  
Design & Methods Development Sec.  
Design Development Branch



GEORGE R. HOLDERBY  
Chief, Design Development Branch  
Structures Division

"If your address has changed, if you wish to be removed from our mailing list, or if the addressee is no longer employed by your organization please notify WL/FIBAD Bldg 45, 2130 Eighth St Ste 1, Wright-Patterson AFB OH 45433-7542 to help us maintain a current mailing list".

Copies of this report should not be returned unless return is required by security considerations, contractual obligations, or notice on a specific document.

# REPORT DOCUMENTATION PAGE

Form Approved  
OMB No. 0704-0188

Public reporting burden for this collection of information is estimated to average 1 hour per response, including the time for reviewing instructions, searching existing data sources, gathering and maintaining the data needed, and completing and reviewing the collection of information. Send comments regarding this burden estimate or any other aspect of this collection of information, including suggestions for reducing this burden, to Washington Headquarters Services, Directorate for Information Operations and Reports, 1215 Jefferson Davis Highway, Suite 1204, Arlington, VA 22202-4302, and to the Office of Management and Budget, Paperwork Reduction Project (0704-0188), Washington, DC 20503.

1. AGENCY USE ONLY (Leave blank)		2. REPORT DATE Dec. 1993	3. REPORT TYPE AND DATES COVERED Final Report - May 1990 to May 1993	
4. TITLE AND SUBTITLE "Integrated Passive and Active Control of Structural Vibrations"			5. FUNDING NUMBERS Contr: F33615-90-C-3205 P.E. 61102F Project 2302 Task N5 Work Unit 09	
6. AUTHOR(S) Vernon H. Neubert			8. PERFORMING ORGANIZATION REPORT NUMBER	
7. PERFORMING ORGANIZATION NAME(S) AND ADDRESS(ES) Department of Engineering Science and Mechanics 227 Hammond Building The Pennsylvania State University University Park PA 16802			10. SPONSORING/MONITORING AGENCY REPORT NUMBER WL-TR-93-3112	
9. SPONSORING/MONITORING AGENCY NAME(S) AND ADDRESS(ES) Dr. V. B. Venkayya (WL/FIBAD) Flight Dynamics Directorate Wright Laboratory (AFMC) Wright-Patterson Air Force Base, Ohio 45433-7542			11. SUPPLEMENTARY NOTES Final Report	
12a. DISTRIBUTION/AVAILABILITY STATEMENT APPROVED FOR PUBLIC RELEASE; DISTRIBUTION IS UNLIMITED			12b. DISTRIBUTION CODE	
13. ABSTRACT (Maximum 200 words) <p>A combination of passive damping and active control is needed on practical structures where sufficient modal damping is not achievable with passive damping alone. The modal theories for structural equations in state space are reviewed and some eigenvector relationship are presented which are not available elsewhere, for use later in the report. Methods for determining sensitivities of eigenvalues and eigenvectors to plant matrix and control inputs are summarized and numerical examples are presented.</p> <p>Procedures are developed for optimizing passive damping through use of the sensitivities of the eigenproperties, for free vibration and forced, random vibrations. Frequency-dependent behavior of viscoelastic damping material by curve-fitting is discussed, which is then used in an overdamped mini-oscillator technique for analysis of an example ten-bar truss. Two approaches are presented for designing the combination of passive viscous damping and full state feedback control. The first is iterative and makes use of eigenvalue sensitivities. The second is based on a perturbation formulation, where the desired changes in eigenvalues and eigenvectors are specified and the corresponding changes in the closed loop characteristic matrix in state space are predicted. Restrictions on the choice of eigenvalues and eigenvectors are discussed in light of related literature on eigenstructure assignment. Fortran computer programs, one coupled with the constrained function minimization program CONMIN, have been written for each type of problem.</p>				
14. SUBJECT TERMS Space Structures, Passive Damping, Active Control, Analysis, Numerical Examples			15. NUMBER OF PAGES 98	
17. SECURITY CLASSIFICATION OF REPORT Unclassified			16. PRICE CODE	
18. SECURITY CLASSIFICATION OF THIS PAGE Unclassified		19. SECURITY CLASSIFICATION OF ABSTRACT Unclassified		20. LIMITATION OF ABSTRACT SAR

## CONTENTS

<b>1. INTRODUCTION</b>	<b>1</b>
<b>2. ANALYTICAL BACKGROUND</b>	<b>2</b>
2.1 Second order differential equations of motion and control.	2
2.1.1 Eigenproperties and orthogonality with no damping.	2
2.1.2 Reconstruction of the $M$ and $K$ matrices from eigenvalues and eigenvectors.	3
2.1.3 Uncoupling of the differential equations and modal control.	3
2.1.4 Criterion for proportional damping or proportional control.	4
2.2. State space form of differential equations.	5
2.2.1 Eigenproperties for symmetric plant matrices.	5
2.2.2 Right and left eigenvectors.	6
2.2.3 Relationships between upper and lower eigenvectors.	7
2.2.4 Conversion from state space to quadratic form and implications.	9
Example 2.1	10
2.2.5 Special cases of combinations of $C_1$ and $K_1$ .	11
Example 2.2	11
Example 2.3	14
2.2.6 Recovery of the $C_1$ and $K_1$ matrices from the eigenproperties.	15
2.2.7 Nonsymmetric control matrices, forced vibration problem.	15
<b>3. SENSITIVITY OF EIGENPROPERTIES TO INDIVIDUAL ELEMENTS IN THE DAMPING AND CONTROL MATRICES.</b>	<b>16</b>
3.1 Eigenvalue sensitivity.	17
3.1.1 Sensitivities of the eigenvalues using the similarity transformation invariants.	19
Example 3.1 System with one degree of freedom.	20
Example 3.2 System with two degrees of freedom.	20
3.1.2 Sensitivities of the eigenvalues in terms of the eigenvectors.	21
Example 3.3 Ten-bar truss with eight degrees of freedom.	23
Example 3.4 Effect of initial passive damping, ten-bar truss.	29
3.1.3 Summary and conclusions.	31
3.2 Sensitivity of the eigenvectors.	32
3.2.1 Representation of eigenvectors by complete modal series.	32
3.2.2 Eigenvector sensitivity by Nelson's single mode approach.	34
3.2.3 Relationship between the complete modal series and single mode approaches.	36
Example 3.5 Eigenvector sensitivity by the complete modal series approach.	37
Example 3.6 Eigenvector sensitivity by the single mode approach.	38

<b>4. PASSIVE DAMPING</b>	<b>39</b>
4.1 Optimization of viscous damping in a truss structure.	39
4.1.1 Achieving uniform modal decay rates for free vibration problems.	39
4.1.2 Critical damping for matrix equations.	40
4.1.3 Optimization of modal damping ratios, ten-bar truss example.	41
4.1.3.1 Formulation of the optimization problem.	41
4.1.3.2 Natural frequencies and mode shapes for proportional damping.	42
4.1.3.3 Sensitivities of modal damping ratios and natural frequencies.	43
4.1.3.4 Modal usurping of damping; variation of $\zeta_5$ and $\zeta_7$ with $C_1$ .	45
4.1.3.5 Optimization of $\zeta_3$ with respect to $C_3$ and $C_4$ .	47
4.2 Representation and optimization of viscoelastic damping in structures.	49
4.2.1 Fitting curves to data for complex moduli of viscoelastic damping materials.	49
4.2.1.1 Equations and parameters.	50
4.2.1.2 Reading data from a composite plot or nomograph.	52
4.2.1.3 Step-by-step procedure for fitting equations to data.	54
4.2.1.4 Results of curve-fitting for Soundcoat 601.	55
4.2.1.5 Improving the fit by modification of the equation for $\eta$ .	57
4.2.1.6 Summary and conclusions.	57
4.2.2 Representation of viscoelastic damping by complex modulus.	58
Example 4.1 Loss factor constant throughout structure.	58
Example 4.2 Loss factor varies among structural elements.	58
4.2.3 Over-damped mini-oscillator approach for representation of viscoelasticity.	60
4.2.3.1 Finite element with two mini-oscillators to represent viscoelastic behavior.	61
4.2.3.2 Representation and optimization of viscoelastic damping in the ten-bar truss.	62
4.2.4 Design and optimization of viscoelastic damping.	64
<b>5. ACTIVE DAMPING AND CONTROL</b>	<b>66</b>
5.1 Constant gain, closed loop control.	67
5.1.1 Uncoupling the differential equations and modal control.	67
5.1.2 Criterion for proportional damping or proportional control.	68
5.1.3 One-step methods for design of viscous damping and control in state space by choosing eigenvalues and/or eigenvectors.	69
5.1.3.1 Method I: Design of the sum of the matrices $[C+G]$ .	70
Example 5.1 One-step design of the $[C+G]$ matrix using Method I.	72
Example 5.2 Same as Example 5.1, but with $N \times N$ matrices and natural control.	74

5.1.3.2	Method II: Design of the entire dA for initially damped or undamped systems.	75
	Example 5.3 Design of damping and control matrices using Method II.	76
5.1.3.3	Method III: Design of damping and control matrices to achieve desired eigenvalues and eigenvectors.	77
	Example 5.4 Design of damping and control matrices using Method III.	78
5.1.4	Shifting poles using eigenvalue sensitivities, symmetric and unsymmetric control.	80
	Example 5.5 Design of a symmetrical control matrix using sensitivities.	80
	Example 5.6 Design of an unsymmetrical control matrix using sensitivities.	82
	Example 5.7 Same as problem Example 5.6, but using a variation of Method I.	83
5.1.5	Nonsymmetrical control matrices, forced vibration problem.	83
5.2	Optimum damping and control by way of performance index and Riccati equation.	85
5.2.1	Performance index and optimal control.	85
5.2.2	The Riccati equation and modal control.	85
	Example 5.8 Conversion of modal control forces to system control forces.	86
	Example 5.9 Same as 5.8, but using pole shifting by natural control method.	88
	Example 5.10 Same as 5.8, but using Method II.	89
5.3	Summary and Conclusions	90
	<b>REFERENCES</b>	91

<b>Accession For</b>	
NTIS GFA&I	<input checked="" type="checkbox"/>
DTIC TAB	<input type="checkbox"/>
Unannounced	<input type="checkbox"/>
Justification	
By	
Distribution/	
<b>Availability Codes</b>	
Dist	Avail and/or special
A-1	

## List of Figures

	Page
Fig. 3.1 Ten-bar truss.	23
Fig. 3.2 Variation of $\zeta_6$ , $\zeta_5$ and $\zeta_8$ with $G_{55}$ .	24
Fig. 3.3 $\partial \zeta_r / \partial G_{55}$ versus $G_{55}$ for $r=6, 5$ and $8$ .	25
Fig. 3.4 $\zeta_5$ , $\zeta_6$ and $\zeta_8$ versus $G_{77}$ .	26
Fig. 3.5 $\omega_5$ , $\omega_6$ and $\omega_8$ versus $G_{77}$ .	26
Fig. 3.6 $\omega_{D5}$ , $\omega_{D6}$ and $\omega_{D8r}$ versus $G_{77}$ .	27
Fig. 3.7 $\zeta_5$ , $\zeta_6$ and $\zeta_8$ versus $G_{75}$ .	27
Fig. 3.8 $\zeta_6$ with effect of $G_{55}$ , $-G_{75}$ , $-G_{57}$ and $G_{77}$ applied simultaneously and superimposed.	29
Fig. 3.9 $\zeta_2$ and $\zeta_4$ versus $G_{18}$ with and without proportional passive damping.	30
Fig. 4.1 Mode shapes of ten-bar truss.	44
Fig. 4.2 Variation of $\zeta_5$ and $\zeta_6$ with $C_1$ .	46
Fig. 4.3 $\partial \zeta_5 / \partial C_1$ and $\partial \zeta_6 / C_1$ versus $C_1$ .	46
Fig. 4.4 Variation of $\zeta_3$ with $C_3$ and $C_4$ .	47
Fig. 4.5 Nomograph for $G$ and $\eta$ as functions of $f$ , $\alpha_T$ and $f \alpha_T$ .	53
Fig. 4.6 $E$ versus $f$ for 601 at $T = 50, 75$ and $125^\circ \text{F}$ .	56
Fig. 4.7 $\eta$ versus $f$ for 601 at $T = 50, 75$ and $125^\circ \text{F}$ .	56

## 1. INTRODUCTION

The goal of the present work is the integration of active and passive control of structural vibrations. First a procedure is developed to achieve maximum passive viscous damping in the frequency range of interest. Then the active control is added to increase the effective damping to the level required.

Passive damping is either viscous damping or that obtained with viscoelastic materials. It is representable by devices connected between two structural nodes or between one node and ground. It is achieved mechanically by special truss members which incorporate dashpots, electro-mechanical devices, or viscoelastic elements where the viscoelastic material is deformed in shear. Viscous damping is represented in matrix form as  $F = C \dot{z}$ . Viscoelastic damping is represented herein by (1) using a complex Young's modulus which is frequency dependent [N3], where the  $F = G(\omega)$  or (2) by using the mini-oscillator approach to represent the frequency dependence of the complex Young's modulus, as presented by McTavish and Hughes [M2]. The fractional calculus method propounded by Bagley and Torvik [B1] is of interest, but has not been pursued in the present study. The active control investigated herein is mainly constant gain, closed loop control. It is assumed to be achievable by control forces, in matrix form, of  $F = -G \dot{z} - H z$ .

The second chapter presents analytical background. Much of control theory is written in state space form, which for structural problems means reformulating  $n$  second-order differential equations into  $2n$  equivalent first-order equations. Part of the cost is that  $n$  redundant first-order equations have to be introduced and a corresponding amount of redundant information can be produced. So some of the features of eigenproblems for both second-order and state space differential equations are reviewed. Also, important relationships are presented between the upper and lower portions of the right and left eigenvectors which, though easy to derive, are not readily available in the literature.

A great deal of emphasis is put on sensitivity of the eigenproperties to damping and control forces. This is summarized in the third chapter. The equations, initially derived by others, for calculation of eigenvalue and eigenvector sensitivities are summarized including some examples. A unique feature is the introduction of sensitivities calculated also from the invariants associated with the similarity transformation between system coordinates and modal coordinates.

In the fourth chapter, optimization of passive damping is summarized. A ten bar truss is used as a practical example and the optimization of both viscous damping and viscoelastic damping is discussed in detail.

Chapter five deals with active damping and control and design of the  $[C+G]$  matrix to achieve the desired combination of passive and active control. The existing theory of natural modal control is reviewed. Two approaches are presented for designing the combination of passive viscous damping and full state feedback control. The first is iterative and makes use of eigenvalue sensitivities. The second is based on a perturbation formulation, where the desired changes in eigenvalues are specified and the corresponding changes in the closed loop characteristic matrix in state space are predicted. Restrictions on the choice of eigenvalues and eigenvectors are discussed in light of related literature on eigenstructure assignment. The concept of cost functions is reviewed and the relationship of solutions of the Riccati equation to the present work is outlined.

## 2. ANALYTICAL BACKGROUND FOR MODAL THEORY

The purpose of this chapter is to review the modal theory and notation for structural vibration problems, with emphasis on assumptions regarding symmetry and proportionality of damping or control. First the second order differential equations of motion are outlined; second, the state space form of the equations.

### 2.1 Second order differential equations of motion.

#### 2.1.1 Eigenproperties and orthogonality with no damping.

With regard to nomenclature, a bold capital letter or any symbols in brackets [ ] represent a rectangular matrix. A vector, or column matrix, is represented by a bold, lower case letter such as  $\mathbf{z}$ , symbols in braces { }, or an underlined Greek letter, as with  $\underline{\phi}$ . A diagonal, square, matrix is represented by a superscript "D" on brackets, that is [ ]<sup>D</sup>.

The differential equations of motion for the case of no damping are

$$\mathbf{M}\ddot{\mathbf{z}} + \mathbf{K}\dot{\mathbf{z}} = \mathbf{F}(t) \quad (2.1)$$

$$\mathbf{M}\dot{\mathbf{z}} + \mathbf{K}\mathbf{z} = -\mathbf{G}\dot{\mathbf{z}} - \mathbf{H}\mathbf{z}. \quad (2.2)$$

where  $\mathbf{M}$  is positive definite and symmetric,  $\mathbf{K}$  is indefinite and symmetric and  $\mathbf{F}(t) = -\mathbf{G}\dot{\mathbf{z}} - \mathbf{H}\mathbf{z}$ . The  $\mathbf{G}$  and  $\mathbf{H}$  are control matrices. The eigenvalue problem is

$$[-\mathbf{M}\omega_r^2 + \mathbf{K}]\underline{\phi}_r = 0 \quad (2.3)$$

The eigenvectors  $\underline{\phi}_r$  may be assembled into an  $n \times n$   $\Phi$  matrix. The orthogonality relationships are

$$\Phi^T \mathbf{M} \Phi = [\mathbf{M}_n]^D \quad (2.4)$$

and

$$\Phi^T \mathbf{K} \Phi = [\mathbf{M}_n \omega_n^2]^D \quad (2.5)$$

### 2.1.2 Reconstruction of the M and K matrices from eigenvalues and eigenvectors.

Note that the M and K matrices may be reconstructed by using

$$\mathbf{M} = \Phi^{-T} [\mathbf{M}_n]^D \Phi^{-1} \quad (2.6)$$

and

$$\mathbf{K} = \Phi^{-T} [\mathbf{M}_n \omega_n^2]^D \Phi^{-1} \quad (2.7)$$

Further, we see that

$$\mathbf{M}^{-1} = \Phi [\mathbf{M}_n]^{-D} \Phi^T \quad (2.8)$$

and

$$\mathbf{M}^{-1} \mathbf{K} = \Phi [\omega_n^2]^D \Phi^{-1} \quad (2.9)$$

### 2.1.3 Uncoupling of the differential equations and modal control.

The differential equations, Eqs. (2.1) and (2.2), are uncoupled by the coordinate transformation

$$\mathbf{z}(t) = \Phi \mathbf{q}(t) \quad (2.10)$$

and pre-multiplying Eq. (2.1) by  $\Phi^T$ .

$$\Phi^T \mathbf{M} \Phi \ddot{\mathbf{q}} + \Phi^T \mathbf{K} \Phi \mathbf{q} = \Phi^T \mathbf{F}(t) = \mathbf{N}(t) \quad (2.11)$$

$$[\mathbf{M}_n]^D \ddot{\mathbf{q}} + [\mathbf{M}_n]^D [\omega_n^2]^D \mathbf{q} = -[\mathbf{g}] \dot{\mathbf{q}} - [\mathbf{h}] \mathbf{q} = \mathbf{N}(t) \quad (2.12)$$

The diagonal matrices on the left side of Eqs. (2.12) indicate decoupling, but if [g] and [h] are non-diagonal, the equations are still coupled. If [g] and [h] are diagonal, which is called natural control [M3], then the equations are uncoupled.

If the control matrices in N(t) are specified, and  $\Phi^T \mathbf{F}(t) = \mathbf{N}(t)$ , then F(t) is found. It is efficient to use the orthogonality relationship, Eq. (2.4), to avoid inverting  $\Phi^T$ .

$$\mathbf{F}(t) = \Phi^{-T} \mathbf{N}(t) = \mathbf{M} \Phi [\mathbf{M}_n]^{-D} \mathbf{N}(t) = -\mathbf{M} \Phi [\mathbf{M}_n]^{-D} \left[ [\mathbf{g}] \dot{\mathbf{q}} + [\mathbf{h}] \mathbf{q} \right] \quad (2.13)$$

Changing back to the z(t) coordinates

$$\mathbf{F}(t) = \Phi^{-T} \mathbf{N}(t) = \mathbf{M} \Phi [\mathbf{M}_n]^{-D} \mathbf{N}(t) = -\mathbf{M} \Phi [\mathbf{M}_n]^{-D} \left[ [\mathbf{g}] \Phi^{-1} \dot{\mathbf{z}} + [\mathbf{h}] \Phi^{-1} \mathbf{z} \right] \quad (2.14)$$

The differential equation with feedback is now

$$\mathbf{M}\ddot{\mathbf{z}} + \mathbf{M} \Phi [\mathbf{M}_n]^{-D} [ [\mathbf{g}] \Phi^{-1} \dot{\mathbf{z}} + [\mathbf{h}] \Phi^{-1} \mathbf{z} ] + \mathbf{K}\mathbf{z} = 0. \quad (2.15)$$

which is 
$$\mathbf{M}\ddot{\mathbf{z}} + \mathbf{G}\dot{\mathbf{z}} + [\mathbf{H} + \mathbf{K}] \mathbf{z} = 0. \quad (2.16)$$

where 
$$\mathbf{G} = \mathbf{M} \Phi [\mathbf{M}_n]^{-D} [\mathbf{g}] \Phi^{-1} \quad \text{and} \quad \mathbf{H} = \mathbf{M} \Phi [\mathbf{M}_n]^{-D} [\mathbf{h}] \Phi^{-1} \quad (2.17)$$

Pre-multiplying Eq. (2.16) by  $\mathbf{M}^{-1}$

$$\ddot{\mathbf{z}} + \Phi [\mathbf{M}_n]^{-D} [ [\mathbf{g}] \Phi^{-1} \dot{\mathbf{z}} + [\mathbf{h}] \Phi^{-1} \mathbf{z} ] + \mathbf{M}^{-1} \mathbf{K}\mathbf{z} = 0. \quad (2.18)$$

or 
$$\ddot{\mathbf{z}} + \mathbf{M}^{-1} \mathbf{G}\dot{\mathbf{z}} + \mathbf{M}^{-1} [\mathbf{H} + \mathbf{K}] \mathbf{z} = 0. \quad (2.19)$$

which is of the form

$$\mathbf{I} \ddot{\mathbf{z}} + \mathbf{C}_1 \dot{\mathbf{z}} + \mathbf{K}_1 \mathbf{z} = 0. \quad (2.20)$$

#### 2.1.4 Criterion for proportional damping or proportional control.

The question now addressed is whether the matrices  $\mathbf{H}$  and  $\mathbf{G}$  in Eq. (2.19) represent proportional control. The test which applies is

$$\text{is } \mathbf{C}_1 \mathbf{K}_1 \stackrel{?}{=} \mathbf{K}_1 \mathbf{C}_1 \quad (2.21a)$$

$$\mathbf{M}^{-1} \mathbf{G} \mathbf{M}^{-1} [\mathbf{H} + \mathbf{K}] \stackrel{?}{=} \mathbf{M}^{-1} [\mathbf{H} + \mathbf{K}] \mathbf{M}^{-1} \mathbf{G} \quad (2.21b)$$

Since  $\mathbf{G}$  and  $\mathbf{H}$  can be chosen separately, the Eq. (2.21b) is separated into two parts:

$$\mathbf{M}^{-1} \mathbf{G} \mathbf{M}^{-1} \mathbf{H} \stackrel{?}{=} \mathbf{M}^{-1} \mathbf{H} \mathbf{M}^{-1} \mathbf{G} \quad (2.22a)$$

$$\mathbf{M}^{-1} \mathbf{G} \mathbf{M}^{-1} \mathbf{K} \stackrel{?}{=} \mathbf{M}^{-1} \mathbf{K} \mathbf{M}^{-1} \mathbf{G} \quad (2.22b)$$

Now substitute for  $\mathbf{M}^{-1} \mathbf{G}$  and  $\mathbf{M}^{-1} \mathbf{K}$  from Eqs. (2.18) and (2.19)

$$\Phi [\mathbf{M}_n]^{-D} [\mathbf{g}] \Phi^{-1} \Phi [\omega_n^2]^{-D} \Phi^{-1} \stackrel{?}{=} \Phi [\omega_n^2]^{-D} \Phi^{-1} \mathbf{M}^{-1} \mathbf{M} \Phi [\mathbf{M}_n]^{-D} [\mathbf{g}] \Phi^{-1} \quad (2.23a)$$

which reduces to

$$[\mathbf{M}_n]^{-D} [\mathbf{g}] [\omega_n^2]^{-D} \stackrel{?}{=} [\omega_n^2]^{-D} [\mathbf{M}_n]^{-D} [\mathbf{g}] \quad (2.23b)$$

The answer is that Eq. (2.23b) does not represent an equality. However, the two sides of the equation will be equal if  $[\mathbf{g}]$  is diagonal, which is then a requirement for proportional control. Then Eq. (2.23b) becomes the following equality

$$[\mathbf{M}_n]^{-D} [\mathbf{g}]^D [\omega_n^2]^{-D} = [\omega_n^2]^{-D} [\mathbf{M}_n]^{-D} [\mathbf{g}]^D \quad (2.24)$$

The advantage of proportional damping or proportional control is that the eigenvectors  $\Phi$  do not change, which means that the coordinate transformations which decouple the original matrices will also decouple the closed loop equations. A direct way to check that this is true is to simply look at the products  $\Phi^T G \Phi$  and  $\Phi^T H \Phi$ .

The latter product 
$$\Phi^T H \Phi = \Phi^T M \Phi [M_n]^{-D} [h] \Phi^{-1} \Phi \quad (2.25)$$

reduces to 
$$\Phi^T H \Phi = [h], \quad (2.26a)$$

and, similarly, 
$$\Phi^T G \Phi = [g]. \quad (2.26b)$$

So, the open loop eigenvectors decouple the closed loop equations, but only if  $[h]$  and  $[g]$  are diagonal matrices.

## 2.2 State space form of differential equations.

### 2.2.1 Eigenproperties for symmetric plant and control matrices.

The differential equations in state space form are

$$M^* \dot{\underline{\eta}} + K^* \underline{\eta} = -G^* \underline{\eta} \quad (2.27)$$

$$I \dot{\underline{\eta}} + A_o \underline{\eta} = -[M^*]^{-1} G^* \underline{\eta} \quad (2.28)$$

which defines  $A_o$ . With  $G^* = 0$ , Eq. (2.27) is written in detail as

$$\begin{bmatrix} M & 0 \\ 0 & -K \end{bmatrix} \begin{Bmatrix} \ddot{z}(t) \\ \dot{z}(t) \end{Bmatrix} + \begin{bmatrix} C & K \\ K & 0 \end{bmatrix} \begin{Bmatrix} z(t) \\ z(t) \end{Bmatrix} = \begin{Bmatrix} 0 \\ 0 \end{Bmatrix}. \quad (2.29)$$

The open-loop eigenproblem is

$$[I\lambda - A_o] \underline{\psi} = 0 \quad (2.30)$$

and the solution to the homogeneous equations is  $\underline{\eta}_r = \underline{\psi}_r e^{\lambda_r t}$ , where  $\underline{\psi}_r$  is the  $r$ th eigenvector.

The  $2n$  eigenvectors may be arranged in columns in a  $2n \times 2n$  matrix, designated  $\Psi$ , and the following orthogonality relationships [N3] exist

$$\Psi^T M^* \Psi = B^D \quad \Psi^T K^* \Psi = -B^D \Lambda \quad (2.31)$$

where the eigenvectors may be normalized so  $B^D = I$ . The matrix  $\Lambda$  is a diagonal matrix of eigenvalues,  $\lambda_r$ .

The  $\underline{\psi}_r$  are sometimes called the right eigenvectors, because many workers in the field of control seem to be in the habit of using right and left eigenvectors, even though left eigenvectors are not needed for decoupling if the plant and control matrices are symmetric. The concept of

left and right eigenvectors is explained in the next section.

### 2.2.2 Right and left eigenvectors

When both right and left eigenvectors are used, the convention herein is to designate the  $r$ th right eigenvector by  $\mathbf{u}_r$  and the  $r$ th left eigenvector by  $\mathbf{v}_r$ . The left eigenvectors are the eigenvectors associated with the transpose of the  $\mathbf{A}$  matrix.

$$[\mathbf{I}\lambda - \mathbf{A}_0^T] \mathbf{v} = \underline{\mathbf{0}} \quad (2.32)$$

The right and left vectors are arranged in columns to form the  $\mathbf{U}$  and  $\mathbf{V}$  matrices, of size  $2n \times 2n$ . Their properties are such that

$$\mathbf{V}^T \mathbf{A}_0 \mathbf{U} = \Lambda \quad (2.33a)$$

and  $\mathbf{V}^T \mathbf{U}$  is diagonal. (2.33b)

Two normalizations are usually performed. The first involves the right vectors. There are various choices for normalizing. If  $\mathbf{M}^*$  and  $\mathbf{K}^*$  are symmetric,  $\mathbf{U} = \Psi$  and the right eigenvectors may be normalized using, from Eq. (2.31),

$$\mathbf{U}^T \mathbf{M}^* \mathbf{U} = \mathbf{B}^D = \mathbf{I}. \quad (2.34)$$

In a more general situation, if  $\mathbf{U}^T \mathbf{M}^* \mathbf{U}$  is not diagonal, the individual vectors may be normalized by

$$\mathbf{u}_r^T \mathbf{M}_a \mathbf{u}_r = 1 \quad (2.35)$$

where  $\mathbf{M}_a$  is an arbitrary matrix, to be defined. Among the possibilities are  $\mathbf{M}_a = \mathbf{M}^*$  or  $\mathbf{M}_a = \mathbf{I}$ .

The lower half of the  $\mathbf{U}$  matrix represents the displacement mode shapes. In Chapters 3 and 5 a special normalization involving only the lower half of the  $\mathbf{U}$  matrix is found to be advantageous.

Having normalized the right eigenvectors, the left are usually normalized by making the diagonal matrix indicated in Eq. (2.33b) equal to the unit matrix, or

$$\mathbf{V}^T \mathbf{U} = \mathbf{I} \quad (2.36)$$

### 2.2.3 Relationships between upper and lower eigenvectors.

The complete eigenvector matrices,  $U$  and  $V$ , in the state space formulation of structural dynamics problems are of size  $2n \times 2n$  while those for the second order differential equation form are only  $n \times n$ . Further, the eigenvectors in state space occur in complex conjugate pairs for underdamped systems. The relationships between the various forms of the vectors has not been documented well in the literature. The purpose of this section is to outline some of the relationships between the portions of the eigenvector matrices. The right eigenvector matrix,  $U$ , is first divided into two  $n \times 2n$  matrices designated  $U_u$  and  $U_l$ , for the upper and lower portions of the  $U$  matrix.

$$U = \begin{bmatrix} U_u \\ U_l \end{bmatrix} \quad (2.37)$$

From the characteristic equation with  $A$  denoting a general characteristic matrix,

$$A U = U \Lambda \quad (2.38)$$

and filling in the submatrices of the  $A$  and  $U$  matrices, the following two sets of equations result

$$-C_1 U_u - K_1 U_l = U_u \Lambda \quad (2.39a)$$

and 
$$U_u = U_l \Lambda. \quad (2.39b)$$

The second equation, (2.39b), shows how simply the upper right vectors are related to the lower right vectors and is true even if  $C_1$  and  $K_1$  are unsymmetric.

The left eigenvector matrix,  $V$ , is subdivided similarly and substituted into the characteristic equation

$$A^T V = V \Lambda \quad \text{or} \quad V^T A = \Lambda V^T \quad (2.40)$$

to yield

$$-V_u^T C_1 + V_l^T = \Lambda V_u^T \quad (2.41a)$$

and

$$-V_u^T K_1 = \Lambda V_l^T. \quad (2.41b)$$

Here the relationship between the upper and lower left vectors is not so simple, unless  $C_1 = 0$ , which is a situation discussed below, under section 2.2.5.

Equations which relate the left and right eigenvectors are derived from the orthogonality relationships. The first involves the characteristic matrix  $A$  and the eigenvalues  $\Lambda$ .

It is 
$$V^T A U = \Lambda \quad (2.42a)$$

which yields 
$$-V_u^T C_1 U_u + V_l^T U_u - V_u^T K_1 U_l = \Lambda. \quad (2.42b)$$

Making use of Eqs. (2.41a) and (2.41b) in (2.43),

$$\Lambda \mathbf{V}_u^T \mathbf{U}_u + \Lambda \mathbf{V}_l^T \mathbf{U}_l = \Lambda \quad (2.43a)$$

so it must be that

$$\mathbf{V}_u^T \mathbf{U}_u + \mathbf{V}_l^T \mathbf{U}_l = \mathbf{I} \quad (2.43b)$$

The orthogonality relationships  $\mathbf{V}^T \mathbf{U} = \mathbf{I}$  can be written in several forms. Since the  $\mathbf{U}$  and  $\mathbf{V}$  matrices are rectangular of size  $n \times 2n$ , the submatrix products of interest may be  $n \times n$  or  $2n \times 2n$ .

The forms which result in  $2n \times 2n$  product matrices are

$$\mathbf{V}^T \mathbf{U} = \mathbf{I} \text{ and } \mathbf{U}^T \mathbf{V} = \mathbf{I} \quad (2.44)$$

and the submatrix product matrices are

$$\mathbf{V}_u^T \mathbf{U}_u + \mathbf{V}_l^T \mathbf{U}_l = \mathbf{I} \quad (2n \times 2n) \quad (2.45a)$$

and 
$$\mathbf{U}_u^T \mathbf{V}_u + \mathbf{U}_l^T \mathbf{V}_l = \mathbf{I} \quad (2n \times 2n) \quad (2.45b)$$

The forms which result in  $n \times n$  product matrices are

$$\mathbf{U} \mathbf{V}^T = \mathbf{I} \text{ or } \mathbf{V} \mathbf{U}^T = \mathbf{I} \quad (2.46)$$

In detail,

$$\mathbf{U} \mathbf{V}^T = \begin{bmatrix} \mathbf{U}_u \mathbf{V}_u^T & \mathbf{U}_u \mathbf{V}_l^T \\ \mathbf{U}_l \mathbf{V}_u^T & \mathbf{U}_l \mathbf{V}_l^T \end{bmatrix} = \begin{bmatrix} \mathbf{I} & \mathbf{0} \\ \mathbf{0} & \mathbf{I} \end{bmatrix} \quad (2.47)$$

and

$$\mathbf{V} \mathbf{U}^T = \begin{bmatrix} \mathbf{V}_u \mathbf{U}_u^T & \mathbf{V}_u \mathbf{U}_l^T \\ \mathbf{V}_l \mathbf{U}_u^T & \mathbf{V}_l \mathbf{U}_l^T \end{bmatrix} = \begin{bmatrix} \mathbf{I} & \mathbf{0} \\ \mathbf{0} & \mathbf{I} \end{bmatrix} \quad (2.48)$$

If the eigenvectors occur in complex conjugate pairs, there is sometimes an advantage to subdividing the upper and lower matrices accordingly with an overbar, as for  $\bar{\mathbf{U}}_{up}$ , meaning the complex conjugate of  $\mathbf{U}_{up}$ .

$$\mathbf{U} = \begin{bmatrix} \mathbf{U}_u \\ \mathbf{U}_l \end{bmatrix} = \begin{bmatrix} \mathbf{U}_{up} & \bar{\mathbf{U}}_{up} \\ \mathbf{U}_{lp} & \bar{\mathbf{U}}_{lp} \end{bmatrix} \quad (2.49)$$

The four submatrices are each  $n \times n$  and can be inverted because the eigenvectors are assumed here to be independent. The diagonal eigenvalue matrix  $\Lambda$  must be rearranged accordingly.

$$\Lambda = \begin{bmatrix} \Lambda_p & \mathbf{0} \\ \mathbf{0} & \bar{\Lambda}_p \end{bmatrix} \quad (2.50)$$

## 2.2.4 Conversion from state space to quadratic form and implications.

Using the upper and lower eigenvector matrices, it is possible to return to the quadratic form of the characteristic equations. The derivations are done without inverting the diagonal matrix  $\Lambda$ , which may be singular.

For the right eigenvectors, using Eq. (2.39b),  $U_u$  is eliminated from Eq. (2.39a) to give the quadratic form.

$$I U_l \Lambda^2 + C_1 U_l \Lambda + K_1 U_l = 0 \quad (2.51)$$

Now, post-multiply (2.51) by  $\Lambda$  and, since  $U_u = U_l \Lambda$ , a quadratic equation in terms of  $U_u$  is

$$I U_u \Lambda^2 + C_1 U_u \Lambda + K_1 U_u = 0 \quad (2.52)$$

Doing the corresponding process for the left vectors, first pre-multiply Eq. (2.41a) by  $\Lambda$ , and then use Eq. (2.41b) to eliminate  $V_l^T$ ,

$$I \Lambda^2 V_u^T + \Lambda V_u^T C_1 + V_u^T K_1 = 0 \quad (2.53)$$

Taking the transpose yields

$$I V_u \Lambda^2 + C_1^T V_u \Lambda + K_1^T V_u = 0. \quad (2.53a)$$

Comparing Eqs. (2.52) and (2.54), it is seen that the  $V_u$  are involved with the eigenvalue problem of the transpose matrices  $C_1^T$  and  $K_1^T$ . If the  $C_1$  and  $K_1$  are symmetric, then  $V_u$ ,  $U_l$ , and  $U_u$  satisfy the same quadratic equation. Thus the corresponding eigenvectors may be equal, or differ at most by a scalar multiplier, which can be different for each mode. An equation involving only  $V_l$  is not as simple, as shown in Eq. (2.53b).

$$-K_1^T V_l \Lambda^2 + C_1^T K_1^T V_l \Lambda + V_l = 0 \quad (2.53b)$$

If the rectangular eigenvector matrices are subdivided into two square submatrices, which are complex conjugates of each other, Eq. (2.51) becomes

$$\begin{bmatrix} U_{l/p} & \bar{U}_{l/p} \end{bmatrix} \begin{bmatrix} \Lambda_p^2 & 0 \\ 0 & \bar{\Lambda}_p^2 \end{bmatrix} + C_1 \begin{bmatrix} U_{l/p} & \bar{U}_{l/p} \end{bmatrix} \begin{bmatrix} \Lambda_p & 0 \\ 0 & \bar{\Lambda}_p \end{bmatrix} + K_1 \begin{bmatrix} U_{l/p} & \bar{U}_{l/p} \end{bmatrix} = \begin{bmatrix} 0 & 0 \end{bmatrix} \quad (2.55)$$

and the results are the  $n$  simultaneous equations which state the eigenvalue problem of the second order differential equations

$$U_{l/p} \Lambda_p^2 + C_1 U_{l/p} \Lambda_p + K_1 U_{l/p} = 0 \quad (2.56a)$$

and

$$\bar{U}_{/p} \bar{\Lambda}_p^2 + C_1 \bar{U}_{/p} \bar{\Lambda}_p + K_1 \bar{U}_{/p} = 0 \quad (2.56b)$$

The Eq. (2.56b) is just the complex conjugate of Eq. (2.56a), since the plant matrices are real.

The orthogonality equation in Eq. (2.57) cannot be further simplified.

$$V_u U_u^T = [V_{up} U_{up}^T + \bar{V}_{up} \bar{U}_{up}^T] = I \quad (2.57)$$

### Example 2.1

This example is for a 4x4 state matrix with viscous damping. The purpose is to show the numerical form of the individual matrices  $\Lambda$ ,  $\Lambda_p$ ,  $U_{/p}$  and the product matrices in the resulting quadratic equation.

$$M^* = \begin{bmatrix} 1 & 0 & 0 & 0 \\ 0 & 2 & 0 & 0 \\ 0 & 0 & -5 & 4 \\ 0 & 0 & 4 & -4 \end{bmatrix} \quad K^* = \begin{bmatrix} 0.4 & -0.2 & 5 & -4 \\ -0.2 & 0.8 & -4 & 4 \\ 5 & -4 & 0 & 0 \\ -4 & 4 & 0 & 0 \end{bmatrix}$$

$$A = \begin{bmatrix} -0.4 & 0.2 & -5 & 4 \\ 0.1 & -0.4 & 2 & 2 \\ 1 & 0 & 0 & 0 \\ 0 & 1 & 0 & 0 \end{bmatrix} \quad \Lambda = \begin{bmatrix} (-0.1376 + 0.5289 i) & 0 & 0 & 0 \\ 0 & (-0.2624 + 2.5745 i) & 0 & 0 \\ 0 & 0 & (-0.1376 - 0.5289 i) & 0 \\ 0 & 0 & 0 & (-0.2624 - 2.5745 i) \end{bmatrix}$$

$$\Lambda_p = \begin{bmatrix} (-0.1376 + 0.5289 i) & 0 \\ 0 & (-0.2624 + 2.5745 i) \end{bmatrix}$$

$$U_{/p} = \begin{bmatrix} 0.5144 + 0.0047 i & -0.8572 + 0.0139 i \\ 0.6064 - 0.0020 i & 0.3646 + 0.0163 i \end{bmatrix}$$

The individual matrices in the quadratic are 2x2 and the numerical values are listed below.

$$U_{/p} \Lambda_p^2 + C_1 U_{/p} \Lambda_p + K_1 U_{/p} = 0.$$

$$U_{/p} \Lambda_p^2 = \begin{bmatrix} -0.1334 - 0.0761 i & 5.6414 + 1.0670 i \\ -0.1584 - 0.0877 i & -2.3697 - 0.5997 i \end{bmatrix}$$

$$C_1 U_{/p} \Lambda_p = \begin{bmatrix} -0.0128 + 0.0444 i & 0.1032 - 1.0711 i \\ -0.0256 + 0.1013 i & -0.0740 + 0.5948 i \end{bmatrix}$$

$$K_1 U_{/p} = \begin{bmatrix} 0.1463 + 0.0318 i & -5.7446 + 0.0041 i \\ 0.1840 - 0.0135 i & 2.4437 + 0.0049 i \end{bmatrix}$$

### 2.2.5 Special cases of combinations of $C_1$ and $K_1$ .

**Special Case 1:**  $C_1$  and  $K_1$  are symmetric.

In general, if  $C_1 = M^{-1} C$  and  $K_1 = M^{-1} K$ , then neither  $C_1$  or  $K_1$  will be symmetric, even though  $C$  and  $K$  are symmetric. An exception would be when  $M$  is equal to a scalar  $\alpha$  times the unit matrix, that is  $M = \alpha I$ .

Another possibility for assuring that  $C_1$  and  $K_1$  are symmetric is to make a change in coordinates, by weighting the original coordinates by the square root of the mass matrix. The result is that

$$C_1 = M^{-1/2} C M^{-1/2} \quad \text{and} \quad K_1 = M^{-1/2} K M^{-1/2} \quad (2.58)$$

which will be symmetric if  $C$  and  $K$  are symmetric. For this special case,  $C_1^T = C_1$  and  $K_1^T = K_1$ , so it is seen by comparing Eqs. (2.53) and (2.51) that the  $V_u$  and  $U_l$  satisfy the same equations. Thus, it could be that  $V_u = U_l$ , but it is more likely that they would differ by a scalar factor because of the normalization. The following example demonstrates this effect.

#### Example 2.2

This example shows that the eigenvalues in  $V_u$  and  $U_l$  differ only by a scalar multiplier when  $C_1 = K_1 = 0$ .

$$M^* = \begin{bmatrix} 2 & 0 & 0 & 0 \\ 0 & 2 & 0 & 0 \\ 0 & 0 & -6 & 3 \\ 0 & 0 & 3 & -7 \end{bmatrix} \quad K^* = \begin{bmatrix} 0.5 & -0.2 & 6 & -3 \\ -0.2 & 0.4 & -3 & 7 \\ 6 & -3 & 0 & 0 \\ -3 & 7 & 0 & 0 \end{bmatrix}$$

$$A = \begin{bmatrix} -0.25 & 0.1 & -3 & 1.5 \\ 0.1 & -0.2 & 1.5 & 3.5 \\ 1 & 0 & 0 & 0 \\ 0 & 1 & 0 & 0 \end{bmatrix} \quad \Lambda = \begin{bmatrix} (-0.0652 + 1.3138 i) & 0 & 0 & 0 \\ 0 & (-0.1598 + 2.1777 i) & 0 & 0 \\ 0 & 0 & (-0.0652 - 1.3138 i) & 0 \\ 0 & 0 & 0 & (-0.1598 - 2.1777 i) \end{bmatrix}$$

$$U_p = \begin{bmatrix} U_{up} \\ U_{lp} \end{bmatrix} = \begin{bmatrix} -0.0245 + 0.7091 i & -0.1078 + 0.9954 i \\ -0.0424 + 0.6003 i & 0.0567 - 1.1758 i \\ 0.5394 & -0.0081 i & 0.4583 & +0.0159 i \\ 0.4574 & +0.0096 i & -0.5389 & +0.0135 i \end{bmatrix}$$

$$V_p = \begin{bmatrix} V_{up} \\ V_{lp} \end{bmatrix} = \begin{bmatrix} -0.0062 - 0.4108 i & 0.0073 - 0.2103 i \\ 0.0073 - 0.3484 i & 0.0062 + 0.2473 i \\ 0.5378 & -0.0492 i & 0.4580 & -0.0278 i \\ 0.4593 & +0.0037 i & -0.5391 & +0.0445 i \end{bmatrix}$$

The result is that  $V_{up} \neq U_{lp}$  but the individual vectors are related by scalar factors. Adding another subscript for eigenvector number,  $V_{up1} = (-0.7616 i) U_{lp1}$  and  $V_{up2} = (-0.4589 i) U_{lp2}$ . Note that two of the four vectors are given, to save space. The other two vectors are the complex conjugates of the two that are given.

**Special Case 2: :  $C_1 = 0$  and  $K_1$  is unsymmetric.**

For this special case, the control forces are zero and there is no damping. It would not be unusual for  $K_1$  to be unsymmetric. Then, from Eqs. (2.39),

$$-K_1 U_l = U_u \Lambda \quad (2.59a)$$

and

$$U_u = U_l \Lambda. \quad (2.59b)$$

The quadratic equation reduces to

$$-K_1 U_l = U_l \Lambda^2 \quad (2.59c)$$

From Eqs. (2.41) obtained from the characteristic equation

$$V_l^T = \Lambda V_u^T \quad (2.60a)$$

and

$$-V_u^T K_1 = \Lambda V_l^T. \quad (2.60b)$$

It is seen in Eq. (2.60a) that the lower left vector  $V_l$  is related simply to  $V_u$ , which is not the case when  $C_1 \neq 0$ .

One quadratic equation is 
$$-V_u^T K_1 = \Lambda^2 V_u^T \quad (2.60c)$$

or

$$-K_1^T V_u = V_u \Lambda^2$$

and that with the  $V_l$

$$-K_1^T V_l = V_l \Lambda^2 \quad (2.60d)$$

The form of  $\lambda_j, \bar{\lambda}_j = -\zeta_j \omega_j \pm i \omega_j \sqrt{1 - \zeta_j^2}$  so  $\zeta_j = 0$  and  $\lambda_j, \bar{\lambda}_j = \pm i \omega_j$ . The eigenvalues of  $K_1^T$  are the same as those for  $K_1$ , but the left-hand vectors are still different from the right-hand vectors.

**Special Case 3:**  $C_1 = 0$  and  $K_1$  is symmetric.

If  $K_1$  is symmetric with no damping, the upper portions of  $U$  and  $V$  satisfy the same quadratic equations as the lower portion of  $U$ , but the lower portion of  $V$  does not. This is seen by inspection of Eqs. (2.51) through (2.54). This means that the eigenvectors are "equal" but they may differ by a scalar, depending on how they are normalized or where  $u_{ur} = u_{lr} \lambda_r$ .

$$U_u = V_u \Lambda^2 \quad (2.61)$$

$$U_u = U_l \Lambda \quad (2.62)$$

$$V_l \Lambda = V_u \Lambda^2 = U_u = U_l \Lambda \quad (2.63)$$

The form of the orthogonality relations  $V^T U = I$  in terms of submatrices is

$$V_u^T U_u + V_l^T U_l = I \quad (2.64)$$

### Example 2.3

In this example,  $C_1 = 0$  and  $K_1$  is symmetric. If  $K$  is symmetric, then  $M$  must be of a special form such as  $M = \beta I$ , where  $\beta$  is a scalar, for  $K_1$  to be symmetric.

$$M = \begin{bmatrix} 2 & 0 \\ 0 & 2 \end{bmatrix} \quad K = \begin{bmatrix} 6 & -3 \\ -3 & 7 \end{bmatrix} \quad K_1 = M^{-1} K = \begin{bmatrix} 3 & -1.5 \\ -1.5 & 3.5 \end{bmatrix}$$

The eigenvalues are

$$\lambda_1 = 1.3150 i, \quad \lambda_2 = 2.1842 i, \quad \lambda_3 = \bar{\lambda}_1 \quad \text{and} \quad \lambda_4 = \bar{\lambda}_2.$$

The eigenvectors are in the same order as the eigenvalues.

$$U = \begin{bmatrix} 0.7095 i & 0.9983 i & -0.7095 i & -0.9983 i \\ 0.6010 i & -1.1785 i & -0.6010 i & 1.1785 i \\ 0.5395 & 0.4571 & 0.5395 & 0.4571 \\ 0.4571 & -0.5395 & 0.4571 & -0.5395 \end{bmatrix}$$

$$V = \begin{bmatrix} -0.4103 i & -0.2093 i & 0.4103 i & 0.2093 i \\ -0.3476 i & 0.2470 i & 0.3476 i & -0.2470 i \\ 0.5395 & 0.4571 & 0.5395 & 0.4571 \\ 0.4571 & -0.5395 & 0.4571 & -0.5395 \end{bmatrix}$$

### 2.2.6 Recovery of the $C_1$ and $K_1$ matrices from the eigenproperties.

The  $A$  matrix can be recovered from the eigenproperties by pre-multiplying Eq. (2.42a) by  $U$  and post-multiplying by  $V^T$ , to produce Eq. (2.65),

$$U \Lambda V^T = A \quad (2.65)$$

which, written out in terms of the submatrices is

$$\begin{bmatrix} U_u \Lambda V_u^T & U_u \Lambda V_l^T \\ U_l \Lambda V_u^T & U_l \Lambda V_l^T \end{bmatrix} = \begin{bmatrix} -C_1 & -K_1 \\ I & 0 \end{bmatrix}. \quad (2.66)$$

### 2.2.7 Nonsymmetric control matrices, forced vibration problem.

To do a forced vibration problem with symmetric, or unsymmetric control matrices,  $G$  and  $H$ , the matrix equations are

$$\begin{bmatrix} M & 0 \\ 0 & -[K+H] \end{bmatrix} \begin{Bmatrix} \ddot{z}(t) \\ \dot{z}(t) \end{Bmatrix} + \begin{bmatrix} [C+G] & [K+H] \\ [K+H] & 0 \end{bmatrix} \begin{Bmatrix} \dot{z}(t) \\ z(t) \end{Bmatrix} = \begin{Bmatrix} F(t) \\ 0 \end{Bmatrix}. \quad (2.67)$$

The advantage of using this special form of the redundant equations is that, if the control matrices are symmetric, the closed loop  $M^*$  and  $K^*$  matrices are again symmetric. The shorthand form of Eq. (2.67) is

$$M^* \dot{\underline{\eta}} + K^* \underline{\eta} = F^*(t) \quad (2.68)$$

or

$$\dot{\underline{\eta}} - A^* \underline{\eta} = [M^*]^{-1} F^*(t) \quad (2.69)$$

The equations are decoupled by substituting

$$\underline{\eta}(t) = U q(t) \quad (2.70)$$

into Eq. (2.69) and pre-multiplying by  $V^T$ .

### 3. SENSITIVITY OF EIGENPROPERTIES TO INDIVIDUAL ELEMENTS IN THE DAMPING AND CONTROL MATRICES.

An essential part of control of vibration of structures is the study of the sensitivity of the eigenproperties, namely damping ratios, natural frequencies, and mode shapes, to elements in the damping and control matrices. The differential equations are  $\mathbf{M} \ddot{\mathbf{z}} + \mathbf{C} \dot{\mathbf{z}} + \mathbf{K} \mathbf{z} = -\mathbf{G} \dot{\mathbf{z}} - \mathbf{H} \mathbf{z}$ , where  $\mathbf{G}$  and  $\mathbf{H}$  are control matrices. The viscous damping matrix  $\mathbf{C}$  is achieved through passive mechanical, electromechanical, or other devices whose forces depend on the relative velocities between two points on a structure or between one point and ground. It is assumed that there is more freedom in designing the active control forces on the right side of the equation, so that it is possible to apply a force  $G_{ij} \dot{z}_j$  at  $i$  proportional to the velocity at  $j$ , for example. This chapter deals with the sensitivity of eigenvalues and eigenvectors to changes in individual elements, primarily in the  $\mathbf{C}$  or  $\mathbf{G}$  matrices.

An alternate form of the differential equation is  $\mathbf{M} \ddot{\mathbf{z}} + [\mathbf{C}+\mathbf{G}] \dot{\mathbf{z}} + [\mathbf{K}+\mathbf{H}] \mathbf{z} = \mathbf{0}$ , from which the closed loop eigenvalues are determined. So, an approach to optimum control is this: achieve as much damping as possible and practical through optimizing the parameters in the  $\mathbf{C}$  matrix and then add what more is needed in the  $\mathbf{G}$  matrix. The idea is to design the  $\mathbf{C}+\mathbf{G}$  matrix and the  $\mathbf{K}+\mathbf{H}$  matrix, rather than the individual matrices, keeping in mind how they are physically achieved.

The publications that are closely related to the present study are summarized. The optimization of viscous damping to minimize free vibrations has been studied by Neubert [N4], Gilheany [G1], Silverberg [S1], McLoughlin [M1], and Inman and Andry [5], who give additional references. Neubert [N6] also presented an approach for optimum sizing and location of viscous damping to minimize forced, random vibrations. Methods of active control are summarized in the book by Meirovitch [M4]. The need for passive damping in feedback controlled flexible structures was emphasized by von Flotow and Vos [F1]. Venkayya and Tischler [V1] discussed the effect of frequency control on the dynamic response of structures. Sensitivity analysis as related to modal control is the subject of the book by Porter and Crossley [P1] in 1972, which summarized the methods that were developed to that time and presented some practical examples for aircraft stabilization systems, cascaded vehicles, and economic and manufacturing systems. Somewhat unique are the sections dealing with systems which have confluent, or repeating, eigenvalues rather than distinct eigenvalue with linearly independent eigenvectors, as assumed herein.

The contributions of the present study that are summarized in this chapter are:

1. The current, classical methods for finding eigenvalue and eigenvector sensitivities are summarized.
2. A direct mathematical relationship is presented between the coefficients in the complete modal series method and Nelson's individual mode method for finding sensitivities of eigenvectors.
3. A new method for finding eigenvalue sensitivities is presented, based on derivatives of the invariants associated with the similarity transformations involved in the eigenvalue solutions.
4. It is demonstrated that increasing damping may sometimes be deleterious, because some modes may usurp, or hog, the damping with the result that damping ratios actually decrease in other modes.
5. Several examples are given, that give an engineer a practical feeling for the sensitivity of damping ratios and natural frequencies to changes in plant and control matrices.

### 3.1 Eigenvalue sensitivity.

In this section, methods are summarized in detail for finding the sensitivity of the eigenvalues. It is assumed that the system is underdamped and the eigenvalues occur in complex conjugate pairs. A typical pair of eigenvalues is  $\lambda_r, \bar{\lambda}_r = -\zeta_r \omega_r \pm i \omega_{Dr}$ . Having the derivative of this pair of eigenvalues with respect to input parameters, the derivatives of the modal damping ratios  $\zeta_r$  and natural frequencies  $\omega_r$  are readily determined.

The eigenvalue derivatives are determined in two ways. In the first method, which was developed during the present study, the eigenvalue derivatives are formulated from the invariants in the similarity transformation. Since the input parameters and the eigenvalues appear explicitly, these derivatives aid greatly in understanding the interaction. The second, standard way, which is more convenient for numerical computations, is to take the derivative of the characteristic equation. The derivative then involves the eigenvectors and the derivative of the characteristic matrix.

The matrix equations are

$$\mathbf{M} \ddot{\mathbf{z}} + \mathbf{C} \dot{\mathbf{z}} + \mathbf{K} \mathbf{z} = -\mathbf{G} \dot{\mathbf{z}} - \mathbf{H} \mathbf{z} \quad (3.1)$$

where the  $n \times n$  matrices  $\mathbf{M}$ ,  $\mathbf{C}$  and  $\mathbf{K}$  are symmetric but  $\mathbf{G}$  and  $\mathbf{H}$  may be unsymmetric. The Eq. (3.1) is multiplied by the inverse of  $\mathbf{M}$  to produce

$$\ddot{\mathbf{z}} + \mathbf{C}_1 \dot{\mathbf{z}} + \mathbf{K}_1 \mathbf{z} = -\mathbf{M}^{-1} [\mathbf{G} \dot{\mathbf{z}} + \mathbf{H} \mathbf{z}] \quad (3.2)$$

where  $\mathbf{C}_1 = \mathbf{M}^{-1} \mathbf{C}$  and  $\mathbf{K}_1 = \mathbf{M}^{-1} \mathbf{K}$ . The matrices  $\mathbf{C}_1$  and  $\mathbf{K}_1$  are usually unsymmetric. The

resulting closed loop equations are written in state space form as

$$\mathbf{I} \dot{\mathbf{y}}(t) - \mathbf{A} \mathbf{y}(t) = \mathbf{0} \quad (3.3)$$

where

$$\mathbf{A} = \begin{bmatrix} -\mathbf{M}^{-1}[\mathbf{C}+\mathbf{G}] & -\mathbf{M}^{-1}[\mathbf{K}+\mathbf{H}] \\ \mathbf{I} & \mathbf{0} \end{bmatrix} \quad (3.4)$$

The solutions of the homogeneous equations are of the form

$$\mathbf{y}(t) = e^{\lambda t} \mathbf{u}, \quad (3.5)$$

and the eigenvalue problem to be solved is

$$[-\lambda \mathbf{I} + \mathbf{A}] \mathbf{u} = \mathbf{0}. \quad (3.6)$$

From Eq. (3.6) the eigenvalues  $\lambda_r$  are determined and are here assumed to be distinct, with no repeated eigenvalues. The right eigenvectors  $\mathbf{u}_r$  satisfy the relationship

$$[-\lambda_r \mathbf{I} + \mathbf{A}] \mathbf{u}_r = \mathbf{0}. \quad (3.7)$$

Since  $\mathbf{A}$  is unsymmetric, there is also a set of left eigenvectors associated with the eigenvector problem involving  $\mathbf{A}^T$ , which is the transpose of  $\mathbf{A}$ . The eigenvalues  $\lambda_r$  are the same as in Eq. (3.7), but the left eigenvectors  $\mathbf{v}_r$  satisfy

$$[-\lambda_r \mathbf{I} + \mathbf{A}^T] \mathbf{v}_r = \mathbf{0}, \quad (3.8)$$

which can also be written in transpose form

$$\mathbf{v}_r^T [-\lambda_r \mathbf{I} + \mathbf{A}] = \mathbf{0}. \quad (3.9)$$

The orthogonality relationships between left and right eigenvectors are

$$\mathbf{v}_r^T \mathbf{u}_s = 0 \quad \text{for } r \neq s \quad (3.10a)$$

and

$$\mathbf{v}_r^T \mathbf{u}_r = 1 \quad \text{for } r = s \quad (3.10b)$$

or, combining (3.10a) and (3.10b),

$$\mathbf{V}^T \mathbf{U} = \mathbf{I} \quad (3.10c)$$

where  $\mathbf{U}$  and  $\mathbf{V}$  are  $2n \times 2n$  matrices of right and left eigenvectors. It can be shown that

$$\mathbf{V}^T \mathbf{A} \mathbf{U} = \Lambda \quad (3.10d)$$

where  $\Lambda$  is a diagonal matrix of the eigenvalues.

Here Eq. (3.10b) is the normalizing condition for the  $\mathbf{v}_r$  vectors, where the  $\mathbf{u}_r$  have first been normalized according to

$$\mathbf{u}_r^T \mathbf{M}^* \mathbf{u}_r = \mathbf{b}_r. \quad (3.11)$$

### 3.1.1 Sensitivities of the eigenvalues using the similarity transformation invariants.

Some of the effects of individual elements in the control matrix can be anticipated from knowledge of the relationship between the matrix  $A$  and the diagonal eigenvalue matrix  $\Lambda$ . The matrices  $\Lambda$  and  $A$  are similar, in that they are related by a similarity transformation. The invariants are those associated with similarity transformations, meaning that the matrices have the same eigenvalues, their traces are equal, and their determinants have the same value. The equality of the traces relates the system damping parameters to the modal damping ratios and natural frequencies, as follows.

$$\text{Tr}(A) = \text{Tr}(-(C+G)) = \text{Tr}(\Lambda) = \sum_r \lambda_r + \bar{\lambda}_r = \sum_r -2 \zeta_r \omega_r \quad (3.12)$$

The fact that the determinants are invariant means that

$$|A| = |M^{-1} K| = \omega_1^2 \omega_2^2 \dots \omega_N^2, \quad (3.13)$$

so that, even though the  $\omega_r^2$ 's change due to changes in  $C+G$ , their product does not change if the mass and stiffness matrices are not altered.

From Eqs. (3.12) and (3.13), relationships for the sensitivities can also be determined by taking derivatives of both sides of the equations with respect to  $A_{ij}$ . Thus the following important results are obtained.

$$\frac{\partial(\text{Tr}(A))}{\partial A_{ij}} = \frac{-\partial(\text{Tr}(C+G))}{\partial A_{ij}} = \frac{\partial(\sum_r \lambda_r + \bar{\lambda}_r)}{\partial A_{ij}} = \frac{\partial(\sum_r (-2 \zeta_r \omega_r))}{\partial A_{ij}} \quad (3.14)$$

$$\frac{\partial |M^{-1} K|}{\partial A_{ij}} = \frac{\partial(\omega_1^2 \omega_2^2 \dots \omega_N^2)}{\partial A_{ij}} \quad (3.15)$$

The Eq. (3.12) is written in detail as Eq. (3.16) and taking the partial of (3.16) with respect to  $A_{ii}$  confirms Eq. (3.33), which is derived separately below.

$$\sum_{r=1}^{2n} \lambda_r = \sum_{i=1}^{2n} A_{ii} = A_{11} + A_{22} + \dots + A_{2n2n} \quad (3.16a)$$

$$\text{and} \quad \sum_{r=1}^{2n} \frac{\partial \lambda_r}{\partial A_{ii}} = 1 \quad (3.16b)$$

### Example 3.1: System with One Degree of Freedom

For the simple one-degree-of-freedom system with a mass  $m$  supported by a spring of stiffness  $k$ , a dashpot with damping rate  $c$ , and a control force of  $-g \dot{x}$  the  $A$  matrix is

$$A = \begin{bmatrix} -m^{-1}(c+g) & -m^{-1}k \\ 1 & 0 \end{bmatrix} \quad (3.17)$$

and the diagonal eigenvalue matrix is

$$\Lambda = \begin{bmatrix} -\zeta_1 \omega_1 + i \omega_{D1} & 0 \\ 0 & -\zeta_1 \omega_1 - i \omega_{D1} \end{bmatrix}. \quad (3.18)$$

The following relationships are obtained by setting the traces and determinants equal,

$$-m^{-1}(c+g) = -2\zeta_1 \omega_1 \quad (3.19)$$

and 
$$m^{-1}k = \zeta_1^2 \omega_1^2 + \omega_{D1}^2 = \omega_1^2. \quad (3.20)$$

Taking the partial derivatives of Eqs. (3.19) and (3.20) with respect to  $g$ , the results are

$$m^{-1} = 2\left(\zeta_1 \frac{\partial \omega_1}{\partial g} + \omega_1 \frac{\partial \zeta_1}{\partial g}\right) \quad (3.21)$$

and 
$$0 = \omega_1 \frac{\partial \omega_1}{\partial g} \quad (3.22)$$

From Eq. (3.22), if  $\omega_1 \neq 0$ , then  $\partial \omega_1 / \partial g = 0$  which shows that changing  $g$  does not result in a change in  $\omega_1$ .

### Example 3.2: System with two degrees of freedom

If the system has two degrees of freedom, with the damping matrix  $C=0$ , and the mass matrix is diagonal, the  $A$  and  $\Lambda$  matrices would be  $4 \times 4$ , as follows.

$$A = \begin{bmatrix} -G & -K \\ I & 0 \end{bmatrix} = \begin{bmatrix} -G_{11}/m_1 & -G_{12}/m_1 & -K_{11}/m_1 & -K_{12}/m_1 \\ -G_{21}/m_2 & -G_{22}/m_2 & -K_{21}/m_2 & -K_{22}/m_2 \\ 1 & 0 & 0 & 0 \\ 0 & 1 & 0 & 0 \end{bmatrix} \quad (3.23)$$

and 
$$\Lambda = \begin{bmatrix} \lambda_1 & 0 & 0 & 0 \\ 0 & \bar{\lambda}_1 & 0 & 0 \\ 0 & 0 & \lambda_2 & 0 \\ 0 & 0 & 0 & \bar{\lambda}_2 \end{bmatrix} \quad (3.24)$$

From the traces and determinants, the following relationships arise.

$$(K_{11}K_{22}-K_{12}K_{21})/(m_1m_2) = \lambda_1 \bar{\lambda}_1 \lambda_2 \bar{\lambda}_2 = \omega_1^2 \omega_2^2 \quad (3.25)$$

$$-G_{11}/m_1 - G_{22}/m_2 = -\lambda_1 - \bar{\lambda}_1 - \lambda_2 - \bar{\lambda}_2 = -2\zeta_1\omega_1 - 2\zeta_2\omega_2 \quad (3.26)$$

The fact that the eigenvalues must be real or occur in complex conjugate pairs is confirmed by Eq. (3.26), since the left side is real. Further it shows that if  $G_{11} = G_{22} = 0$  and  $G_{12} \neq 0$ , then the system will be unstable since  $\zeta_1$  and  $\zeta_2$  must then be real and of opposite signs, with  $\omega_1$  and  $\omega_2$  real and positive.

By taking the partial derivative of Eqs. (3.25) and (3.26) with respect to  $G_{11}$ , equations for the sensitivities are obtained.

$$0 = \omega_1^2 \frac{\partial \omega_2}{\partial G_{11}} + \omega_2^2 \frac{\partial \omega_1}{\partial G_{11}} \quad (3.27)$$

and

$$1/(2m_1) = \zeta_1 \frac{\partial \omega_1}{\partial G_{11}} + \zeta_2 \frac{\partial \omega_2}{\partial G_{11}} + \omega_1 \frac{\partial \zeta_1}{\partial G_{11}} + \omega_2 \frac{\partial \zeta_2}{\partial G_{11}} \quad (3.28)$$

An interesting situation arises according to Eq. (3.27), namely that a change in  $G_{11}$  could produce changes in  $\omega_1$  and  $\omega_2$  and if one of them increases, the other must decrease.

### 3.1.2 Sensitivities of the eigenvalues in terms of the eigenvectors.

To find the sensitivity of the eigenvalues  $\lambda_r$  with respect to a parameter in location  $A_{ij}$ , take the partial derivative of Eq. (3.7) with respect to  $A_{ij}$ . The well known equation [R1,W1] for solving for this derivative in terms of the eigenvectors and the derivative of  $A$  is given in Eq. (3.29).

$$\frac{\partial \lambda_r}{\partial A_{ij}} = \mathbf{v}_r^T \frac{\partial \mathbf{A}}{\partial A_{ij}} \mathbf{u}_r \quad (3.29)$$

The right-hand side of Eq. (3.29) is a scalar. Taking the partial of  $A$  with respect to  $A_{ij}$  results in a matrix having unity in the  $ij$  position and zeroes for all the other matrix elements. , using  $v_{ir}$  to designate the  $i$ th element of the vector  $\mathbf{v}_r$  and  $u_{jr}$  the  $j$ th element of  $\mathbf{u}_r$ , the Eq. (3.29) becomes

$$\frac{\partial \lambda_r}{\partial A_{ij}} = v_{ir} u_{jr} \quad (3.30)$$

The  $2n \times 2n$  sensitivity matrix  $S_r$  is now formed [P1], which shows how each element  $A_{ij}$  affects the eigenvalue  $\lambda_r$ .

$$S_r = \left[ \frac{\partial \lambda_r}{\partial A_{ij}} \right] = v_r u_r^T \quad (r, i, j = 1, 2, \dots, 2n) \quad (3.31)$$

The sums of sensitivity matrices are of interest and, from Eqs. (3.31) and (3.10c), are

$$\sum_{r=1}^{2n} S_r = V U^T = I \quad (3.32)$$

where the  $U$  and  $V$  are  $2n \times 2n$  matrices made up of the right and left eigenvectors respectively.

Writing the Eq. (3.32) explicitly for the sum of the diagonal elements of the sensitivity matrices shows a significant result in Eq. (3.33), which is the same as Eq. (3.16b).

$$\sum_{r=1}^{2n} S_{iir} = \sum_{r=1}^{2n} \frac{\partial \lambda_r}{\partial A_{ii}} = 1 \quad \text{for } i=j \quad (3.33)$$

For the off-diagonal terms, 
$$\sum_{r=1}^{2n} S_{ijr} = \sum_{r=1}^{2n} \frac{\partial \lambda_r}{\partial A_{ii}} = 0 \quad \text{for } i \neq j. \quad (3.34)$$

The product of two sensitivity matrices for two different eigenvalues is zero, as can be seen from the following, which follow from Eqs. (3.10).

$$S_r S_s = v_r u_r^T v_s u_s^T = 0 \quad (r \neq s) \quad (3.35a)$$

$$S_r S_r = v_r u_r^T v_r u_r^T = S_r \quad (r=s) \quad (3.35b)$$

If the system is underdamped, the eigenvalues occur in complex conjugate pairs, and the following relationships apply:

$$\lambda_r = -\zeta_r \omega_r + i \omega_r (1 - \zeta_r^2)^{\frac{1}{2}} = -\zeta_r \omega_r + i \omega_{Dr} \quad (3.36a)$$

$$\lambda_r \bar{\lambda}_r = \omega_r^2 \quad \text{and} \quad \lambda_r + \bar{\lambda}_r = -2\zeta_r \omega_r. \quad (3.36b)$$

If there are  $2n$  eigenvalues, there are only  $n$  different modal frequencies  $\omega_r$ . The  $\omega_{Dr}$  is the modal frequency of damped free vibrations.

By differentiating the two expressions in Eq. (3.36b) with respect to  $A_{ij}$ , the derivatives of the modal damping ratio and natural frequency, that is  $\partial \zeta_r / \partial A_{ij}$  and  $\partial \omega_r / \partial A_{ij}$ , are readily determined in terms of the derivatives of  $\lambda_r$  and  $\bar{\lambda}_r$ .

### EXAMPLE 3.3: Ten-bar truss with eight degrees of freedom

The ten-bar truss studied, and shown in Fig. 3. 1, is one that has been suggested by some investigators as one of a group of "standard" trusses and was used as an example in references [N4] and [N6] . It is not necessarily a practical truss, but is used for comparison purposes. The truss lies in the x-y plane and has four moving nodal points, numbered 1, 2, 3, and 4, which are free to move in the x- and y-directions. There are two anchored nodal points, numbered 5 and 6. Each truss bay is square, 360 inches on each side. The cross-sectional areas are given in Table 3.1. The material of each bar is aluminum with a Young's Modulus  $E=10 \times 10^6$  psi. Half the mass of each bar was lumped at each end of the bar in the present analysis.

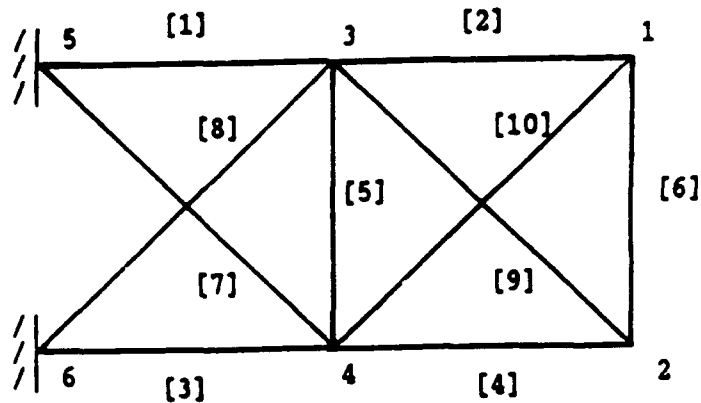


Fig. 3.1 Ten-bar truss

Table 3.1. Areas of Truss Bars

Bar No. m	Area(in <sup>2</sup> ) $A_m$	Bar No. m	Area(in <sup>2</sup> ) $A_m$
1	31.5	6	0.5
2	0.1	7	7.5
3	23.0	8	20.5
4	15.5	9	21.0
5	0.1	10	0.1

Optimization of passive viscous damping, representable by dashpots connected between nodal points, was presented in [N4] and [N6] for this truss. In practice, the control forces represented by the  $G\dot{x}$  would be superimposed on the damping forces generated by  $C\dot{x}$ . In order to isolate the effects of the control forces, no passive damping is included in these first examples, so the matrix  $C=0$  initially.

It is assumed that a control force can be located at any of the four moving truss nodes and that it is proportional to velocity at that or any other node, in the x- or y-direction. The positions in the G matrix follow the numbering of the nodes on the truss. Thus rows 1, 2 and 3 correspond to  $1x$ ,  $1y$  and  $2x$  on the truss, where  $2x$  means the displacement at node 2 in the x-direction.

Hence  $G_{23}=G_{1y,2x}$  and  $G_{57}=G_{3x,5x}$  for example. The sensitivities of the eigenvalues to individual elements in the  $G$  matrix were found using Eq. (3.12). The relationships in Eqs. (3.22)-(3.23) help to understand and confirm the results, but they were not used directly in the computations of sensitivities.

The modal damping ratios  $\zeta_r$  of the closed loop system are of particular interest. For this truss, it was found that the damping ratios in different modes are affected by various choices of location and magnitude of  $G_{ij}$ . In Fig. 3.2, the damping ratios  $\zeta_6$ ,  $\zeta_5$  and  $\zeta_8$  are plotted for both positive and negative values of  $G_{55}$ . It is seen that for small, positive values of  $G_{55}$  the damping ratios  $\zeta_5$  and  $\zeta_6$  are both positive and increase almost linearly with  $G_{55}$ . All the modal damping ratios are positive in this range and the system is stable. For larger values of  $G_{55}$ ,  $\zeta_6$  increases at a faster rate and  $\zeta_5$  decreases, but they remain positive. The curves are antisymmetrical with respect to the origin.

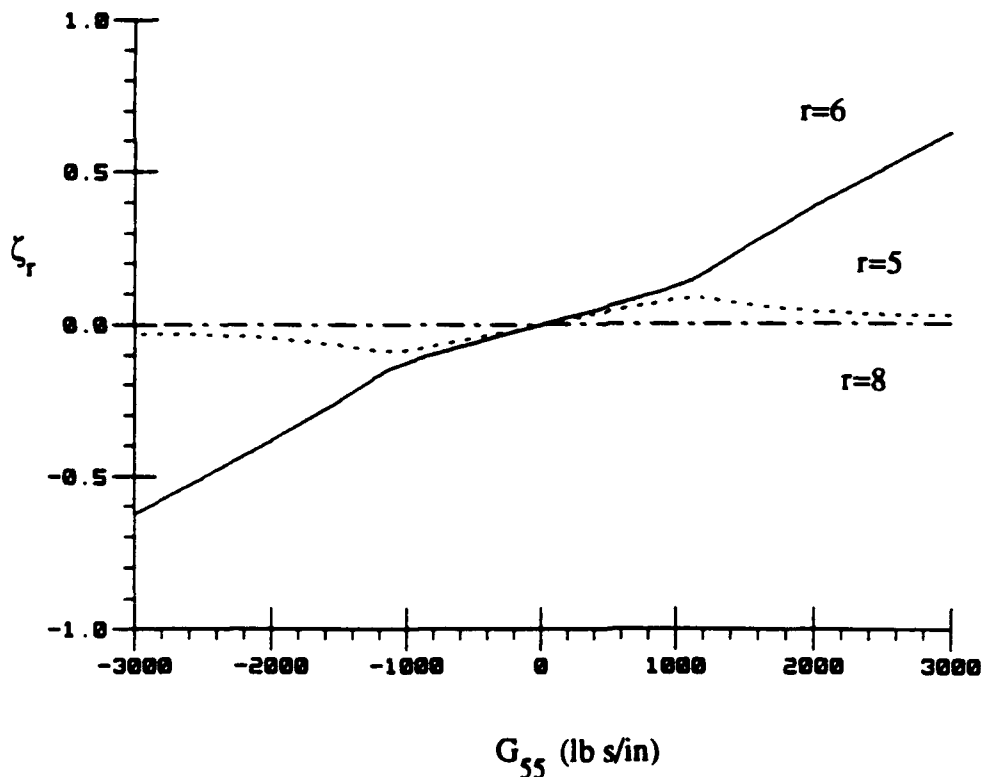


Fig. 3.2 Variation of  $\zeta_6$ ,  $\zeta_5$  and  $\zeta_8$  with  $G_{55}$

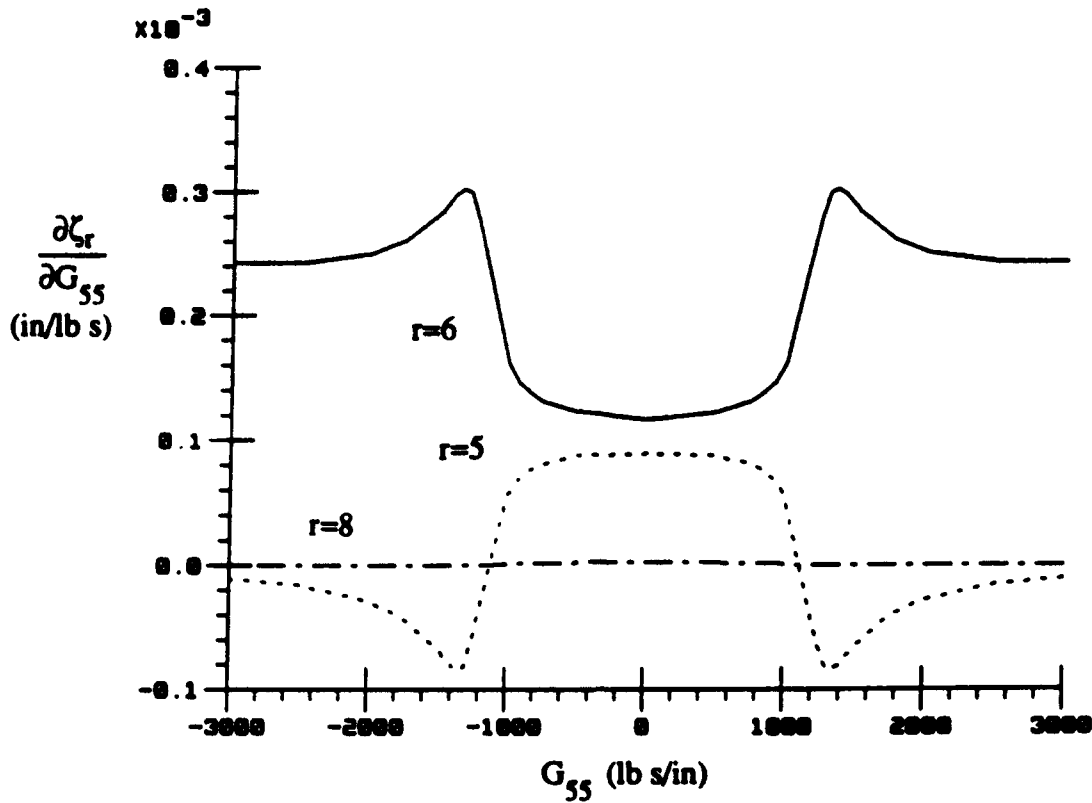


Fig. 3.3  $\partial\zeta_r/\partial G_{55}$  versus  $G_{55}$  for  $r = 6, 5$  and  $8$

The sensitivities, or derivatives of  $\zeta_5$ ,  $\zeta_6$  and  $\zeta_8$  with respect to  $G_{55}$  are shown in Fig. 3.3. These are related directly to the slopes of the curves in Fig. 3.2. When the sensitivity is positive, the damping ratio is increasing. Thus for  $\zeta_6$ , the slope is seen to be always positive, while for  $\zeta_5$ , the slope is positive for small  $G_{55}$  and negative for larger values.

The damping ratios of the same three modes are shown in Fig. 3.4 versus  $G_{77}$ . The corresponding natural frequencies  $\omega_r$  are shown in Fig. 3.5 and the damped natural frequencies  $\omega_{Dr}$  are plotted in Fig. 3.6 versus  $G_{77}$ . It is seen that damping is highest in the 8th mode and that  $\zeta_8$  approaches 1.0 or critical damping as  $G_{77}$  becomes large, while  $\zeta_5$  and  $\zeta_6$ , as well as the damping ratios for the other five modes, remain relatively small. The range of the natural frequencies for small damping is from 131 to 796 rad/s. When  $\zeta_8=1.0$ , the damped natural frequency  $\omega_{D8}=0$  and the modal frequency  $\omega_8=598$  rad/s, so there is a decrease of about 25 % in  $\omega_8$ . At the same time the other seven modes all show increases of from 0.03 to 7.5 % for their  $\omega_r$ 's.

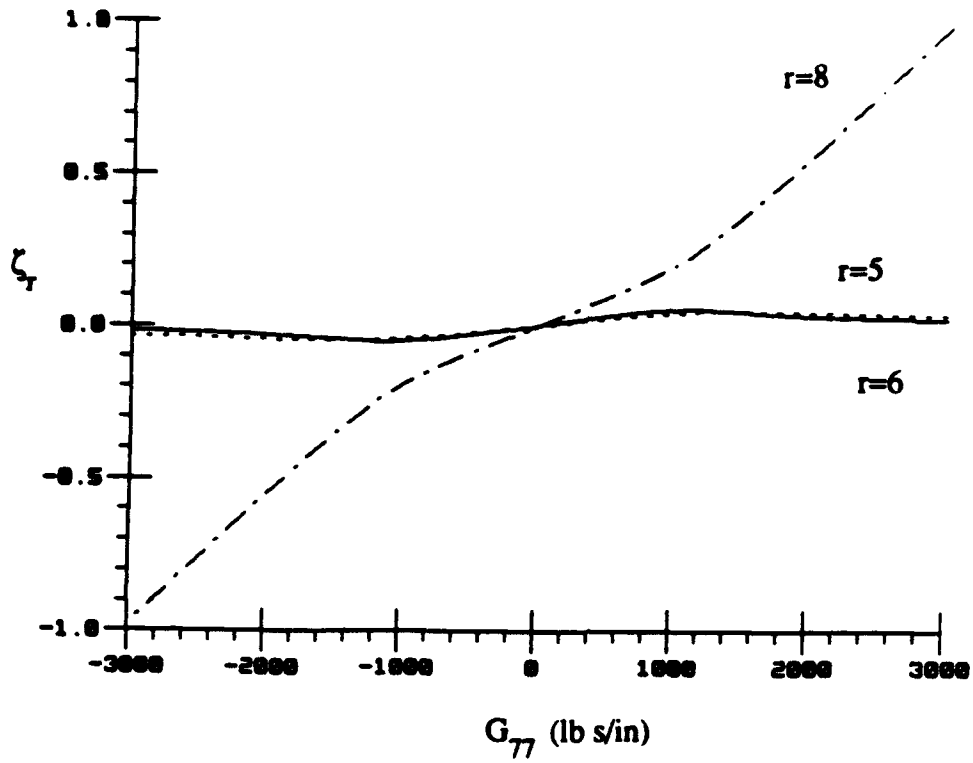


Fig. 3.4  $\zeta_5, \zeta_6$ , and  $\zeta_8$  versus  $G_{77}$

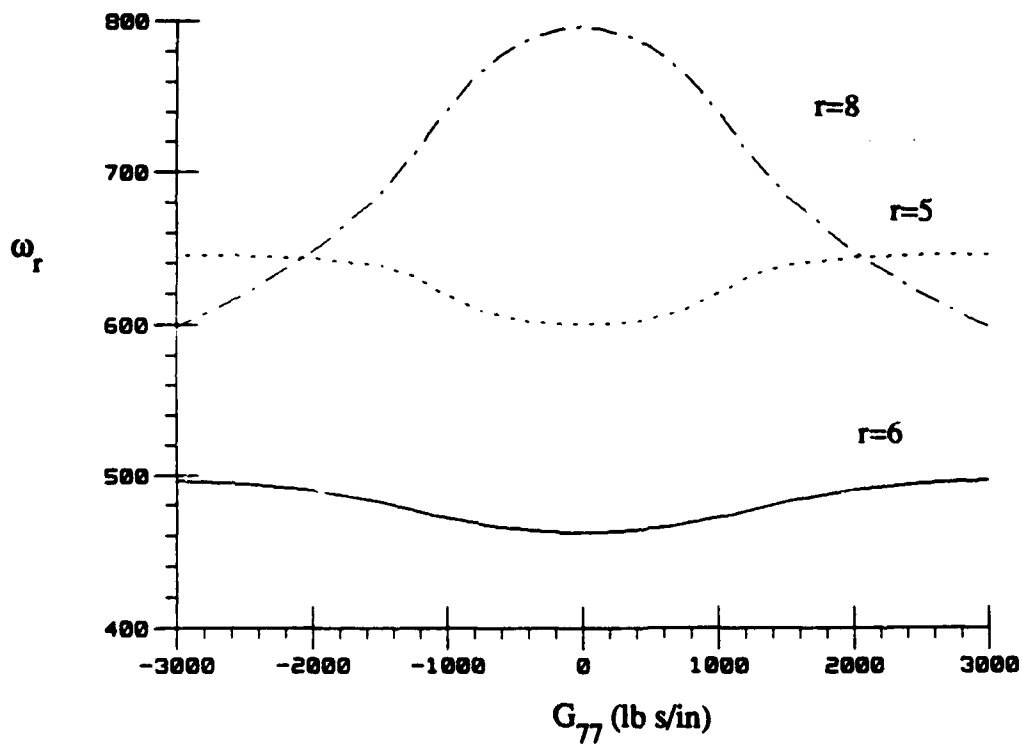


Fig. 3.5  $\omega_5, \omega_6$ , and  $\omega_8$  versus  $G_{77}$

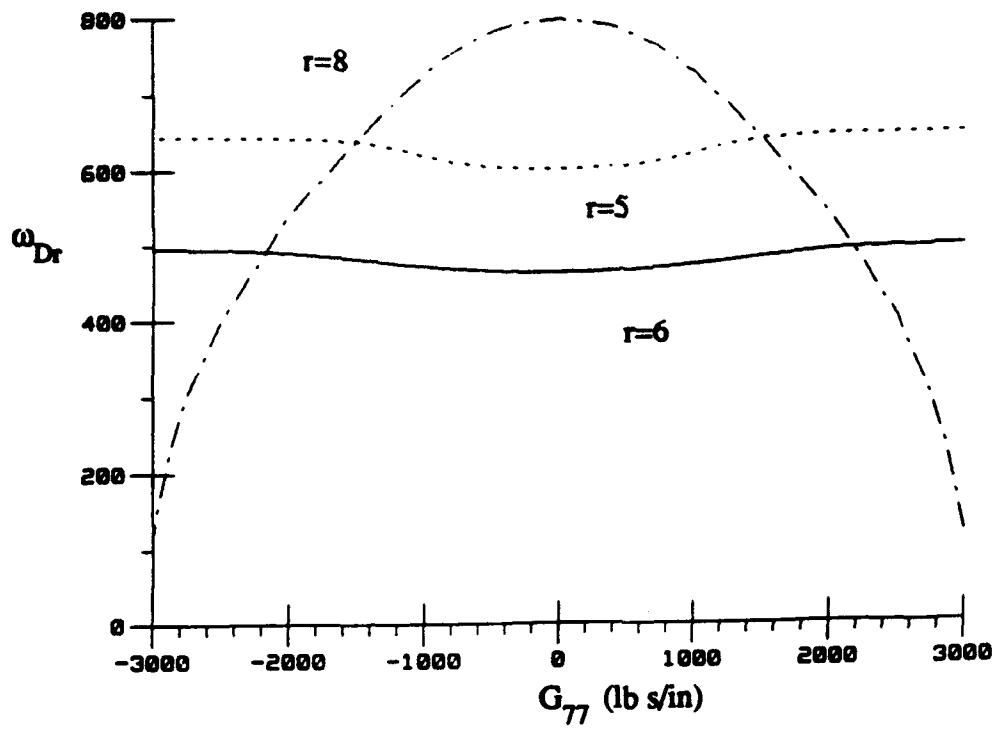


Fig. 3.6  $\omega_{D5}$ ,  $\omega_{D6}$ , and  $\omega_{D8}$  versus  $G_{77}$

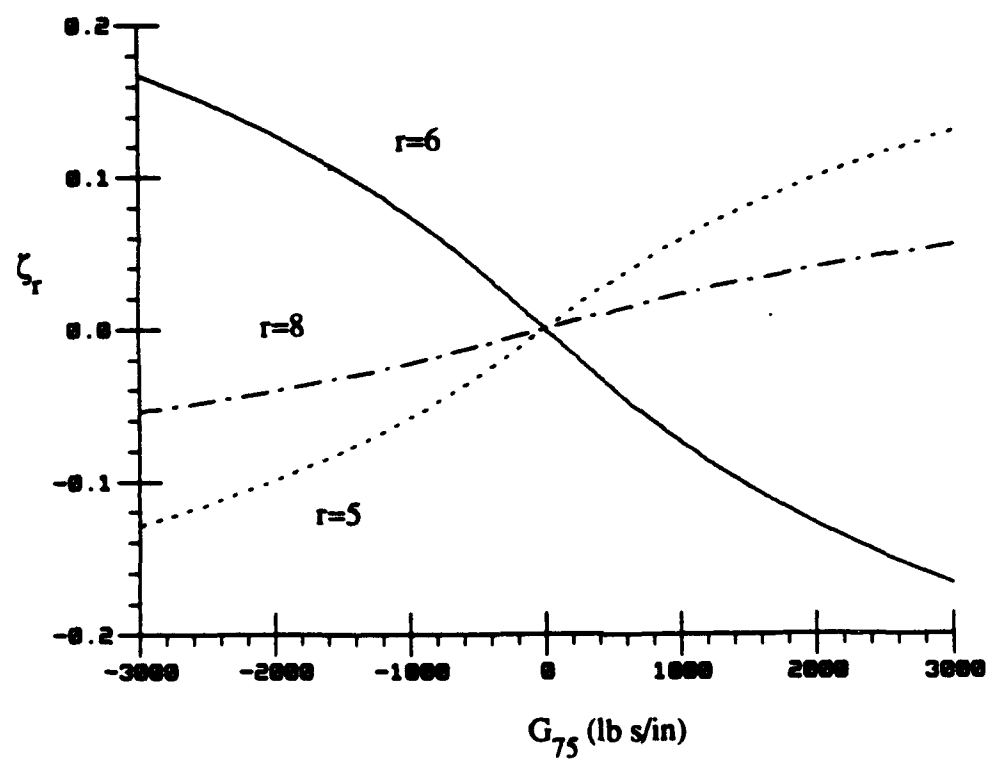


Fig. 3.7  $\zeta_5$ ,  $\zeta_6$ , and  $\zeta_8$  versus  $G_{75}$

It should be mentioned that it becomes difficult to trace the modes as the modal damping ratio increases. The mode numbers are here decided in association with small control forces. If the modes are ordered according to the magnitude of  $\omega_{Dr}$ , the damped natural frequency, then what was the eighth mode for small control forces becomes the first, or lowest frequency, mode for large control forces.

In Fig. 3.7, the damping ratios are plotted for an input control force for  $G_{75}$ . The sensitivities are not plotted, but are readily visualized as the slope of the  $\zeta_r$  curves. The  $\zeta_5$  and sensitivities are positive for positive  $G_{75}$  but  $\zeta_6$  shows a negative, decreasing trend in region. Thus the system is unstable if only the  $G_{75}$  control force is applied. If it is desired to increase the damping in modes 5 and 8 and decrease that in mode 6, then a positive  $G_{75}$  should be used. A negative  $G_{75}$  would produce the reverse effect. The effect of  $G_{57}$  on the modal damping ratios is similar to that of  $G_{75}$ .

The relationships between  $\zeta_r$  and  $G_{ii}$  or  $G_{ij}$  are nonlinear. The plots show a nearly linear range only for small control forces. These nonlinearities are due to changes in mode shapes. Large viscous damping or velocity-proportional control forces tend to stiffen the structure and change the mode shapes. The eigenvectors are, in general, complex and their sensitivities are readily calculated, as discussed in Section 3.2.

Because of the nonlinear behavior, the question arises as to how well the effects of  $G_{55}$ ,  $G_{75}$ ,  $G_{57}$ , and  $G_{77}$  superimpose. This is answered graphically in the plots in Fig. 3.8, where  $\zeta_6$  is shown for the four control forces applied simultaneously, with  $G_{55}$  and  $G_{77}$  positive but with  $G_{75}$  and  $G_{57}$  negative, to increase  $\zeta_6$ . For the dashed line, the separate effects were added, while for the solid line, the forces were applied simultaneously. It is clear that superposition applies for small control forces only. Note that the range of the control force on Fig. 3.8 is much smaller than on the previous figures. As the magnitude of the four control forces, applied simultaneously, approaches 3000 lb s/in, the value of  $\zeta_6=1.77$  and the damping ratios of all the other modes are less than 0.1, so mode 6 usurps the dissipation.

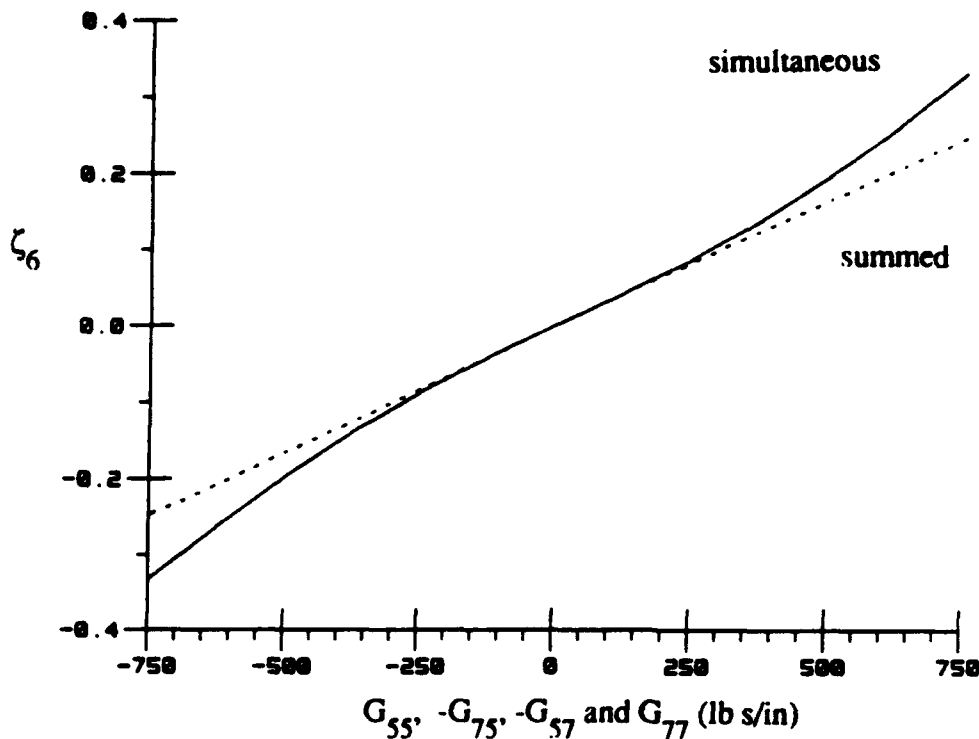


Fig. 3.8  $\zeta_6$  with effects of  $G_{55}$ ,  $-G_{75}$ ,  $-G_{57}$  and  $G_{77}$  applied simultaneously (solid) and superimposed (dashed)

#### Example 3.4 Effect of initial passive damping, ten-bar truss

Passive viscous damping, which is representable mathematically by dashpots connected in parallel to each truss member, tends to produce dissipation in every mode of vibration and the system is stable. If there is passive damping and only one active control force is added in an off-diagonal position, such as  $G_{18}$ , then the resulting motion can be stable or unstable, depending on the relative magnitudes of the passive and active forces. Using the ten-bar truss as an example, proportional damping was included by having a dashpot parallel to each truss member, so the  $C = \beta K$ , with  $\beta = 3.1623 \times 10^{-4}$  s. Then the value of  $G_{18}$  was varied from -200 to 200 lb/in s. The result is shown in Fig. 3.9 as a plot of  $\zeta_2$  and  $\zeta_4$  versus  $G_{18}$ . The damping ratios for the other six modes are not small, but they are affected little by  $G_{18}$ . The solid line is for the system with both viscous damping and the single control force. The dot-dash line represents the values when the viscous damping is zero and only the single control force is active. For the latter situation, the trace of  $C+G$  is zero, so  $\zeta_2$  and  $\zeta_4$  tend to have opposite signs and the system is unstable. When the passive damping is added, the curves shift upward and the system becomes more stable.

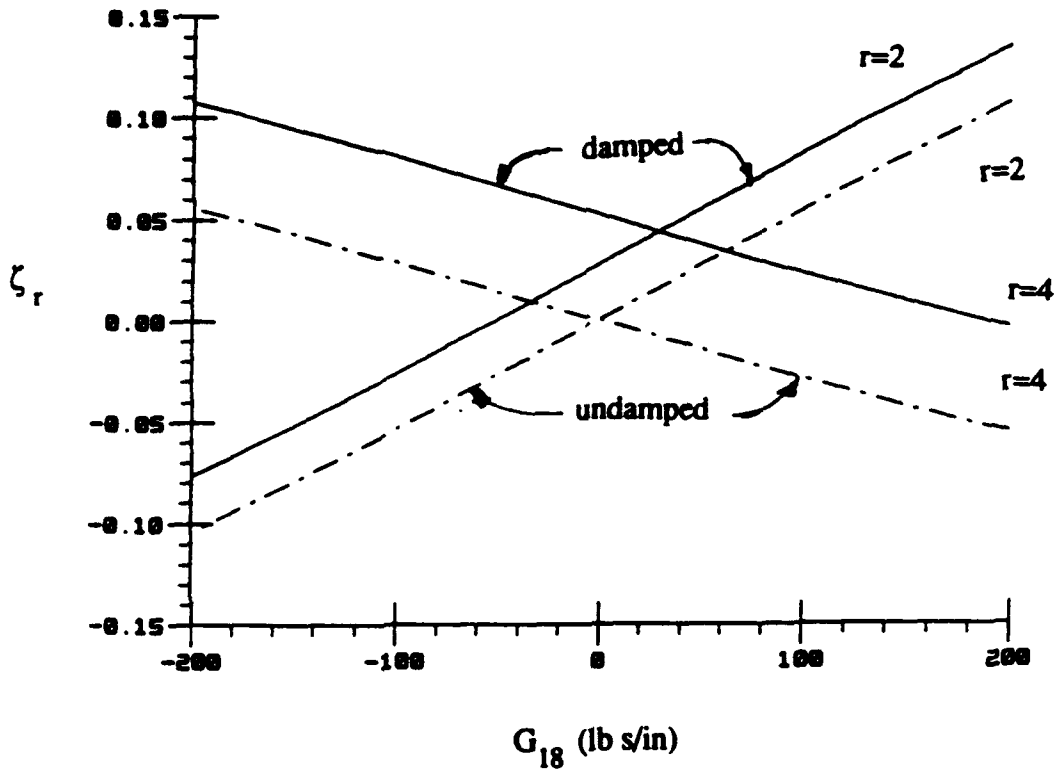


Fig. 3.9  $\zeta_2$  and  $\zeta_4$  versus  $G_{18}$  with and without proportional passive damping.

### 3.1.3 Summary and conclusions

1. The modal damping ratios,  $\zeta_r$ , are odd functions of the  $G_{ij}$ , so their sensitivities  $\partial\zeta_r/\partial G_{ij}$  are even functions. If there is no passive damping, the  $\zeta_r$  tend to be positive when the diagonal elements  $G_{ii}$  are positive. However, the  $\zeta_r$  can be positive or negative when the off-diagonal elements  $G_{ij}$  are positive.
2. The  $\zeta_r$  are nonlinear functions of the various  $G_{ij}$ . For small control forces, the relationship is nearly linear. The nonlinearity for larger  $G_{ij}$  is due to a changes in mode shapes.
3. In view of the changes in mode shapes, complex eigenvectors must be used and proportional damping cannot be assumed except for small  $\zeta_r$ .
4. The study emphasized the effects of individual elements  $G_{ij}$  in the G matrix. If combinations of the  $G_{ij}$  are used, corresponding to mutiple control forces, their individual effects superimpose accurately only for small control forces. This is because the changes in mode shapes for individual  $G_{ij}$  are not the same as for combinations of  $G_{ij}$ .
5. As has been well known previously, the addition of passive damping tends to have a stabilizing effect in combination with the types of control forces considered herein.

### 3.2 Sensitivity of the eigenvectors. .

The sensitivity of eigenvectors to changes in the plant matrices is of interest when modal solutions are used. Some of the instances where they are important are as follows:

1. In predicting changes in kinetic or potential energies, the modal derivatives appear explicitly.
2. When a perturbation technique is used for pole placement, it may be advantageous to predict the change in eigenvectors.
3. If proportional damping is assumed, then the corresponding assumption is that the mode shapes do not change. The eigenvectors derivatives indicate how much change, or error, is acceptable in the plant matrix parameters in order to be able to assume that changes in mode shape are negligible.

An important point is, even if mode shapes representing displacements do not change, the eigenvectors in State Space do change if the eigenvalues change. This is because the upper right vectors, for example, are equal to the lower vectors (the mode shapes) times the eigenvalue matrix, even for non-symmetric plant matrices.

#### 3.2.1 Sensitivity of the eigenvectors by the complete modal series method.

The eigenvector derivative  $\frac{\partial \mathbf{u}_i}{\partial a_{kl}}$  is written in short-hand as  $\mathbf{u}_{i,akl}$ . For the derivative of the  $i$ th vector, start by taking the derivative of  $[\mathbf{A} - \lambda_i \mathbf{I}] \mathbf{u}_i = \mathbf{0}$ .

$$[\mathbf{A} - \lambda_i \mathbf{I}] \mathbf{u}_{i,akl} + [\mathbf{A}_{,akl} - \lambda_{i,akl} \mathbf{I}] \mathbf{u}_i = \mathbf{0} \quad (3.37)$$

It is known that the derivative of the eigenvalue is found from

$$\lambda_{i,akl} = \mathbf{v}_i^T \mathbf{A}_{,akl} \mathbf{u}_i \quad (3.38)$$

It appears that the eigenvector derivative might be found by simply inverting the  $[\mathbf{A} - \lambda_i \mathbf{I}]$  matrix in Eq. (3.37), but that matrix is singular and cannot be inverted, so another approach must be found. Two possibilities are summarized. First, a common approach when working with eigenvectors is to represent a solution in terms of a weighted sum of the eigenvectors [P1], so that  $\mathbf{u}_{i,akl}$  is expressed as

$$\mathbf{u}_{i,akl} = \sum_{j=1}^{2n} \gamma_{ij} \mathbf{u}_j = \mathbf{U} \underline{\gamma}_i \quad (3.39)$$

The Eq. (3.39) requires that all the  $u_j$  be known. Substituting Eq. (3.39) into (3.37) gives

$$[A - \lambda_i I] \sum_{j=1}^{2n} \gamma_{ij} u_j + [A_{,ak/} - \lambda_i A_{,ak/} I] u_i = 0 \quad (3.40)$$

To solve for the  $\gamma_{ij}$ , pre-multiply Eq. (3.40) by  $v_n^T$  and make use of the relationships

$$v_n^T A u_j = 0 \quad n \neq j \quad (3.41a)$$

$$v_n^T A u_j = \lambda_j \quad n = j \quad (3.41b)$$

Thus, only the  $j$ th term in the series is non-zero, with the result

$$(\lambda_j - \lambda_i) \gamma_{ij} = v_n^T A_{,ak/} u_i \quad (3.42)$$

or

$$\gamma_{ij} = - \frac{v_j^T A_{,ak/} u_i}{(\lambda_j - \lambda_i)} \quad \text{for } i \neq j. \quad (3.43)$$

For  $i = j$ , the denominator of Eq. (3.43) goes to zero, so  $\gamma_{ii}$  must be found from a different equation.

It is interesting to repeat the derivation more efficiently by substituting the matrix representation of  $u_{i, ak/}$  of Eq. (3.39) into Eq. (3.37) and pre-multiply by  $V^T$ , the full matrix of left eigenvectors.

$$V^T [A - \lambda_i I] U \gamma_i = - V^T A_{,ak/} u_i \quad (3.44)$$

Now

$$V^T A U = \Lambda = \begin{bmatrix} \lambda_1 & & \\ & \lambda_2 & \\ & & \ddots \\ & & & \lambda_{2n} \end{bmatrix} \quad (3.45)$$

and suppose, for example, that  $i=2$ . Then Eq. (3.44) becomes

$$\begin{bmatrix} \lambda_1 - \lambda_2 & & \\ & \lambda_2 - \lambda_2 & \\ & & \ddots \\ & & & \lambda_{2n} - \lambda_2 \end{bmatrix} \begin{Bmatrix} \gamma_{21} \\ \gamma_{22} \\ \vdots \\ \gamma_{2n} \end{Bmatrix} = - V^T A_{,ak/} u_2 \quad (3.46)$$

and Eq. (3.43) follows.

To determine  $\gamma_{ii}$  we may use the normalizing condition

$$\begin{matrix} 1 \times 2n & 2n \times 2n & 2n \times 1 \\ u_i^T & M & u_i \end{matrix} = b_i \quad (3.47)$$

and take its derivative with respect to  $a_{k/}$ .

This gives 
$$\mathbf{u}_{i,ak}^T \mathbf{M} \mathbf{u}_i + \mathbf{u}_i^T \mathbf{M}_{,ak} \mathbf{u}_i + \mathbf{u}_i^T \mathbf{M} \mathbf{u}_{i,ak} = 0 \quad (3.48)$$

If  $\mathbf{M}$  is symmetric, the equation can be written

$$\mathbf{u}_i^T \mathbf{M}_{,ak} \mathbf{u}_i + 2 \mathbf{u}_i^T \mathbf{M} \mathbf{u}_{i,ak} = 0 \quad (3.49)$$

and the derivative of the vector is replaced by its series form

$$\mathbf{u}_i^T \mathbf{M}_{,ak} \mathbf{u}_i + 2 \mathbf{u}_i^T \mathbf{M} \sum_{j=1}^{2n} \gamma_{ij} \mathbf{u}_j = 0 \quad (3.50)$$

or 
$$\mathbf{u}_i^T \mathbf{M}_{,ak} \mathbf{u}_i + 2 b_i \gamma_{ii} + 2 \mathbf{u}_i^T \mathbf{M} \sum_{\substack{j=1 \\ j \neq i}}^{2n} \gamma_{ij} \mathbf{u}_j = 0 \quad (3.51)$$

yielding, finally, for  $\gamma_{ii}$ .

$$\gamma_{ii} = -\frac{1}{2 b_i} \left( 2 \mathbf{u}_i^T \mathbf{M} \sum_{\substack{j=1 \\ j \neq i}}^{2n} \gamma_{ij} \mathbf{u}_j + \mathbf{u}_i^T \mathbf{M}_{,ak} \mathbf{u}_i \right) \quad (3.52)$$

Having the  $\gamma_{ij}$ , the eigenvector derivative may be calculated from Eq. (3.39).

Before leaving this derivation, it is worthwhile to contemplate the expression in Eq. (3.47), namely,  $\mathbf{u}_i^T \mathbf{M} \mathbf{u}_i = b_i$ . One simplification would occur if the vectors were normalized so that  $b_i = 1$ . A benefit would also accrue from prudent choice of  $\mathbf{M}$ , such that  $\mathbf{u}_j^T \mathbf{M} \mathbf{u}_i = 0$ . For symmetric plant matrices, this would occur if  $\mathbf{M} = \mathbf{M}^*$

### 3.2.2 Eigenvalue sensitivity by Nelson's single mode approach.

The disadvantages of the complete series approach are that all the modal vectors must be known and summing them for each eigenvector derivative is tedious.

In developing Nelson's [N2] single mode approach, substitute Eq.(3.38) into (3.37) to obtain

$$\begin{aligned} [\mathbf{A} - \lambda_i \mathbf{I}] \mathbf{u}_{i,ak} &= -\mathbf{A}_{,ak} \mathbf{u}_i + [\mathbf{v}_i^T \mathbf{A}_{,ak} \mathbf{u}_i] \mathbf{u}_i \\ &= \mathbf{F}_i \end{aligned} \quad (3.53)$$

Rather than use a modal series to represent the solution, Nelson represented  $\mathbf{u}_{i,ak}$  as the sum of a homogeneous and a particular solution, namely

$$\mathbf{u}_{i,ak} = \mathbf{h}_i + \alpha_{ij} \mathbf{u}_j \quad (3.54)$$

The contribution of Nelson is that the vector  $\mathbf{h}_i$  may be calculated directly, without knowing the

remaining eigenvectors. Suppose that  $u_{i, ak/}$  is represented by

$$u_{i, ak/} = \begin{Bmatrix} h_1 \\ 0 \\ h_2 \end{Bmatrix} + \alpha_{ii} \begin{Bmatrix} u_1 \\ u_j \\ u_b \end{Bmatrix} \quad (3.55)$$

where the sub 1 and 2 just mean portions of the vectors  $h_i$  and  $u_i$ . Then, the special form of the vector  $h_i$  is solved for by zeroing out the  $j$ th row and column of the  $[A - \lambda_i I]$  matrix. Since the rank of the reduced  $[A - \lambda_i I]$  must be  $2n-1$ , the remaining  $(2n-1) \times (2n-1)$  matrix may be inverted. The appearance of the partitioned matrices is as follows,

$$\begin{bmatrix} [A - \lambda_i I]_{11} & 0 & A_{13} \\ 0 & 1 & 0 \\ A_{31} & 0 & [A - \lambda_i I]_{33} \end{bmatrix} \begin{Bmatrix} h_1 \\ h_j \\ h_2 \end{Bmatrix} = \begin{Bmatrix} F_1 \\ 0 \\ F_2 \end{Bmatrix} \quad (3.56)$$

which is easy to program on the computer. By inserting the digit 1 in location  $jj$  on the main diagonal of the matrix on the left, the matrix is restored to size  $2n \times 2n$  and  $h_j = 0$  is assured by zeroing the  $F$  vector in the same row. The choice of which vector to designate as the  $j$ th row is arbitrary, but to avoid numerical difficulties Nelson suggested finding the row where the components of the vectors  $u_i$  and  $v_i$  are large by investigating the products of the absolute values  $\text{abs}(u_{ji}) \text{abs}(v_{ji})$ .

The  $\alpha_{ii}$  is found from the normalizing condition, Eq.(3.11), after taking the derivative as in Eq. (3.49) above

$$u_i^T M_{,ak/} u_i + 2 u_i^T M u_{i,ak/} = 0 \quad (3.49)$$

$$u_i^T M_{,ak/} u_i + 2 u_i^T M [h_i + \alpha_{ii} u_i] = 0 \quad (3.57)$$

so

$$\alpha_{ii} = -\frac{1}{2b_i} \left( u_i^T M_{,ak/} u_i + 2 u_i^T M h_i \right) \quad (3.58)$$

Here a simplification will result if  $M$  is chosen such that  $M_{,ak/} = 0$ .

### 3.2.3 Relationships between the complete series approach and the single mode method.

In using the complete series representation, from Eq. (3.39), the eigenvector derivative is given by

$$\mathbf{u}_{i, ak/} = \sum_{j=1}^{2n} \gamma_{ij} \mathbf{u}_j = \mathbf{U} \underline{\gamma}_i \quad (3.39)$$

By Nelson's single mode approach, the derivative is given by Eq. (3.45)

$$\mathbf{u}_{i, ak/} = \mathbf{h}_i + \alpha_{ii} \mathbf{u}_i \quad (3.45)$$

It is possible to represent  $\mathbf{h}_i$  as a series summation of all the modal vectors, weighted by a factor  $\eta_{ij}$ , as

$$\mathbf{u}_{i, ak/} = \sum_{j=1}^{2n} \eta_{ij} \mathbf{u}_j + \alpha_{ii} \mathbf{u}_i \quad (3.59)$$

It follows that the series coefficients are related by

$$\gamma_{ij} = \eta_{ij} \quad \text{for } i \neq j \quad (3.60a)$$

$$\gamma_{ii} = \eta_{ii} + \alpha_{ii} \quad \text{for } i = j. \quad (3.60b)$$

### Example 3.5. Eigenvector sensitivity by the complete series approach

The matrices in this example are given in state space form.

$$\mathbf{M}^* = \begin{bmatrix} 1 & 0 & 0 & 0 \\ 0 & 2 & 0 & 0 \\ 0 & 0 & -5 & 4 \\ 0 & 0 & 4 & -4 \end{bmatrix} \quad \mathbf{K}^* = \begin{bmatrix} 0 & 0 & 5 & -4 \\ 0 & 0 & -4 & 4 \\ 5 & -4 & 0 & 0 \\ -4 & 4 & 0 & 0 \end{bmatrix} \quad (3.61)$$

so

$$\mathbf{A} = [\mathbf{M}^*]^{-1} \mathbf{K}^* = \begin{bmatrix} 0 & 0 & -5 & 4 \\ 0 & 0 & 2 & -2 \\ 1 & 0 & 0 & 0 \\ 0 & 1 & 0 & 0 \end{bmatrix} \quad (3.62)$$

The right eigenvectors were normalized according to  $\mathbf{U}^T \mathbf{M}^* \mathbf{U} = \mathbf{I}$ . The sensitivities calculated are those of the right eigenvectors with respect to  $\mathbf{A}_{12}$  or  $\mathbf{u}_{,a12}$ . The right eigenvectors are:

$$\mathbf{U} = \begin{bmatrix} -0.3645 & -0.3645 & -0.6059 & -0.6059 \\ -0.4284 & -0.4284 & 0.2577 & 0.2577 \\ 0.6672 i & -0.6672 i & 0.2341 i & -0.2341 i \\ 0.7843 i & -0.7843 i & -0.0996 i & 0.0996 i \end{bmatrix} \quad (3.63)$$

The eigenvalues are  $\lambda_1, \lambda_2 = \pm 0.5463 i$ ;  $\lambda_3, \lambda_4 = \pm 2.5887 i$ .

The sensitivities  $\lambda_{1,a12} = 0.1562$   $\lambda_{2,a12} = -0.1562$   $\lambda_{3,a12} = -0.1562$   $\lambda_{4,a12} = 0.1562$

The values of  $\gamma_{ij}$  are listed in matrix form, their subscripts determining their position in the matrix.

$$[\gamma_{ij}] = - \begin{bmatrix} 0 & 0.1429 i & -0.1271 i & 0.0828 i \\ -0.1429 i & 0 & -0.0828 i & 0.1271 i \\ -0.0460 i & -0.0300 i & 0 & -0.0302 i \\ 0.0300 i & 0.0460 i & 0.0302 i & 0 \end{bmatrix} \quad (3.64)$$

The partial derivatives of the right vectors are arranged in columns

$$\mathbf{u}_{,a12} = \frac{\partial \mathbf{u}_i}{\partial \mathbf{A}_{12}} = - \begin{bmatrix} -0.0253 i & 0.0253 i & 0.0460 i & -0.0460 i \\ -0.0727 i & 0.0727 i & 0.0248 i & -0.0248 i \\ 0.1445 & 0.0145 & 0.0036 & 0.0036 \\ 0.0912 & 0.0912 & 0.0156 & 0.0156 \end{bmatrix} \quad (3.65)$$

**Example 3.6 Eigenvector sensitivity by the single mode approach.**

The plant matrices and the eigenvectors are the same as in Example 1. The matrices for finding the  $u_{1,a12}$  are.

$$F_1 = -A_{a12} u_1 + [v_1^T A_{a12} u_1] u_1 = \begin{Bmatrix} 0.3715 \\ -0.0669 \\ 0.1042 i \\ 0.1225 i \end{Bmatrix} \quad (3.66)$$

The  $[A - \lambda_1 I]$  matrix, after modification of the third row and third column is

$$\text{Modified } [A - \lambda_1 I] = \begin{bmatrix} -0.5463 i & 0 & 0 & 4 \\ 0 & -0.5463 i & 0 & -2 \\ 0 & 0 & 1 & 0 \\ 0 & 1 & 0 & 0 \end{bmatrix} \quad (3.67)$$

$$\text{Modified } F_1 = \begin{Bmatrix} 0.3715 \\ -0.0669 \\ 0 \\ 0.1225 i \end{Bmatrix} \quad (3.68)$$

Now the matrix  $h_1$  is found by multiplying the inverse of the modified  $[A - \lambda_1 I]$  matrix times the modified  $F_1$  matrix.

$$\text{Thus } h_1 = \begin{Bmatrix} 0.1042 i \\ 0.1654 i \\ 0 \\ 0.0786 \end{Bmatrix} \quad (3.69)$$

Since  $M_{a12} = 0$  and  $b_1 = 1.0$

$$\alpha_{11} = -u_1^T M^* h_1 = 0.2166 i \quad (3.70)$$

$$\text{and } u_{i,a12} = h_1 + \alpha_{11} u_1 = \begin{Bmatrix} 0.0253 i \\ 0.0727 i \\ -0.1445 \\ -0.0912 \end{Bmatrix} \quad (3.71)$$

which agrees with the first column in the Eq. (3.65) above, obtained by the complete series method.

## 4. OPTIMIZATION OF PASSIVE DAMPING

### 4.1 Optimization of viscous damping.

#### 4.1.1 Achieving uniform modal decay rates for free vibration problems.

In the present context, passive viscous damping is that representable by dashpots, which may be connected to ground or between two points on a structure.

$$\mathbf{M} \ddot{\mathbf{z}} + \mathbf{C} \dot{\mathbf{z}} + \mathbf{K} \mathbf{z} = \mathbf{0} \quad (4.1)$$

In free vibration problems, it is sometimes desirable for the motion of each mode to decay at the same rate. This may be achieved with mass-proportional damping, such that  $\mathbf{C} = 2 \alpha \mathbf{M}$ . The displacements are represented in terms of modal coordinates.

$$\mathbf{z}(t) = \Phi \mathbf{q}(t) \quad (4.2)$$

Then, if  $\Phi^T \mathbf{M} \Phi = \mathbf{I}$ , the product  $\Phi^T \mathbf{C} \Phi = \alpha \mathbf{I}$  and a typical equation for the  $r$ th mode is

$$\ddot{q}_r + 2 \alpha \dot{q}_r + \omega_r^2 q_r = 0. \quad (4.3)$$

The eigenvalues are

$$\lambda_r, \bar{\lambda}_r = -\alpha \pm i \sqrt{\omega_r^2 - \alpha^2} = -\alpha \pm i \omega_D \quad (4.4)$$

so the decay rate is the same in each mode.

If the mass matrix is diagonal, of size  $n \times n$ , then  $n$  dashpots are theoretically required. If the system is three-dimensional, a dashpot is required at each mass in each direction, and one end must be connected to an effective ground. Thus achieving mass-proportional damping may not always be practical.

For stiffness-proportional damping,  $\mathbf{C} = \beta \mathbf{K}$  and  $\Phi^T \mathbf{C} \Phi = \beta [\omega_r^2]^D$  and the decoupled equations are of the form

$$\ddot{q}_r + \beta \omega_r^2 \dot{q}_r + \omega_r^2 q_r = 0.$$

The standard form of the decoupled equations in terms of the modal damping ratio  $\zeta_r$  is

$$\ddot{q}_r + 2 \zeta_r \omega_r \dot{q}_r + \omega_r^2 q_r = 0. \quad (4.5)$$

so the equivalent modal damping ratio is found from

$$2 \zeta_r \omega_r = \beta \omega_r^2$$

which shows that the higher modes decay fastest, unless the  $\zeta_r$  are designed so they decrease with frequency. Practically, stiffness-proportional damping may be easier to achieve than mass-proportional damping because mechanical devices can be connected between nodes, rather than to ground. But then active control may need to be added to provide sufficient dissipation in the lower frequency modes.

#### 4.1.2 Critical damping for matrix equations

The idea of a critical damping matrix was presented by Inman and Andry [I2] in 1980. Usually the mass matrix  $\mathbf{M}$  and the stiffness matrix  $\mathbf{K}$  are positive definite, although  $\mathbf{K}$  may be positive semi-definite for a free structure which possesses rigid body modes.

Now change variables by letting  $\mathbf{x} = \mathbf{M}^{1/2} \mathbf{z}$ .

$$\ddot{\mathbf{x}} + \mathbf{M}^{-1/2} \mathbf{C} \mathbf{M}^{-1/2} \dot{\mathbf{x}} + \mathbf{M}^{-1/2} \mathbf{K} \mathbf{M}^{-1/2} \mathbf{x} = \mathbf{0} \quad (4.6a)$$

$$\ddot{\mathbf{x}} + \mathbf{C}_1 \dot{\mathbf{x}} + \mathbf{K}_1 \mathbf{x} = \mathbf{0} \quad (4.6b)$$

Now critical damping is defined in reference [I3] as  $\mathbf{C}_1 = 2 \mathbf{K}_1^{1/2}$ .

The following cases are then possible:

1. If  $\mathbf{C}_1 = \tilde{\mathbf{C}}_1$  the system is critically damped and each eigenvalue is a repeated negative real number. All the eigenvectors are real.
2. If  $\mathbf{C}_1 - \tilde{\mathbf{C}}_1$  is positive definite then the system is overdamped and each eigenvalue is a negative real number. All the eigenvectors are real.
3. If  $\mathbf{C}_1 - \tilde{\mathbf{C}}_1$  is negative definite then the system is underdamped and the eigenvalues occur in complex conjugate pairs, each with a negative real part.
4. If  $\mathbf{C}_1 - \tilde{\mathbf{C}}_1$  is indefinite or sign variable, then mixed damping occurs. At least one mode will be overdamped and at least one mode will be underdamped.

Related references and concepts were summarized in the paper by Liang, Tong, and Lee [L1] who give definitions for strongly complex and weakly complex eigenvectors. Caughey and O'Kelly [C2] gave a necessary and sufficient condition for decoupling of the Eqs. (4.6).

### 4.1.3 Optimization of modal damping ratios, ten-bar truss example.

#### 4.1.3.1 Formulation of the optimization problem.

In a practical truss, bars are connected at pinned joints. The viscous damping force  $F_j$  on pin  $j$  may be  $F_j = C_m (\dot{z}_j - \dot{z}_{j+1})$  if the dashpot is between stations  $j$  and  $j+1$ . If the dashpot is connected between station  $j$  and ground, then  $F_j = C_m \dot{z}_j$ . It is expensive to connect damping devices between each pair of nodes. So the questions to be addressed are:

1. Which modal damping ratios are to be maximized?
2. If a limited number of dashpots are to be used, where should they be connected on the structure?
3. Once the best locations are determined, how much damping should be used at each location?

For the underdamped situation, the complex eigen pairs are written as in Eq. (4.7), with  $\zeta_i$  modal damping ratio.

$$\lambda_i, \bar{\lambda}_i = -\zeta_i \omega_i \pm j \omega_i \sqrt{1 - \zeta_i^2} \quad (4.7)$$

The optimization problem is specified by defining appropriate objective functions. Suppose it is desired to maximize the damping ratios of certain modes. Then the objective function, OBJ, could be specified as

$$\text{OBJ} = \sum_i \alpha_i \zeta_i \quad (4.8)$$

where the  $\alpha_i$  are arbitrary weighting factors to be chosen as positive real numbers or zero. In addition a bound is put on the total amount of damping to be used. This is done by defining a constraint function  $G(1)$ , using weighting factors  $\gamma_m$  and  $C_m$  as the viscous dashpot constants.

$$G(1) = \sum_m \gamma_m C_m - C_T \leq 0.0 \quad (4.9)$$

#### 4.1.3.2 Natural frequencies and mode shapes for proportional damping.

The ten-bar truss of interest lies in the x-y plane as shown in Fig. 3.1, page 23 . The connections are assumed to be frictionless pins. The nodes 5 and 6 are anchored and the other four nodes are free to move, with x and y components of motion. The bar numbers are in brackets. The bar material is aluminum with  $E_m = 10 \times 10^6$  psi for each bar. The dashpots are not shown, but each dashpot is connected between the same two nodes as a parallel bar, with the same element number, so  $C_m$  is connected parallel to bar m. The axial stiffness of each bar is

$K_m = \frac{A_m E}{L_m}$ . The bar cross-sectional areas are listed in Table 4.1. The truss was originally designed to carry heavy vertical loads at nodes 2 and 4 . Consequently, the bars 2, 5, 6 and 10 have a much smaller cross-sectional area than the other six bars. The truss bays are square, 360 inches on each side.

The stiffness-proportional dashpot constant is arbitrarily defined as  $C_m = \frac{\beta_m K_m}{\sqrt{E}}$ , where  $\beta_m$  is a factor to be chosen. If  $\beta_m$  is a constant, then the damping is stiffness proportional. For the first example, all  $\beta_m = 1.0$  . The mass matrix is diagonal, with half the mass of each bar lumped at the node at each bar end. The damping ratios and natural frequencies for this situation are given in Table 4.2. The damping factors for the higher modes are the largest. The natural frequencies range from 131.13 to 796.21 rad/s and are well separated.

The mode shapes for zero damping, or for proportional damping, are shown in Figs. 4.1. For modes 1 and 3, the shapes are somewhat like lateral bending modes of the entire truss. For the higher frequency modes, the stretching of the lighter bars, namely bars 2, 6 and 10, dominates the motion.

Table 4.1 Member areas, lengths, stiffnesses, and damping factors for  $\beta_m = 1.0$  .

m	$A_m$ (in <sup>2</sup> )	$L_m$ (in)	$K_m$ (lb/in)	$C_m$ (lb-s/in)
1	31.5	360.000	875 000	276.699 30
2	0.1	360.000	2 778	0.878 41
3	23.0	360.000	638 889	202.034 41
4	15.5	360.000	430 556	136.153 62
5	0.1	360.000	2 778	0.878 41
6	0.5	360.000	13 890	4.392 05
7	7.5	509.117	147 314	46.584 75
8	20.5	509.117	402 658	127.331 65
9	21.0	509.117	412 479	130.437 30
10	0.1	509.117	1 964	0.621 13

**Table 4.2 Damped modal damping ratios and natural frequencies for  $\beta_m = 1.0$ .**

$i$	$\zeta_i$	$\omega_i$ (rad/s)
1	0.0207 3350	131.1301
2	0.0274 1571	173.3921
3	0.0426 4408	269.7048
4	0.0515 5221	326.0448
5	0.0730 5049	462.0119
6	0.0948 6770	599.9960
7	0.1051 3561	664.9360
8	0.1258 9253	796.2143

#### 4.1.3.3 Sensitivities of modal damping ratios and natural frequencies.

The first derivatives,  $\partial \zeta_i / \partial C_m$  were calculated by the methods of section 3.1.2, after determining the derivatives of each eigenvalue  $\partial \lambda_i / \partial C_m$  and its complex conjugate  $\partial \bar{\lambda}_i / \partial C_m$ . The derivatives of the damping ratios are tabulated in Table 4.3. There are 80 entries in the table, since there are 8 modes and 10 bars. The total of each row and column is also given and the sub-totals add to an overall total of 10.27867. There is a big variation in the magnitudes of the sensitivities, which is the reason for listing values to six decimal places. The list of dashpot locations in order of sensitivities is 2, 10, 6, 5, 4, 9, 3, 8, 1, 7. By bar stiffness, from smallest to the largest, the order is 10, 2, 5, 6, 7, 8, 9, 4, 3, 1. Thus, there is a direct correlation between sensitivities and stiffnesses, with largest sensitivities going with dashpots parallel to bars with lowest stiffnesses. Location 7 seems to be most out of order, but notice that there are two negative values in the column for bar 7. In a ranking of potential effectiveness according to the absolute sum of the columns, the value for dashpot 7 would be 0.037637 and it would precede dashpot 3 in the sensitivity list.

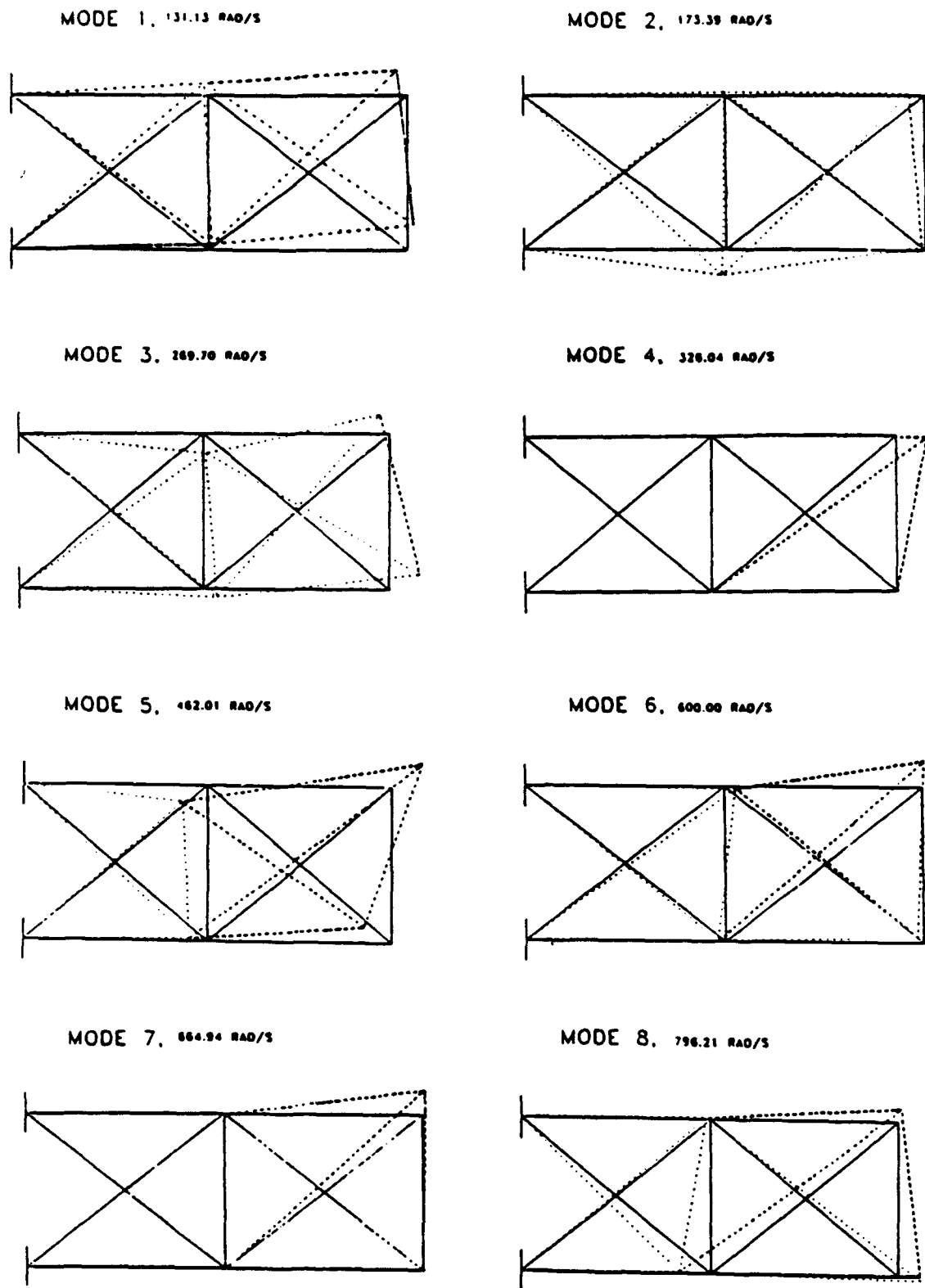


Fig. 4.1 Mode shapes of the undamped ten-bar truss.

Table 4.3 Sensitivities  $\frac{\partial \zeta_i}{\partial C_m} \times 10^2$  at  $\beta_m = 1.0$ .

i	m=1	m=2	m=3	m=4	m=5	m=6
1	0.002 025	0.004 389	0.000 900	0.001 138	0.007 674	0.000 035
2	0.000 197	0.021 051	0.001 518	0.000 001	0.154 036	0.000 238
3	0.000 180	0.004 650	0.005 255	0.010 230	0.006 373	0.000 355
4	0.000 054	4.336 100	0.000 037	0.000 021	0.000 486	0.000 238
5	0.008 992	0.045 043	0.004 783	0.001 471	0.007 432	0.001 360
6	0.011 616	0.009 531	0.005 680	0.000 325	0.000 890	0.069 406
7	0.000 203	0.018 862	0.000 531	0.000 367	0.000 079	2.122 320
8	<u>0.007 902</u>	<u>0.000 946</u>	<u>0.017 544</u>	<u>0.051 749</u>	<u>0.000 016</u>	<u>0.007 902</u>
	0.023 581	4.440 572	0.036 248	0.065 302	0.176 986	2.234 647

i	m=7	m=8	m=9	m=10	All m
1	-0.001 810	0.006 954	0.001 747	0.007 211	0.030 263
2	-0.012 466	0.000 762	0.000 059	0.029 303	0.194 699
3	0.006 633	0.007 399	0.001 391	0.045 729	0.045 729
4	0.000 104	0.000 117	0.000 000	1.853 090	6.223 040
5	0.003 230	0.014 265	0.012 294	0.039 581	0.138 451
6	0.003 364	0.003 603	0.031 427	0.081 899	0.217 741
7	0.000 344	0.000 039	0.001 667	1.164 520	3.308 932
8	<u>0.009 686</u>	<u>0.000 024</u>	<u>0.010 797</u>	<u>0.020 834</u>	<u>0.119 812</u>
	0.009 085	0.033 163	0.061 254	3.197 829	10.278 67

#### 4.1.3.4 Modal usurping of damping; variation of $\zeta_5$ and $\zeta_6$ with $C_1$ .

As the values of  $C_m$  are increased and the damping becomes nonproportional, the mode shapes change and the eigenvectors become complex numbers, so the eigenvalue derivatives change. The variation of  $\zeta_5$  and  $\zeta_6$  with  $C_1$  is shown in Fig. 4.2. All the other  $C_m$  were taken as zero. The plot shows that for  $0 \leq C_1 \leq 3$ , both  $\zeta_5$  and  $\zeta_6$  increase almost monotonically. However, for  $C_1 > 3$ , the rate of increase of  $\zeta_6$  becomes larger while that of  $\zeta_5$  decreases. The slopes of these lines, which are the sensitivities, are plotted in Fig. 4.3, where it is seen that  $\partial \zeta_5 / \partial C_1$  changes sign and finally approaches zero as  $C_1$  increases. So mode 6 usurps the increased damping and mode 5 damping approaches zero, because of changes in mode shapes.

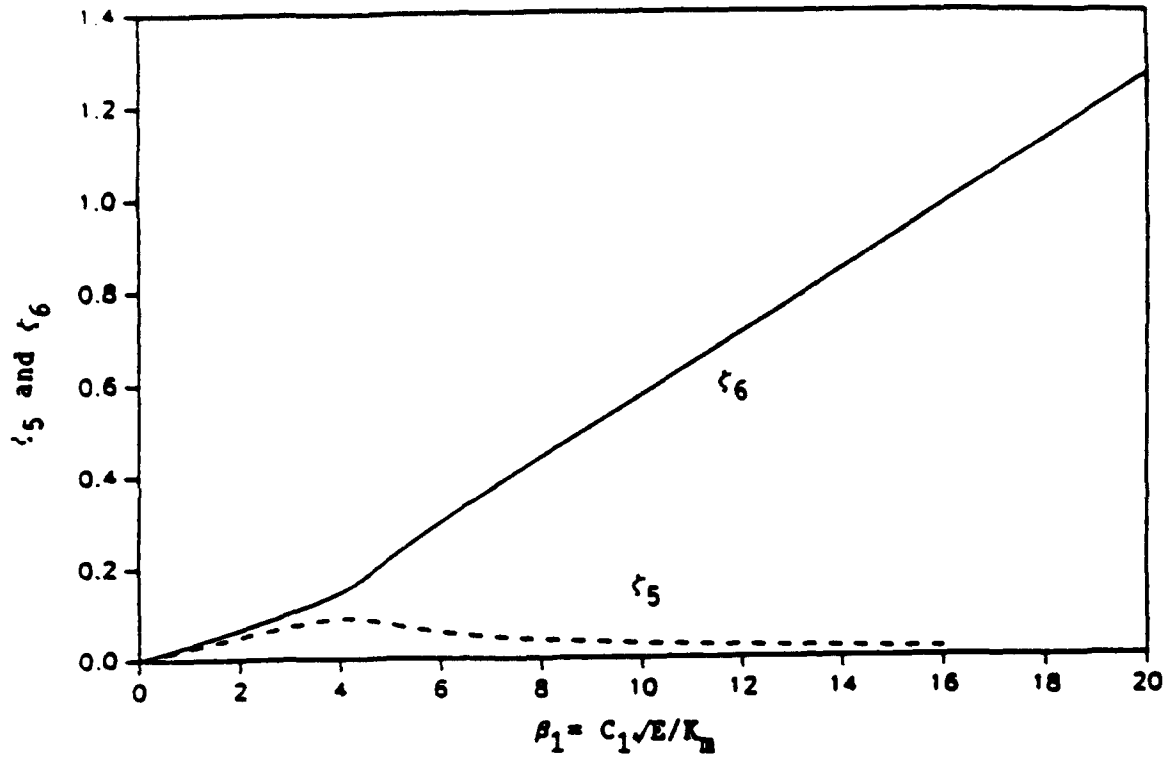


Fig. 4.2 Variation of  $\zeta_5$  and  $\zeta_6$  with  $C_1$ .

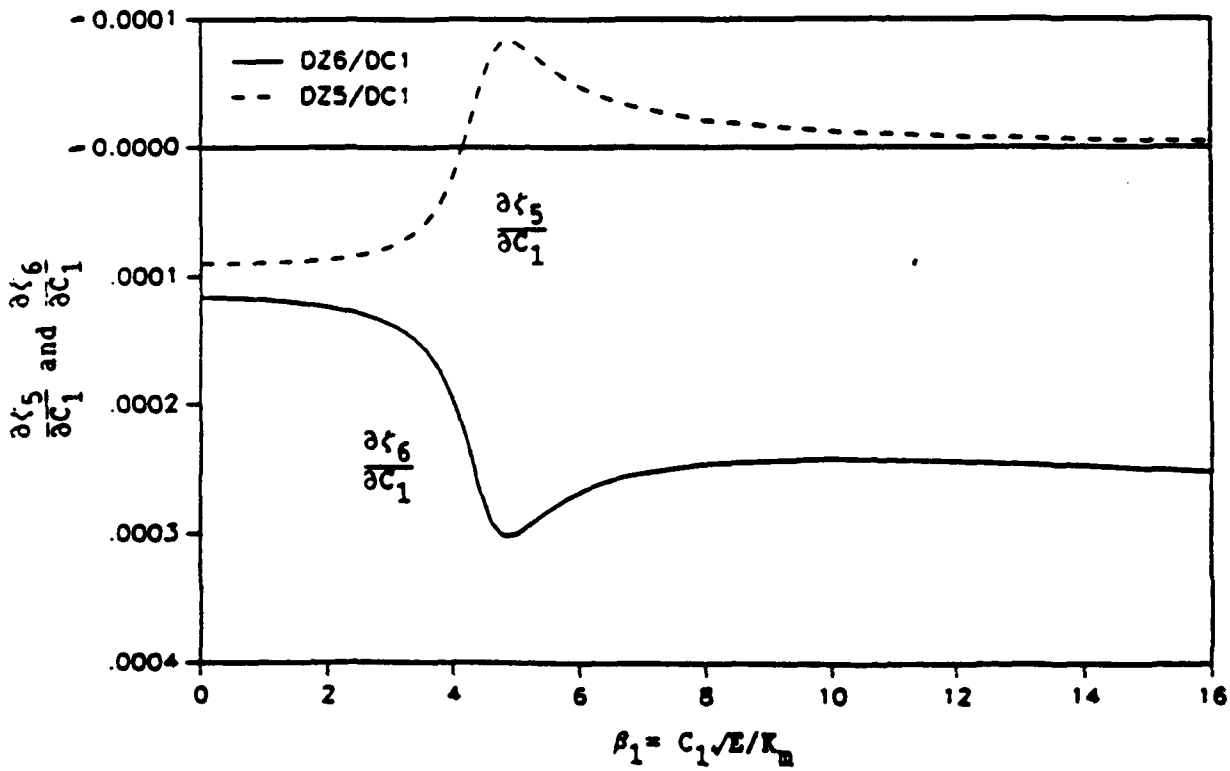


Fig. 4.3  $\frac{\partial \zeta_5}{\partial C_1}$  and  $\frac{\partial \zeta_6}{\partial C_1}$ .

#### 4.1.3.5 Optimization of $\zeta_3$ with respect to $C_3$ and $C_4$ .

Now we return to the optimization problem stated at the beginning of this chapter. The goal is to optimize the damping ratio of mode 3 by placing dashpots parallel to bars 3 and 4, which are horizontal members at the bottom of the truss. The table of sensitivities shows us that the  $\zeta_3$  is quite sensitive to dashpots placed in these positions.

The objective function is taken as  $\zeta_3$  with the design variables  $C_3$  and  $C_4$  in the constraint function  $G(1)$ .

$$\text{OBJ} = \zeta_3$$

$$G(1) = C_3 + C_4 - C_T \leq 0.0$$

An advantage to limiting the design variables to two is that a two-dimensional plot can be shown of the interaction between  $\zeta_3$  and the two design variables. Contours for  $\zeta_3 = 0.05, 0.10, 0.15$  and  $0.20$  are shown in Fig. 4.4. The straight lines are constraint lines which were chosen to be approximately tangent to the given contour lines. Thus each constraint line corresponds to a different value of  $C_T$  in  $G(1)$ . The slopes would be  $-45^\circ$  if the vertical and horizontal scales were equal. Since the contour lines are convex toward the feasible region, the optimum solution, which maximizes  $\zeta_3$ , will be along the constraint boundary line.

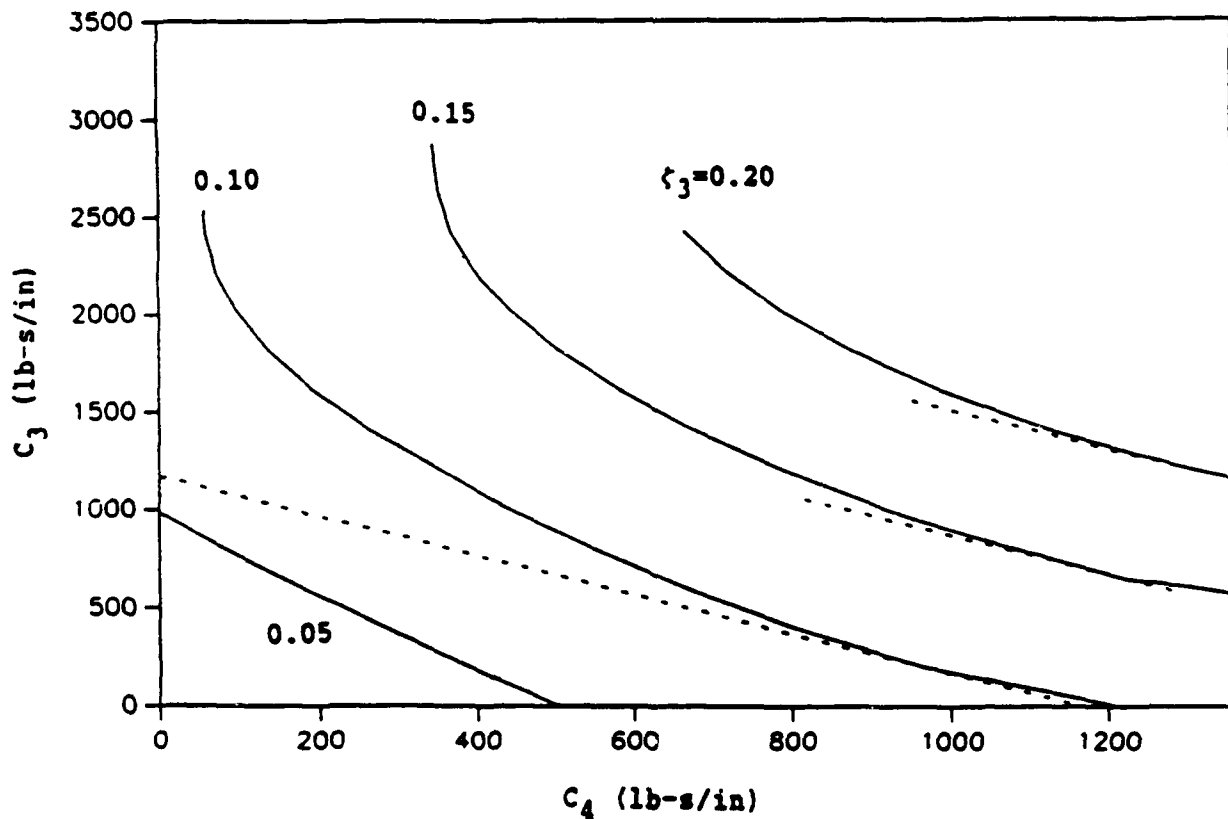


Fig. 4.4 Variation of  $\zeta_3$  with  $C_3$  and  $C_4$ .

The results are summarized in Table 4.4 for three values of  $C_T$ , namely  $C_T = 1157.3$ , 1838.5 and 2525.4 lb-s/in. The associated values of optimum  $\zeta_3$  are close to 0.10, 0.15 and 0.20. It is interesting to note that, even though the increments in  $\zeta_3$  are constant at 0.05, the corresponding increments in  $C_3$  and  $C_4$  are not constant, indicating the nonlinear nature of the optimization problem.

Table 4.4 Optimum values of  $\zeta_3$  with  $C_3$  and  $C_4$  the design variables.

$C_3$	$C_4$	$\zeta_3$	$C_T$
160.928	996.373	0.0994 46	1157.301
719.330	1119.184	0.1470 48	1838.514
1240.957	1284.475	0.2015 59	2525.432

## 4.2 Representation and optimization of viscoelastic damping in structures.

### 4.2.1 Fitting curves to data for complex moduli of viscoelastic damping materials.

A great deal of data exists, in chart form, for the Young's Modulus and loss factor of commercially available materials that are used for damping structural vibrations. Typically all the data is presented in one nomograph as a function of frequency, reduced frequency and temperatures. It is more convenient to represent the data in equation form, using only three short equations and seven parameters for each material.

The basic equations are not new, but a method of fitting is suggested which is better than currently used in the outside literature. A step-by-step procedure is outlined for finding the seven parameters. As an example, specific values are given for the parameters for Soundcoat 601, which has a transition temperatures of 75° F. In reference [N7], curve-fitting is also done for Soundcoat 606 and 609, which have transition temperatures of 125 and 175° respectively. The fit obtained is demonstrated in plots of Young's modulus  $E$ , loss factor  $\eta$ , and loss modulus  $E\eta$  which compare the fitted curves with experimental data which was supplied by the manufacturer.

#### List of Symbols

$\alpha_T$	=	Shift factor depending on temperature $T$
$\beta$	=	Used for initial frequency shift at $T=T_0$ .
$C_1$	=	Constant in equation for $\alpha_T$ .
$E_u$	=	Maximum value of $E$ , occurring at high frequencies
$E_l$	=	Minimum value of $E$ , occurring at low frequencies
$E(\omega, T)$	=	Real part of Young's Modulus
$E^*(\omega, T)$	=	Complex modulus = $E(\omega, T) [1 + j \eta(\omega, T)]$
$E(\omega, T)\eta(\omega, T)$	=	Loss modulus
$f$	=	$\omega/2\pi$ = frequency (Hz).
$n$	=	Shape and magnitude parameter for $E(\omega, T)$ and $\eta(\omega, T)$
$\eta(\omega, T)$	=	Loss factor
$T$	=	Variable temperature
$T_0$	=	Transition temperature for material
$T_\infty$	=	Temperature parameter in equation for $\alpha_T$ .
	=	Frequency (rad/s).

#### 4.2.1.1 Equations and parameters

There are three basic equations for the curve fitting, as given in Ref. [N1] . They are expressions for the Young's Modulus  $E(\omega,T)$ , the loss factor  $\eta(\omega,T)$ , and the temperature shift factor  $\alpha_T$  .

$$E(\omega,T) = E_l + E_u \left[ 1 - \frac{1}{1 + (\beta\omega\alpha_T)^n} \right] \quad (4.10)$$

$$\eta(\omega,T) = \frac{n \pi E_u (\beta\omega\alpha_T)^n}{2 E(\omega,T) [1 + (\beta\omega\alpha_T)^n]^2} \quad (4.11)$$

$$\log \alpha_T = \frac{C_1(T-T_0)}{(T-T_\infty)} \quad (4.12)$$

There are seven parameters involved, namely  $E_l$ ,  $E_u$ ,  $C_1$ ,  $T_0$ ,  $T_\infty$ ,  $\beta$  and  $n$ . It can be seen in Eq. (4.10) that the vertical position of the  $E(\omega,T)$  curve is controlled by  $E_l$  and  $E_u$ . Further, when  $\omega=0$ ,  $E(\omega,T) = E_l$  and when  $\omega$  is large,  $E(\omega,T) = E_u$ . The shape of the curves and also the magnitude of  $\eta(\omega,T)$  are directly controlled by  $n$ . The  $\alpha_T$  and  $\beta$  are factors of frequency  $\omega$  and have the effect of shifting the curves.

Note that when  $T = T_0$  the value  $\alpha_T=1$ , so there is no temperature shift. The temperature  $T_0$  is called the transition temperature of the material and the maximum value of  $\eta(\omega,T)$  usually occurs near that temperature. Thus the  $\beta$  may be used to locate the  $E(\omega,T)$  in the correct lateral position on a frequency scale, when  $T=T_0$ . Then at other temperatures, the  $\alpha_T$  automatically accounts for the temperature changes, if it is chosen correctly. Since the  $\alpha_T$  in Eq. (4.12) depends greatly on two parameters,  $C_1$  and  $T_\infty$ , finding the best combination is not always easy. . The temperature  $T_\infty$  is usually chosen somewhere in the glassy region and the value of  $C_1$  often lies between 1 and 12.

In the book by Nashif, etal [N1] it is suggested that some of the fitting can be done by knowing where the loss modulus  $E(\omega,T)\eta(\omega,T)$  reaches its maximum. From Eqs. (4.10) and (4.11), the loss modulus is

$$E(\omega,T) \eta(\omega,T) = \frac{n \pi E_u (\beta\omega\alpha_T)^n}{2 [1 + (\beta\omega\alpha_T)^n]^2} \quad (4.13)$$

Taking the derivative with respect to  $\omega$  yields

$$(\beta\omega\alpha_T)^n = 1 \text{ at } \beta\omega \text{ for max. loss modulus.} \quad (4.14)$$

Using this result in Eq. (4.13), the maximum value of the loss modulus is obtained.

$$\left[ E(\omega, T) \eta(\omega, T) \right]_{\max} = \frac{n \pi E_u}{8} \quad (4.15)$$

It is suggested that, if the other parameters are known, then the value of  $n$  may be calculated from Eq. (4.15). A practical problem arises in using this relationship for Soundcoat 601 because the maximum of the loss modulus occurs at a frequency higher than the range covered by the given composite plot. This was overcome by extending the frequency scale to  $f=1.0E8$  and by extending the straight temperature lines to the higher frequency range.

It is easier to find the maximum value of the loss factor, which occurs near the transition temperature and is easily identified, as can be seen in Fig. 4.5. Hence, the derivative of the loss factor  $\eta(\omega, T)$  is needed with respect to  $\omega$ . Taking the derivative and setting the result equal to zero gives the following relationship.

$$(\beta \omega \alpha_T)^{2n} = \frac{E_l}{E_l + E_u} \quad (4.16)$$

It is convenient to take the square root and define the resulting specific value of  $(\beta \omega \alpha_T)^n$  where the maximum occurs as  $R$ .

$$(\beta \omega \alpha_T)^n = \left[ \frac{E_l}{E_l + E_u} \right]^{0.5} \equiv R \quad (4.17)$$

The expression for the maximum value of loss factor is, in terms of  $R$ , and using Eqs. (4.10) and (4.11),

$$\eta(\omega, T, \alpha_T)_{\max} = \frac{n \pi E_u R}{2 \left\{ E_l + E_u \left[ \frac{R}{1+R} \right] \right\} [1+R]^2} \quad (4.18)$$

For many practical materials  $R$  is small compared to 1, or  $R \ll 1$  because  $E_l \ll E_u$ . Taking advantage of these inequalities, Eq. (4.18) becomes

$$\eta(\omega, T, \alpha_T)_{\max} = \frac{n \pi E_u R}{2 \{ E_l + E_u R \}} \quad (4.19)$$

If it is also true that  $E_l \ll E_u R$ , then Eq. (4.18) may be simplified to Eq. (4.20), but Eq. (4.18) is preferred for its accuracy.

$$\eta(\omega, T, \alpha_T)_{\max} = \frac{n \pi E_u R}{2 \{ E_u R \}} = \frac{n \pi}{2} \quad (4.20)$$

The Eqs. (4.16) -(4.20) do not appear in Ref. [N1] and have been developed by the writer. It appears that Eq. (4.20) may be used easily to find the value of  $n$ , but since  $n$  also controls the "bandwidth" of the  $\eta(\omega, T, \alpha_T)$  curve, judgment is deferred until a fit of actual data is attempted below.

#### 4.2.1.2 Reading data from a composite plot or nomograph.

The data for Soundcoat 601 is shown in Fig. 4.5. There are three vertical scales. On the right the value of frequency  $f$  in Hz is the ordinate; on the left, the values of  $E$  and  $\eta$ . On the bottom horizontal scale the value of  $\alpha_T f$  may be read. This value may be used to find  $\alpha_T$ .

In obtaining data from the plot for a certain temperature and frequency, the procedure is to start with a combination of frequency  $f$  and temperature  $T$ , for example say  $f=1000$  Hz and  $T=75^\circ$  F. So draw a horizontal line through  $f=10^3$  Hz and find its intersection with the slanting temperature line where  $T=75^\circ$  F. Then drop a vertical line from that intersection point and mark the crossing points on the  $E$  and  $\eta$  curves. The values of  $E$  and  $\eta$  are then read on the left hand scales. But now an important point is this: if the vertical line is projected down to the horizontal scale, the value of  $f\alpha_T$  may be read and, knowing  $f$ , the value of  $\alpha_T$  is readily calculated. For this example  $f\alpha_T = 10^3$  Hz, so  $\alpha_T = 1$  because both  $T$  and  $T_0 = 75^\circ$  F. If  $T=50^\circ$ F, then the value of  $\alpha_T = 27$ , and the same value should result no matter what value of frequency  $f$  is taken for this  $T$ .

In Table 4.5, the values of  $E$ ,  $\eta$  and  $E\eta(\omega, T)$  are listed for Soundcoat 601 for a temperature of  $75^\circ$ F.

Table 4.5 Dynamic Properties of Soundcoat 601

f(Hz)	E(psi)	601	
		$\eta E$ (psi)	$\eta$
$T = 75^\circ$ F			
1	210	57	0.28
10	360	180	0.50
100	1 260	945	0.75
1000	6 900	6 900	1.00
4000	18 000	14 400	0.80
1.0E4	30 900	18 450	0.60
4.0E4	90 000	32 400	0.36
1.0E5	180 000	43 200	0.24
4.0E5	210 000	37 800	0.18
1.0E6	240 000	31 200	0.13
4.0E6	270 000	21 600	0.08
1.0E7	300 000	19 500	0.065
4.0E7	300 000	12 000	0.04

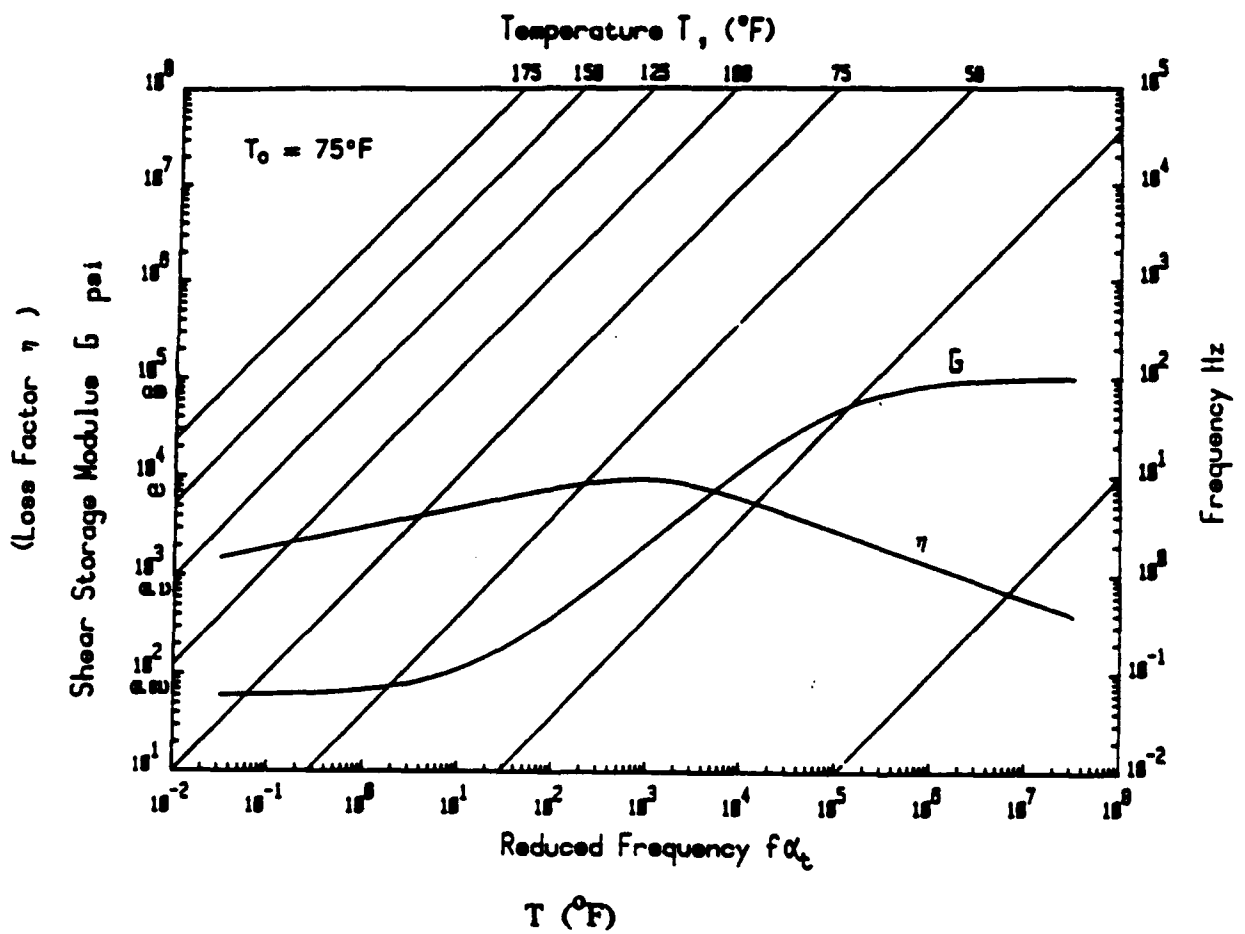


Fig. 4.5 Nomograph for  $G$  and  $\eta$  as functions of  $f$ ,  $\alpha_T$ , and  $f\alpha_T$ .

### 4.2.1.3 Step-by-step procedure for fitting equations to data.

Now the following procedure for determining the parameters is proposed.

1. Read the values of  $E_l$  and  $E_u$  from the curve of  $E$  vs  $f \alpha_T$ . For 601 the values are  $E_l = 180$  psi and  $E_u = 300,000$  psi.
2. Read the value of  $\eta_{max}$  from the curve. Use this to calculate  $n$  from Eq. (4.20). For 601,  $\eta_{max} = 1.00$  and the value of  $n = 0.637$ . To check using Eq. (4.18),  $R = 0.02449$  and  $n = 0.669$ , which results from the more accurate calculation.
3. On the loss factor curve, at the transition temperature  $T_0$ , read the value of  $f \alpha_T$  at which the loss factor is maximum. Since  $\alpha_T = 1$  at the transition temperature, the value of  $f_m = 1000$  Hz for 601.
4. Read the value of  $E$  at frequency  $\omega_m = 2\pi f_m$  at temperature  $T_0$ . This value of  $E$  will be used to calculate  $\beta$ , the shift factor, when  $\alpha_T = 1$ .

$$E(\omega_m, T_0) = E_l + E_u \left[ 1 - \frac{1}{1 + (\beta \omega_m)^n} \right] \quad (4.21)$$

or

$$(\beta \omega)^n = \frac{E_u}{E_u + E_l - E(\omega_m, T_0)} - 1 \quad (4.22)$$

For 601,  $E(\omega_m, T_0) = 6900$  psi, so  $(\beta \omega_m)^{0.669} = 0.022913$  and  $\beta = 5.63E-07$ .

5. Next, account for the effect of the variable temperature  $T$ , by determining  $\alpha_T$ . Since the data for 601 is plotted versus  $f \alpha_T$ , the value of  $\alpha_T$  may be read directly for each frequency  $f$  at any temperature  $T$ . The values so determined are listed in Table 4.6 for 601. From any two pairs of values,  $T$  and  $\alpha_T$ , the values of  $C_1$  and  $T_\infty$  may be calculated for use in Eq. (4.12), which may then be used to find the value of  $\alpha_T$  for any temperature.

Table 4.6. Values of  $\alpha_T$  versus Temperature for Soundcoat 601

$T$ ( $^{\circ}$ F)	$\alpha_T$
0	1.0 E7
25	3.0 E3
50	2.7 E1
75	1.0
100	8.0 E-2
125	1.2 E-2
150	2.0 E-3
175	4.3 E-4

#### 4.2.1.4 Results of curve-fitting for Soundcoat 601.

The values of  $\alpha_T$  at the highest and lowest temperature listed in Table 4.6 were used to determine  $C_1$  and  $T_\infty$ , which are listed in Table 4.7. These values of  $C_1$  and  $T_\infty$  were then used to calculate the  $\alpha_T$  at all temperatures.

Table 4.7 Listing of Parameters for Curve-fitting for Soundcoat 601

$T_0$	75 <sup>0</sup> F
$E_u$	300,000
$E_l$	180
$(E\eta)_{\max}$	43,200
at $f=$	100,000
$\eta_{\max}$	1.00
at $f_m=$	1000
R	0.02449
$\beta$	5.630 E-07
n	0.669
$T_\infty$	-115.75 <sup>0</sup> F
$C_1$	9.788

The correctness of  $\beta$  is best checked at the transition temperature, when  $\alpha_T = 1.0$ . In Figs. 4.5 and 4.6, plots of  $E$ ,  $\eta$ , and  $E\eta$  are depicted versus  $f$  for 601 for three temperatures  $T=50$ , 75 and 125<sup>0</sup>F. In Fig. 4.5, the comparison of the manufacturer's data (dotted) and Eq. (4.10) fit (solid) is especially good for  $E(\omega)$  at the transition temperature  $T_0=75^0$ F and in the frequency range near 1000 Hz. This shows that the value of  $\beta$  is well chosen. The shape of the curve at higher and lower frequencies is not as good and depends in part on choice of  $n$ . At the other two temperatures,  $T=50$  and 125<sup>0</sup>F the fit in the center region of the curves is excellent indicating that the  $\alpha_T$  is about correct. Again the fit is not as good at the ends of the curves.

Both the maximum value of  $\eta$  and the shape of the  $\eta(\omega, T)$  curve depend on  $n$ . Plots of  $\eta$  versus frequency  $f$  for the three temperatures are shown in Fig. 4.6. The maximum value matches well and the shape of the curve is reasonable, but the fit near the ends of the curves is not as good. On the log-log plot, the shape of the  $\eta$  vs.  $f$  is symmetrical and covers several decades in magnitude while the experimental data is unsymmetrical and covers little over one decade in magnitude.

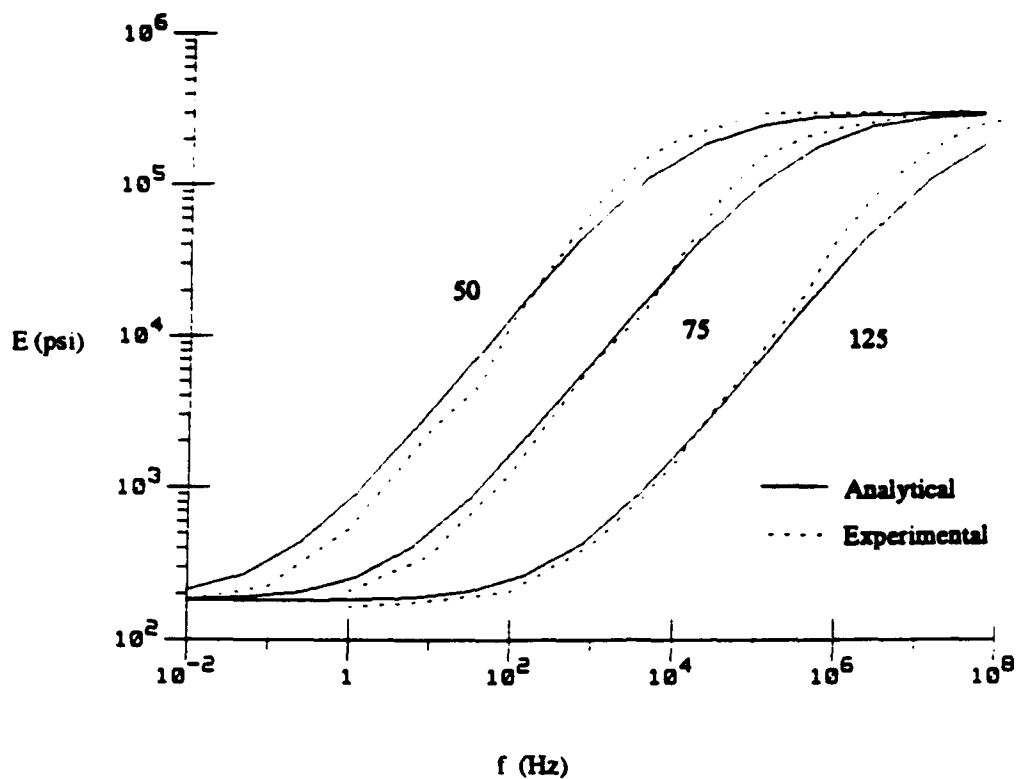


Fig. 4.6  $E$  vs.  $f$  for 601 at  $T = 50, 75,$  and  $125^{\circ}$  F, experimental and analytical.

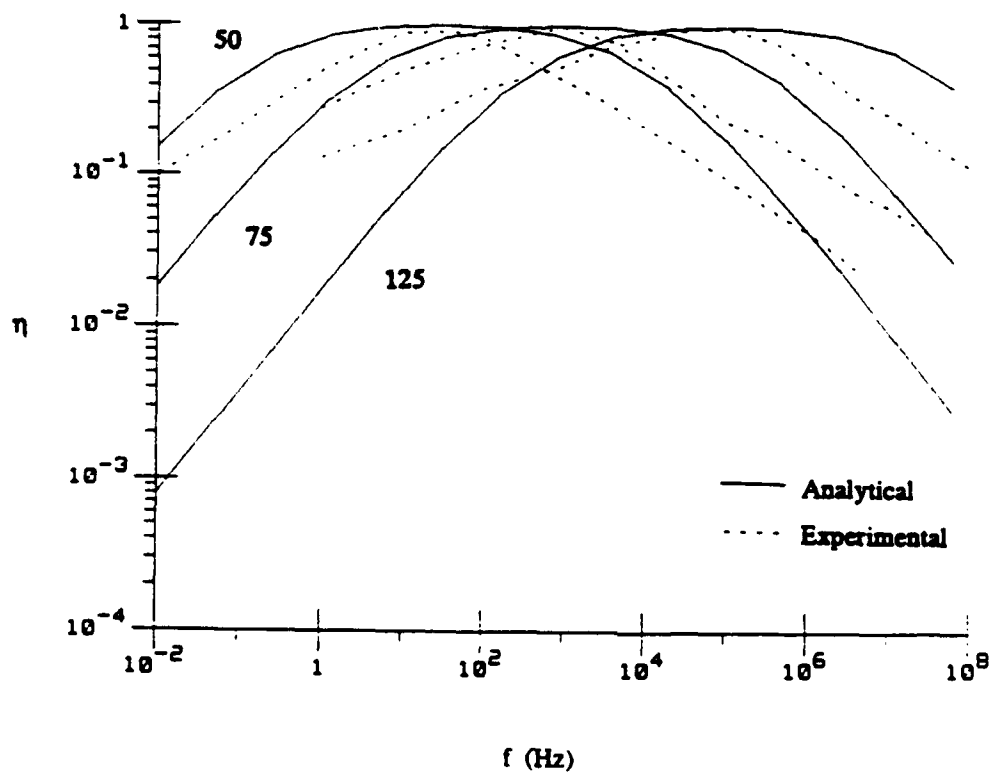


Fig. 4.7  $\eta$  vs.  $f$  for 601 at  $T = 50, 75$  and  $125^{\circ}$  F.

#### 4.2.1.5 Improving the fit by modification of the equation for $\eta$ .

The fit of  $\eta$  depends greatly on the value of  $n$ , which affects both the magnitude of  $\eta$  and the curve shape. A larger value of  $n$  produces an  $\eta$  curve of sharper curvature; a smaller  $n$  flattens the  $\eta$  curve. However, if the value of  $n$  is increased over those listed in Table 4.7 for any one of the three example materials, then the magnitude of the maximum of  $\eta$  will be too high. Hence it is suggested that the Eq. (4.11) for  $\eta(\omega, T)$  be modified to include another constant  $C_\eta$  to adjust the magnitude of  $\eta(\omega, T)$  as in Eq. (4.23). Then the  $n$  may be used mainly to control the curvature of effective bandwidth of the curve. Unfortunately the choice of  $n$  affects  $\beta$ .

$$\eta(\omega, T) = \frac{C_\eta n_t \pi E_u (\beta \omega \alpha_T)^{n_t}}{2 E(\omega, T) [1 + (\beta \omega \alpha_T)^{n_t}]^2} \quad (4.23)$$

The following procedure is therefore suggested for improving the fit of  $\eta(\omega, T)$ . Follow the usual procedure as outlined in the steps above to find  $n$ . Then modify  $n$  slightly to improve the fit and call this value  $n_t$  for "trial value of  $n$ ". Use this value  $n_t$ , in Eq. (4.24) to find  $\beta$ . The value of  $C_\eta$  is calculated simply by taking the ratio of the  $n$ 's or  $C_\eta = n / n_t$ . Some typical numbers for several values of  $n_t$  are given in Reference [N7].

$$(\beta \omega \alpha_T)^{n_t} = \left[ \frac{E_l}{E_b + E_l} \right]^{0.5} \quad (4.24)$$

#### 4.2.1.6 Summary and conclusions

Based on the standard equations, a new procedure is suggested for calculating the required parameters. The resulting parameters are listed in tabular form in Table 4.7 and curves are presented showing that the fits for  $E$  and  $E\eta$  are good. The fit for  $\eta$  is not as good, but in calculations using the complex modulus as  $E^* = E(1+j\eta)$  the value of  $E\eta$  is important and not the value of  $\eta$  itself. However, a method is suggested for improving the prediction of  $\eta$  and it happens that the prediction of  $E$  and  $E\eta$  is also improved, as demonstrated in Figs. 12-14, over the frequency range of 10 to  $10^6$  Hz. The predictions are made for temperatures from 50 to 200°F.

#### 4.2.2 Representation of viscoelastic damping by complex modulus.

As has been explained, the complex modulus of practical damping materials varies with frequency. However, in the frequency range where the loss factor is a maximum, the plot of loss factor versus frequency is fairly flat. So, if the natural frequencies of the structure are in a narrow range, reasonable estimates of the eigenproperties may be obtained by using the complex modulus in that frequency range and assuming it is constant.

For simple structures, the element stiffness is proportional to Young's modulus of the material. If the Young's modulus is complex, as  $E^* = E(1+i\eta)$  and the natural frequencies will be of the form  $\omega_n^2 (1 + i \eta_n)$ . The eigenvalues found in the state space will be of the form of  $\lambda_n = \text{sqrt}(-\omega_n^2 (1 + i \eta_n))$ . Thus the loss factor for each mode is determined by the complex natural frequencies and if the structure has the same loss factor throughout, each mode will have the same loss factor and the eigenvectors will be real and the same as for the undamped structure. This is demonstrated in Example 4.1

##### Example 4.1

$$\mathbf{M} = \begin{bmatrix} 1 & 0 \\ 0 & 2 \end{bmatrix} \quad \mathbf{K} = (1 + 0.1 i) \begin{bmatrix} 300 & -50 \\ -50 & 400 \end{bmatrix}$$

The eigenvalues and eigenvectors of  $\mathbf{M}^{-1} \mathbf{K}$  are

$$\omega_1^2 = 188.76 + i 18.88, \quad \omega_2^2 = 311.24 + i 31.12$$

so  $\eta_1 = \eta_2 = 0.10$

and

$$\Phi = \begin{bmatrix} 0.3029 & 0.9530 \\ 0.6739 & -0.2142 \end{bmatrix}$$

The eigenvalues and eigenvectors in state space are

$$\lambda_{1,2} = \pm (-0.6861 + i 13.7562) \quad \lambda_{3,4} = \pm (-0.8810 + i 17.6639)$$

with 
$$\mathbf{U}_l = \begin{bmatrix} 0.3029 & 0.3029 & 0.9530 & 0.9530 \\ 0.6739 & 0.6739 & -0.2142 & -0.2142 \end{bmatrix} \quad \text{and} \quad \mathbf{U}_u = \mathbf{U}_l \Lambda$$

In Example 4.2, the loss factors vary from 0.05 to 0.10 for the elements in the stiffness matrix. As a result, the loss factors for the two modes are found to be 0.054 and 0.096, as shown in the Example. In addition, the mode shapes are complex.

##### Example 4.2

$$\mathbf{M} = \begin{bmatrix} 1 & 0 \\ 0 & 2 \end{bmatrix} \quad \mathbf{K} = \begin{bmatrix} 300(1 + i 0.10) & -50(1 + i 0.08) \\ -50(1 + i 0.08) & 400(1 + i 0.05) \end{bmatrix}$$

The eigenvalues and eigenvectors of  $\mathbf{M}^{-1} \mathbf{K}$  are

$$\omega_1^2 = 188.86 + i 10.19, \quad \omega_2^2 = 311.14 + i 29.81$$

so

$$\eta_1 = 0.054, \quad \eta_2 = 0.096$$

and

$$\Phi = [\underline{\varphi}_1 \quad \underline{\varphi}_2] = \begin{bmatrix} 0.2988 - i 0.0263 & 0.9547 + i 0.0082 \\ 0.6751 + i 0.0058 & -0.2113 + i 0.0186 \end{bmatrix}$$

From the state space, the eigenvalues are

$$\lambda_{1,2} = \pm (-0.3705 + i 13.7476) \quad \lambda_{3,4} = \pm (-0.8441 + i 17.6594)$$

with

$$U_l = [\underline{\varphi}_1 \quad \underline{\varphi}_1 \quad \underline{\varphi}_2 \quad \underline{\varphi}_2] \quad \text{and} \quad U_u = U_l \Lambda$$

### 4.2.3 Overdamped mini-oscillator approach for representation of viscoelastic elements.

As mentioned above, the problem with mathematical representation of viscoelastic damping is that the material properties, particularly the elastic moduli, vary with frequency. Since, for free vibrations, each mode vibrates at its natural frequency, a different elastic modulus should be used for each mode. But that does not result in a typical eigenvalue problem. For forced vibration problems where the excitation is at a discrete frequency, the solution is relatively simple using a complex modulus if only the forced vibration is of interest. If the spectrum of the forcing frequency covers a spectrum of frequencies then, again, a different complex modulus should be used at each frequency involved. McTavish and Hughes [M2] set up a mathematical formulation by which the modulus of viscoelastic material is represented in terms of a power series in the frequency domain. The terms of the series are factored into products of quadratics, each quadratic appearing like that of single-degree-of-freedom system, but the idea is much more sophisticated than just connecting extra oscillators to represent damping.

From the theory of linear viscoelasticity [C.3], the constitutive equation which could represent the one-dimensional behavior of a material is

$$\sigma(t) = G(t) \varepsilon(0) + \int_0^t G(t-\tau) \frac{d\varepsilon(\tau)}{d\tau} \varepsilon(\tau) d\tau. \quad (4.25)$$

Here  $G(t)$  is the stress response due to a unit step strain input, which is the definition of the material relaxation function.

Taking the Laplace Transform of Eq. (4.25), the result is expressed symbolically as

$$\tilde{\sigma}(s) = s \tilde{G}(s) \tilde{\varepsilon}(s) \quad (4.26)$$

where  $s \tilde{G}(s)$  is the material dissipation function.

The series presented in detail in [M2] is as follows, where the fraction represents the behavior of over-damped mini-oscillators, with the proper choice of parameters:

$$s \tilde{G}(s) = \tilde{G}^0 \left[ 1 + \sum_k \alpha_k \frac{(s^2 + 2 \zeta_k \omega_k s)}{(s^2 + 2 \zeta_k \omega_k + \omega_k^2)} \right] \quad (4.27)$$

where  $\omega_k > 0$  and  $\zeta_k > 1$ , for overdamping in the mini-oscillators.

The complex modulus  $G^*(\omega) = j \omega \tilde{G}(j\omega) = G'(\omega) + j G''(\omega)$ . The material loss factor  $\eta$  is defined by

$$\eta(\omega) = \frac{G''(\omega)}{G'(\omega)}. \quad (4.28)$$

In [M2], the generalized viscoelastic finite element is represented as follows. The global linear matrix second-order system consists of the following, where  $n$ ,  $m$ , and  $l$  are integers:

- $n_e$  finite elements, subscripted 'i'.
- $m_j$  material moduli, subscripted 'j'.
- $l_{ij}$  mini-oscillator terms, subscripted 'k'.

The stiffness, mass and damping matrices for the  $i$ th element are  $\mathbf{K}_i^e$ ,  $\mathbf{M}_i^e$ , and  $\mathbf{C}_i^e$  respectively. The element stiffness matrix is represented as a linear sum of contributions from the  $m_j$  moduli

$$\mathbf{K}_i^e = \sum_{j=1}^{m_j} G_{ij}^0 \mathbf{K}_{ij}^e \quad (4.29)$$

where  $G_{ij}^0$  is the equilibrium value of the  $j$ th modulus. Further, it is suggested that the  $\mathbf{K}_{ij}^e$  matrices may be diagonalized, using the eigenvector matrices  $\mathbf{R}_{ij}$ , by

$$\mathbf{R}_{ij}^T \mathbf{K}_{ij} \mathbf{R}_{ij} = \Lambda_{ij} \quad (4.30)$$

where  $\Lambda_{ij}$  is a diagonal matrix. Further, the relationships exist such that

$$\mathbf{R}_{ij}^T \mathbf{R}_{ij} = \mathbf{I}, \text{ so } \mathbf{K}_{ij} = \mathbf{R}_{ij} \Lambda_{ij} \mathbf{R}_{ij}^T \quad (4.31)$$

The mini-oscillator representation for the  $j$ th material of the  $i$ th element is

$$s \tilde{\mathbf{G}}_{ij}(s) = \tilde{\mathbf{G}}_{ij}^0 \left[ 1 + \sum_{k=1}^{l_{ij}} \alpha_{ijk} \frac{(s^2 + 2 \zeta_{ijk} \omega_{ijk} s)}{(s^2 + 2 \zeta_{ijk} \omega_{ijk} + \omega_{ijk}^2)} \right] \quad (4.32)$$

#### 4.2.3.1 Finite element with two mini-oscillators to represent viscoelastic damping.

The finite element with two mini-oscillators to represent viscoelastic damping will have the following differential equations

$$\begin{bmatrix} \mathbf{M}^e & & & \\ & \frac{\alpha_1 G^0}{\bar{\omega}_1^2} \mathbf{K}^e & & \\ & & \frac{\alpha_2 G^0}{\bar{\omega}_2^2} \mathbf{K}^e & \\ & & & \end{bmatrix} \begin{Bmatrix} \ddot{\mathbf{q}} \\ \ddot{z}_1 \\ \ddot{z}_2 \end{Bmatrix} + \begin{bmatrix} \mathbf{0} & & & \\ & \frac{\alpha_1 G^0 2\zeta_1}{\bar{\omega}_1} \mathbf{K}^e & & \\ & & \frac{\alpha_2 G^0 2\zeta_2}{\bar{\omega}_2} \mathbf{K}^e & \\ & & & \end{bmatrix} \begin{Bmatrix} \dot{\mathbf{q}} \\ \dot{z}_1 \\ \dot{z}_2 \end{Bmatrix} \\ \begin{bmatrix} G^0 (1 + \alpha_1 + \alpha_2) \mathbf{K}^e & \alpha_1 G^0 \mathbf{K}^e & \alpha_2 G^0 \mathbf{K}^e \\ \alpha_1 G^0 \mathbf{K}^e & \alpha_1 G^0 \mathbf{K}^e & 0 \\ \alpha_2 G^0 \mathbf{K}^e & 0 & \alpha_2 G^0 \mathbf{K}^e \end{bmatrix} \begin{Bmatrix} \mathbf{q} \\ z_1 \\ z_2 \end{Bmatrix} = \begin{Bmatrix} \mathbf{f}(t) \\ \mathbf{0} \\ \mathbf{0} \end{Bmatrix} \quad (4.33)$$

Recall that the bold-face, lower case letters, here  $\mathbf{q}$ ,  $z_1$ ,  $z_2$ , and  $\mathbf{f}(t)$ , represent column matrices, or vectors.

For the  $i$ th bar undergoing only axial deformation, the stiffness matrix is

$$\mathbf{K}_i = G_i^0 \mathbf{K}_i^e = \frac{A_i G_i^0}{l_i} \begin{bmatrix} 1 & -1 \\ -1 & 1 \end{bmatrix} \quad (4.34)$$

McTavish and Hughes [M2] suggest diagonalizing this matrix. Eigenvalues are  $\lambda_{1,2}^e = 0, 2 \frac{AE}{l}$ .

The matrix of normalized eigenvectors is

$$\mathbf{R} = \frac{1}{\sqrt{2}} \begin{bmatrix} 1 & 1 \\ -1 & 1 \end{bmatrix} \quad (4.35a)$$

and

$$\mathbf{R}^T \mathbf{K}^c \mathbf{R} = \Lambda = \frac{A}{l} \begin{bmatrix} 2 & 0 \\ 0 & 0 \end{bmatrix} \quad (4.35b)$$

If the diagonalized  $\mathbf{K}^c$  matrix is used, then a coordinate change is involved and the physical picture of an actual mini-oscillator connected in the system becomes more obscure. However, using the diagonalized matrix makes the computation slightly more efficient. To make the change in coordinates, let  $\mathbf{z} = \mathbf{R} \mathbf{w}$  and pre-multiply the second and third set of equations by  $\mathbf{R}^T$ . Then Eqs. (4.33) become

$$\begin{bmatrix} \mathbf{M}^e & & \\ & \frac{\alpha_1 G^0}{\bar{\omega}_1^2} \mathbf{K}^c & \\ & & \frac{\alpha_2 G^0}{\bar{\omega}_2^2} \mathbf{K}^c \end{bmatrix} \begin{Bmatrix} \ddot{\mathbf{q}} \\ \ddot{\mathbf{w}}_1 \\ \ddot{\mathbf{w}}_2 \end{Bmatrix} + \begin{bmatrix} \mathbf{0} & & \\ & \frac{\alpha_1 G^0 2\zeta_1}{\bar{\omega}_1} \mathbf{K}^c & \\ & & \frac{\alpha_2 G^0 2\zeta_2}{\bar{\omega}_2} \mathbf{K}^c \end{bmatrix} \begin{Bmatrix} \dot{\mathbf{q}} \\ \dot{\mathbf{w}}_1 \\ \dot{\mathbf{w}}_2 \end{Bmatrix}$$

$$\begin{bmatrix} G^0 [1 + (\alpha_1 + \alpha_2)] \mathbf{K}^c & \alpha_1 G^0 \mathbf{K}^c \mathbf{R} & \alpha_2 G^0 \mathbf{K}^c \mathbf{R} \\ \alpha_1 G^0 \mathbf{R}^T \mathbf{K}^c & \alpha_1 G^0 \Lambda & 0 \\ \alpha_2 G^0 \mathbf{R}^T \mathbf{K}^c & 0 & \alpha_2 G^0 \Lambda \end{bmatrix} \begin{Bmatrix} \mathbf{q} \\ \mathbf{w}_1 \\ \mathbf{w}_2 \end{Bmatrix} = \begin{Bmatrix} \mathbf{f}(t) \\ \mathbf{0} \\ \mathbf{0} \end{Bmatrix} \quad (4.36)$$

The matrix  $\mathbf{R}^T \mathbf{K}_i^c = \frac{A_i}{l_i} \begin{bmatrix} 2 & -2 \\ 0 & 0 \end{bmatrix}$ .

#### 4.2.3.2 Representation and optimization of viscoelastic damping in the ten-bar truss.

Viscoelastic material might be applied as a thin layer on the sides of a bar of square cross-section. The present analysis assumes that there is an outer, rigid constraining layer, which is anchored to ground, which is not entirely realistic. A more reasonable assumption would be to represent the constraining layer as a rigid mass, free to move in the direction parallel to the axis of the bar. The configuration might then be called a dynamic absorber, with the viscoelastic material furnishing the stiffness and damping while the constraining layer is the absorber mass, which is the idea pursued by Carabetta [C1]

A reasonable approximation to the shape of the real and imaginary parts of a practical damping material is given by a two-term representation, based on the following values of the parameters.

$$\begin{array}{lll} \alpha_1 = 0.5 & \zeta_1 = 15.0 & \omega_1 = 60,000 \\ \alpha_2 = 1.5 & \zeta_2 = 10.0 & \omega_2 = 10,000 \end{array}$$

If the viscoelastic material is applied to the side of a truss bar and it is deforming primarily in shear, then the area  $A_1$  would be the glue area between the material and the bar and the length  $l_1$  would be the thickness of the viscoelastic layer, possibly in the range of 0.025 to 0.100 inches. In Table 4.8, the eigenvalues are listed for the ten-bar truss with two mini-oscillators on each of bars 3 and 4. The mini-oscillator parameters are as shown above. Since bars 3 and 4 are of different cross-sectional area, the  $A_1/l_1$  for the viscoelastic layer were taken in the ratio

$$\frac{G_4^0 A_4 / l_4}{G_3^0 A_3 / l_3} = 0.8209.$$

The modal damping ratios and natural frequencies are listed in Table 4.8 for three different choices for a parameter "par<sub>3</sub>" defined as  $\text{par}_3 = \frac{G_3^0 A_3 / l_3}{18.42} = 10^3, 10^4 \text{ and } 10^5$ . The structural modes occur in complex conjugate pairs, as usual. The fictitious modes are overdamped and the eigenvalues are real and negative. It is difficult to decide which pairs of overdamped modes to take together for the purpose of computing equivalent damping ratios and natural frequencies for the fictitious modes, but if the modes are not strongly coupled, the eigenvectors aid in identifying the pairs. Thus the pairs were combined using the following relationships

$$\lambda_r \cdot \lambda_{r+1} = \omega_r^2 \quad \text{and} \quad \lambda_r + \lambda_{r+1} = 2 \zeta_r \omega_r$$

and the values of  $\zeta_r$  and  $\omega_r$  are calculated, with the results as given in Table 4.8. The frequencies of the mini-oscillators themselves were 10,000 and 60,000 rad/s so the results of the pairings seem reasonable.

Table 4.8 Values of  $\zeta_r$  and  $\omega_r$  using overdamped mini-oscillators.

$\text{par}_3 = \frac{G_3^0 A_3 / l_3}{18.42}$	$10^3$		$10^4$		$10^5$	
	$\zeta_r$	$\omega_r$	$\zeta_r$	$\omega_r$	$\zeta_r$	$\omega_r$
	0.000 99	131.17	0.008 91	131.69	0.021 62	136.85
	0.000 47	173.42	0.004 41	173.75	0.019 37	178.10
	0.006 26	270.76	0.053 80	281.73	0.078 11	366.37
	0.000 02	326.05	0.000 22	326.07	0.000 46	325.72
	0.001 36	462.56	0.014 19	467.50	0.194 19	642.52
	0.000 91	600.52	0.007 22	604.55	0.058 28	556.67
	0.000 13	665.05	0.000 57	665.69	0.002 02	664.77
	0.010 37	809.80	0.079 10	940.63	0.141 36	1953.15
	60.77	59,237.	65.57	54,905.	68.90	52,252.
	10.01	59,962.	10.06	59,623.	10.62	56,438.
	15.11	9,930.	16.70	8,979.	36.39	4,118.
	15.05	9,968.	15.53	9,660.	23.28	6,440.

For low modulus damping material, the results show that modes 3, 5 and 8 experience the highest damping ratios, in the first column, for  $\text{par}_3 = 10^3$ . This is in line with the sensitivities calculated in Table 4.3 for viscous damping. When the effective material modulus is increased by a factor of 10, the  $\zeta_r$  increase by almost the same factor for the structural modes, as shown in the third column with  $\text{par}_3 = 10^4$ . But when there is another increase, to  $10^5$ , the effect becomes more nonlinear and there are large changes in the  $\omega_r$ 's. There is a stiffening effect from the viscoelastic material, so some of the natural frequencies increase while others decrease as the damping layer is stiffened. As the parameter  $\text{par}_3$  is increased to  $10^6$ , the modal damping ratios begin to decrease so those shown in the table are near the optimum values.

#### 4.2.4 Design and optimization of viscoelastic damping.

The use of added viscoelastic damping is desirable but the behavior is still hard to predict, for many reasons. Testing and test data is essential and it is difficult to perform tests of viscoelastic material, taking into account the preload, temperature, frequency, previous loading history, and damping mechanism. Having the material properties, then the following factors must be considered..

1. The damping mechanism. The viscoelastic material damps best when deformed in shear.
2. Optimum configuration. In a truss, load-carrying members could include a slip joint where the damping material transmits the axial load in shear. If the damping material has to transmit all the structural load, then it must have appreciable shear strength at low frequencies. Viscoelastic damping layers might be glued to the sides of bars used as truss members, with a constraining layer used as a cover. If the constraining layer has the same axial strain as that of the bar, then there is no shear deformation of the viscoelastic layer and little damping is produced. Therefore patches of viscoelastic material have been suggested by some investigators. These patches then have the appearance of dynamic absorbers, where the viscoelastic material supports the absorber mass, which is that of the constraining layer.
2. The temperature range. Viscoelastic materials have an optimum operating temperature, so material must be chosen which has a high loss factor in that range.
3. Heating during operation. The energy is dissipated as heat, so arrangements must be made to assure that heat generated can vented away.
4. Heating during fabrication. Some structural fabrication processes involve heating. Care must be taken not to overheat the viscoelastic material. For example, some materials are irreparably damaged if heated above 350° F.
5. Frequency range of operation. It is important that damping material is chosen which has desirable properties in the frequency range where damping is required.
6. Optimum location in the structure. This topic is addressed in Chapter 2. The optimum location for viscoelastic damping may, or may not be, the same as the optimum location for viscous damping.
7. Optimum amount of viscoelastic material. This has to do with the area and thickness of

individual pads of material.

With regard to the present investigation, in addition to the work summarized above, the optimum design of constrained layer damping in beams was a topic of parallel study. Given a beam material, such as aluminum or steel, then one must choose the damping material of optimum thickness and optimum Young's modulus. Optimum designs are discussed in [N8], based on formulas given in [N1].

A senior engineering student, Smith, did an honors thesis [S2] dealing with optimization of the thickness and elastic modulus of an added damping and constraining layer in a beam in bending. He made a finite element model and worked in the frequency domain, with the assumption that the loss factor of the viscoelastic material was  $\eta = 1.0$ , which is a typical value for some practical materials. He found effective loss factors  $\eta$  as high as 0.38 for beam bending modes, which correspond to modal damping ratio  $\zeta = 0.19$ . He also found modes in which the constraining layer moved parallel to the beam axis, which was very efficient for placing the damping layer in shear, with maximum  $\zeta = 0.42$ . An unexpected discovery was that, due to the low axial stiffness of the damping layer, additional low frequency modes are produced in which the constraining layer moves out of phase with the beam. The maximum modal damping ratio of  $\zeta = 0.48$  was reported. He called it a dynamic-absorber type mode, because the damping layer is acting like an absorber spring, but it is a stretching of the viscoelastic material which allows the constraining layer to move perpendicular to the axis of the beam.

In another phase of the study, a senior engineering student, Carabetta [C1], studied damping produced by four dynamic absorbers attached to an individual clamped-free truss bar undergoing axial deformation. The dissipation can be maximized by tuning the absorber frequency. An advantage of this arrangement is that the viscoelastic material does not have to carry the static load in the truss member. The viscoelastic material provided the damping and spring stiffness, in shear, and a rigid mass was attached. The dynamic modulus of the viscoelastic material was represented by the mini-oscillator approach [M2] described above, using only one term in the series. Carabetta predicted modal damping ratios of  $\zeta$  ranging from 0.10 to 0.57. Further study of the representation of practical viscoelastic material properties is needed, but the results of this study of the dynamic absorber arrangement are very encouraging.

## 5. ACTIVE DAMPING AND CONTROL.

In many practical situations, it is advantageous to augment passive damping with a sufficient level of active control to achieve specified goals for the eigenvalues. If the purpose of active control is to increase the damping ratio in certain modes, then the poles must be shifted. An example showing the effect, on eigenvalue sensitivities, of superimposing of control forces on viscous damping forces is given in reference [N9] and in section 3.1.2.

This chapter deals with the design of passive damping and active control, without the use of observers to reconstruct the state. Emphasis is on designing systems with desirable modal damping, using feedback control of the form  $-G \dot{z} - H z$ . The control may be devised in *system space*, *system modal space*, *state space* or *state modal space*.

*Direct output feedback control in system space* is explained by Meirovitch [M4, p.252]. It is advantageous to have as many actuators as sensors. The motion is sensed and control forces proportional to velocity and/or displacement are fed directly back to the structure. For semidefinite systems, with rigid body modes, one of the goals may be to stabilize the system with displacement feedback. Quite often, the reason for adding control forces is to achieve a desired level of dissipation for each mode, which means to place the closed loop poles in specified locations in the complex plane.

An advantage of using modal coordinates is that the differential equations of motion are decoupled. If they are recoupled due to the nature of the control forces, the control is called *coupled modal control*. Another change in coordinates may be made to decouple the modal equations. If the control forces are chosen so the modal differential equations remain uncoupled, the control is called *natural control* and the associated damping is proportional. If the passive damping is initially small enough to be neglected, natural control is readily designed and an example is given in [M3] where the control forces are chosen in *system modal space* so the closed loop natural frequencies are the same as those of the open loop structure.

Much of control theory was developed in *state space*, but not by engineers concerned with structural dynamics problems. For example, Moore [M6] discussed the possibility of designing the entire eigenstructure and presented related necessary and sufficient conditions for prescribing both eigenvalues and eigenvectors. This idea was expanded by Andry, *et al*, [A1], for three types of feedback, namely: full state, output and constrained output. Neither paper dealt with the special form of the state equations for structural vibrations. However, an important concept is that the mode shapes, as well as the eigenvalues, may be designed. Inman [I3] gave a related example, but in *system modal space* and not *state modal space*. Starek and Inman [S5] presented a solution in *state space* to the so-called inverse problem, where mass, damping and stiffness matrices are constructed based on changing all, or part of, the system eigenvalues and eigenvectors, with rigid body modes included. They extended the formulation to include the case where only a portion of the eigenvalues and eigenvectors are known. To assure that the constructed system mass, stiffness, and damping matrices would be symmetric when solving the inverse problem, Starek, Inman, and Kress [S6] started with symmetric matrices and applied constraints to the chosen eigenstructure. Juang, Lim and Junkins [J1] considered the closed loop control problem with either state or output feedback and used a QR decomposition to generate the orthonormal basis that spans admissible eigenvector space corresponding to each assigned eigenvalue. Neubert [N11, N12] considered the problem of combined damping and control and full state feedback and presented two approaches, one based on using eigenstructure sensitivities and the other based on a perturbation approach, which is shown to be related to the inverse eigenvalue problem.

If the dimension of the control vector is less than that of the state vector, natural control is

not possible and the modes are coupled by the control forces. If only a limited number of modes are controlled, then the question of spillover arises.

In modern control theory, optimum timewise control forces may be found by way of an objective function and solution of the Riccati equation. In the present chapter, an example from [M4] is discussed where the optimum timewise control forces are determined in state modal space. These control forces can then be converted to system space.

The contributions of the present study that are summarized in this chapter are:

1. The equations for natural modal control in system space are given and related to the criteria for proportional damping.
2. Examples are presented for designing symmetric or unsymmetric control matrices using the eigenvalue sensitivities.
3. One-step perturbation methods are presented for designing the control and damping matrices of a structure to produce desired changes in the eigenvalues or eigenvectors.
4. An example from reference [M4], where the optimum timewise control forces were found in state modal space by way of the Riccati equation, is discussed in light of the present work.

## 5.1 Constant gain, closed loop control.

### 5.1.1 Uncoupling of the differential equations and modal control.

In system space, the differential equations are of second order. Excluding viscous damping, Eqs. (2.1), are uncoupled by the coordinate transformation

$$z(t) = \Phi q(t) \quad (5.1)$$

Substituting Eq. (5.1), pre-multiplying Eq. (2.1) by  $\Phi^T$ , and using  $\Phi^T M \Phi = [M_n]^D$

$$\Phi^T M \Phi \ddot{q} + \Phi^T K \Phi q = \Phi^T F(t) = N(t) \quad (5.2)$$

$$[M_n]^D \ddot{q} + [M_n]^D [\omega_n^2]^D q = -[g] \dot{q} - [h] q = N(t) \quad (5.3)$$

The diagonal matrices on the left side of Eq. (5.3) indicate decoupling, but if  $[g]$  and  $[h]$  are non-diagonal, the equations are still coupled. If  $[g]$  and  $[h]$  are diagonal, which is called natural control, then the equations are uncoupled.

If the control matrices in  $N(t)$  are specified, and  $\Phi^T F(t) = N(t)$ , then  $F(t)$  is found through the use of the orthogonality relationships, so

$$F(t) = \Phi^{-T} N(t) = M \Phi [M_n]^{-D} N(t) = -M \Phi [M_n]^{-D} [ [g] \dot{q} + [h] q ] \quad (5.4)$$

Changing back to the  $z(t)$  coordinates

$$F(t) = \Phi^{-T} N(t) = M \Phi [M_n]^{-D} N(t) = -M \Phi [M_n]^{-D} [ [g] \Phi^{-1} \dot{z} + [h] \Phi^{-1} z ] \quad (5.5)$$

The differential equations with feedback are now

$$M \ddot{z} + M \Phi [M_n]^{-D} [ [g] \Phi^{-1} \dot{z} + [h] \Phi^{-1} z ] + K z = 0. \quad (5.6)$$

which is

$$M \ddot{z} + G \dot{z} + [H + K] z = 0 \quad (5.7)$$

where 
$$\mathbf{G} = \mathbf{M} \Phi [\mathbf{M}_n]^{-D} [g] \Phi^{-1} \quad \text{and} \quad \mathbf{H} = \mathbf{M} \Phi [\mathbf{M}_n]^{-D} [h] \Phi^{-1} \quad (5.8)$$

Pre-multiplying Eq. (5.6) by  $\mathbf{M}^{-1}$

$$\ddot{\mathbf{z}} + \Phi [\mathbf{M}_n]^{-D} [g] \Phi^{-1} \dot{\mathbf{z}} + [h] \Phi^{-1} \mathbf{z} + \mathbf{M}^{-1} \mathbf{K} \mathbf{z} = 0. \quad (5.9)$$

or 
$$\ddot{\mathbf{z}} + \mathbf{M}^{-1} \mathbf{G} \dot{\mathbf{z}} + \mathbf{M}^{-1} [\mathbf{H} + \mathbf{K}] \mathbf{z} = 0. \quad (5.10)$$

which is of the form

$$\mathbf{I} \ddot{\mathbf{z}} + \mathbf{C}_1 \dot{\mathbf{z}} + \mathbf{K}_1 \mathbf{z} = 0. \quad (5.11)$$

### 5.1.2 Criterion for proportional damping or proportional control.

The question is when do  $\mathbf{C}_1$  and  $\mathbf{K}_1$  represent proportional damping or control.

In matrix form the question is 
$$\mathbf{C}_1 \mathbf{K}_1 \stackrel{?}{=} \mathbf{K}_1 \mathbf{C}_1 \quad (5.12a)$$

or 
$$\mathbf{M}^{-1} \mathbf{G} \mathbf{M}^{-1} [\mathbf{H} + \mathbf{K}] \stackrel{?}{=} \mathbf{M}^{-1} [\mathbf{H} + \mathbf{K}] \mathbf{M}^{-1} \mathbf{G} \quad (5.12b)$$

Since  $\mathbf{G}$  and  $\mathbf{H}$  can be chosen separately, the Eq. (5.12b) is separated into two parts:

$$\mathbf{M}^{-1} \mathbf{G} \mathbf{M}^{-1} \mathbf{H} \stackrel{?}{=} \mathbf{M}^{-1} \mathbf{H} \mathbf{M}^{-1} \mathbf{G} \quad (5.13a)$$

$$\mathbf{M}^{-1} \mathbf{G} \mathbf{M}^{-1} \mathbf{K} \stackrel{?}{=} \mathbf{M}^{-1} \mathbf{K} \mathbf{M}^{-1} \mathbf{G} \quad (5.13b)$$

Now substitute for  $\mathbf{M}^{-1} \mathbf{G}$  and  $\mathbf{M}^{-1} \mathbf{K}$  by comparing Eqs. (5.10) and (5.9)

$$\Phi [\mathbf{M}_n]^{-D} [g] \Phi^{-1} \Phi [\omega_n^2]^{-D} \Phi^{-1} \stackrel{?}{=} \Phi [\omega_n^2]^{-D} \Phi^{-1} \mathbf{M}^{-1} \mathbf{M} \Phi [\mathbf{M}_n]^{-D} [g] \Phi^{-1} \quad (5.14a)$$

which reduces to

$$[\mathbf{M}_n]^{-D} [g] [\omega_n^2]^{-D} \stackrel{?}{=} [\omega_n^2]^{-D} [\mathbf{M}_n]^{-D} [g] \quad (5.14b)$$

The answer is that Eq. (5.14b) does not represent an equality. However, the two sides of the equation will be equal if  $[g]$  is diagonal, which is then a requirement for proportional control. Then Eq. (5.14b) becomes the following equality

$$[\mathbf{M}_n]^{-D} [g]^D [\omega_n^2]^{-D} = [\omega_n^2]^{-D} [\mathbf{M}_n]^{-D} [g]^D \quad (5.15)$$

The advantage of proportional damping or proportional control is that the eigenvectors  $\Phi$  do not change, which means that the coordinate transformations which decouple the original matrices will also decouple the closed loop equations. A direct way to check that this is true is to simply look at the products  $\Phi^T \mathbf{G} \Phi$  and  $\Phi^T \mathbf{H} \Phi$ .

The latter product 
$$\Phi^T \mathbf{H} \Phi = \Phi^T \mathbf{M} \Phi [\mathbf{M}_n]^{-D} [h] \Phi^{-1} \Phi \quad (5.16)$$

reduces to 
$$\Phi^T \mathbf{H} \Phi = [h], \quad (5.17)$$

and, similarly, 
$$\Phi^T \mathbf{G} \Phi = [g]. \quad (5.18)$$

So, the open loop eigenvectors decouple the closed loop equations, but only if  $[h]$  and  $[g]$  are diagonal matrices.

### 5.1.3 One-step methods for design of viscous damping and control in state space by choosing eigenvalues and/or eigenvectors.

Natural modal control and the closely related IMSC method [M4] are usually presented as a one-step method for designing control matrices in system space starting with plant matrices where there is no viscous damping or where the viscous damping is proportional. One of the usual features is that there is no change in mode shape from those the undamped, open loop system. A perturbation method is presented in [M5] by which the changes are predicted in eigenvalues and eigenvectors due to a small change in a real matrix A. The changes are predicted using a eigenvectors of the unperturbed system. A different, more direct, approach was developed as part of the present study and are presented as three separate methods.

The three methods require only one step. The goal is, given an initial system with or without viscous damping, what is the change  $dA$  in the matrix A to achieve the desired eigenvalues and eigenvectors. The matrix A is in state space and is unsymmetric. The desired right and left eigenvectors U and V and the diagonal matrix of distinct eigenvalues,  $\Lambda$ , are known or chosen.

More specifically, given the desired changes  $d\Lambda$  and  $dU$ , in eigenvalues and eigenvectors, respectively, find the required change  $dA$  in the state space matrix A. The three methods are arbitrarily numbered I, II, and III. They are as follows:

Method I. The sum  $[C + G]$ , initially zero, is designed to achieve a desired change in eigenvalues using the eigenvectors and mode shapes of the undamped system.

Method II. The matrices  $C_1$  and  $K_1$  of the closed loop system are designed to achieve desired changes in the eigenvalues with no change in mode shapes, but with the eigenvectors "corrected".

Method III. The matrices  $C_1$  and  $K_1$  of the closed loop system are designed to achieve desired changes in the eigenvalues, mode shapes and eigenvectors.

First of all, the A matrix can be recovered from the given eigenproperties from the relationship

$$U \Lambda V^T = A \quad (5.19)$$

The Eq. (5.19) is not new, with regard to recovering the original A from the eigenproperties on the left side. However, some interest has been apparent lately in extending the equation to specify desired eigenproperties. The in references [S5], [S6] and [J1] are especially relevant, as summarized on page 66. In the present work, an iteration approach, and a related FORTRAN computer program were written early in the study. The idea was to specify a desired increment  $d\Lambda$  in  $\Lambda$ , estimate the corresponding increments in U and V, and use (5.19) to find the corresponding  $dA$ . It was found that the iteration usually converged in one cycle but the essential form of the A matrix was not always preserved. Further investigation led to the formulation of the problem as a one step perturbation approach.

The basis of the perturbation approach is to take small variations are taken in the matrices in the Eq. (5.19), as follows.

$$(U + dU)(\Lambda + d\Lambda)(V^T + dV)^T = A + dA \quad (5.20)$$

Expanding Eq. (5.20) gives

$$\begin{aligned}
 & \mathbf{U} \Lambda \mathbf{V}^T + \Lambda d\mathbf{V}^T + d\mathbf{U} \Lambda \mathbf{V}^T + d\mathbf{U} \Lambda d\mathbf{V}^T \\
 & \mathbf{U} d\Lambda \mathbf{V}^T + \mathbf{U} d\Lambda d\mathbf{V}^T + d\mathbf{U} d\Lambda \mathbf{V}^T + d\mathbf{U} d\Lambda d\mathbf{V}^T = \mathbf{A} + d\mathbf{A}
 \end{aligned} \tag{5.21}$$

Taking advantage of Eq. (5.19) and dropping terms involving products of two or three small variations, but keeping  $d\mathbf{U} \Lambda d\mathbf{V}^T$  in some cases, the remaining terms are

$$\mathbf{U} d\Lambda \mathbf{V}^T + \mathbf{U} \Lambda d\mathbf{V}^T + d\mathbf{U} \Lambda \mathbf{V}^T + d\mathbf{U} \Lambda d\mathbf{V}^T = d\mathbf{A} \tag{5.22}$$

If the changes in eigenvectors are small enough, the increments in the eigenvectors may be negligible. Otherwise, some method is needed to estimate  $d\mathbf{V}$  and  $d\mathbf{U}$ , or an iteration process must be used. If the  $d\Lambda$  is chosen such that there is no change in eigenvectors, then the result is straightforward to carry out, and is simply

$$\mathbf{U} d\Lambda \mathbf{V}^T = d\mathbf{A} \quad \text{for } d\mathbf{U} = d\mathbf{V} = \mathbf{0} \tag{5.23}$$

At this stage it is important to divide the eigenvector matrices into their upper and lower portions, as in Section 2.2.2, that is

$$\mathbf{U} = \begin{bmatrix} \mathbf{U}_u \\ \mathbf{U}_l \end{bmatrix} \tag{5.24}$$

and recall that, in general,  $\mathbf{U}_u = \mathbf{U}_l \Lambda$ , so taking variations,

$$\mathbf{U}_u + d\mathbf{U}_u = (\mathbf{U}_l + d\mathbf{U}_l) (\Lambda + d\Lambda) \tag{5.25}$$

$$d\mathbf{U}_u = \mathbf{U}_l d\Lambda + d\mathbf{U}_l \Lambda + d\mathbf{U}_l d\Lambda \tag{5.26}$$

So, if the mode shapes do not change and  $d\mathbf{U}_l = \mathbf{0}$ ,  $d\mathbf{U}_u = \mathbf{U}_l d\Lambda \neq \mathbf{0}$ . So, even if the mode shapes do not change, the eigenvectors in state space will change if the eigenvalues change, because the upper  $n \times 2n$  portion of the  $\mathbf{U}$  matrix changes. Further, under the usual normalization, the fact that the lower right vectors do not change may go unrecognized unless a special normalization procedure is used. In this section then, the  $r$ th right eigenvector is normalized using the  $n \times n$  mass matrix  $\mathbf{M}$  by

$$(5. \quad \begin{matrix} 1 \times n & n \times n & n \times 1 & 1 \times 1 \\ \mathbf{u}_{rl}^T & \mathbf{M} & \mathbf{u}_{rl} & = & 1 \end{matrix}$$

Then  $\mathbf{U}_u$  is found from

$$\mathbf{U}_u = \mathbf{U}_l \Lambda \tag{5.28}$$

and  $\mathbf{V}$  from

$$\mathbf{V}^T = \mathbf{U}^{-1} \tag{5.29}$$

While the eigenvector matrices are square, and are assumed to be invertible because the vectors are independent, their upper and lower portions are rectangular, of size  $n \times 2n$ , and are not invertible.

### 5.1.3.1 Method I: Design of the sum of the matrices, $[\mathbf{C}+\mathbf{G}]$ .

In this method, the damping and control matrices are initially zero, so  $\mathbf{C} = \mathbf{G} = \mathbf{H} = \mathbf{0}$  and the desired change  $d\Lambda$  in the eigenvalue matrix is given. The  $2n \times 2n$  matrix  $d\mathbf{A}$  consists of four  $n \times n$  submatrices as shown here

$$dA = \begin{bmatrix} dA_{uu} & dA_{u/} \\ dA_{/u} & dA_{//} \end{bmatrix} = \begin{bmatrix} dC_1 & 0 \\ 0 & 0 \end{bmatrix} \quad (5.30)$$

Taking  $dU=0$  and  $dV=0$ , there results from Eqs. (5.23) and (5.24)

$$dA = U d\Lambda V^T = \begin{bmatrix} U_u d\Lambda V_u^T & U_u d\Lambda V_l^T \\ U_l d\Lambda V_u^T & U_l d\Lambda V_l^T \end{bmatrix} \quad (5.31)$$

Now it happens  $U_l d\Lambda V_l^T \neq 0$  but it is in the wrong position in the  $dA$  matrix, so in Method I, the approach is to add it to  $dA_{uu}$  and set  $dA_{//} = 0$ . In fact, it is easily shown that, if  $C_1 = 0$ ,

$$U_l d\Lambda V_l^T = U_u d\Lambda V_u^T \quad (5.32)$$

which follows from Eqs. (2.39b) and (2.41a) that give

$$U_u = U_l \Lambda \quad \text{and} \quad \Lambda V_u^T = V_l^T \quad \text{when} \quad C_1 = 0 \quad (5.33)$$

Hence, in Method I, the desired change in  $C_1$  is

$$dC_1 = U_l d\Lambda V_l^T + U_u d\Lambda V_u^T \quad (5.34a)$$

with

$$dK_1 = 0 \quad (5.34b)$$

In order to further understand the effect of perturbation, it is of interest to perturb the other related equations, since the Eq. (5.21) came from perturbing the equation  $U\Lambda V^T$ .

The new eigenvectors,  $U + dU$  and  $V + dV$ , would be normalized so there results

$$(V^T + dV^T)(U + dU) = I \quad (5.35)$$

Cancelling  $V^T U = I$  and neglecting the products of increments, Eq. (5.35) becomes,

$$dV^T U + V^T dU = 0 \quad (5.36)$$

Taking variations in the characteristic equations involving the right eigenvectors yields

$$(A + dA)(U + dU) = (U + dU)(\Lambda + d\Lambda) \quad (5.37a)$$

$$A dU + dA U = U d\Lambda + dU \Lambda \quad (5.37b)$$

Similarly, for the left eigenvectors,

$$A^T dV + dA^T V = V d\Lambda + dV \Lambda \quad (5.38a)$$

$$dV^T A + V^T dA = d\Lambda V^T + \Lambda dV^T \quad (5.38b)$$

Now, in the iteration process, it is noticed that, sometimes, the resulting  $dA_{uu} = dA_{//}$ , so the question is, under what conditions does this occur.

$$\begin{matrix} n \times 2n & 2n \times 2n & 2n \times n & n \times 2n & 2n \times 2n & 2n \times n \\ U_u & d\Lambda & V_u^T & U_l & d\Lambda & V_l^T \end{matrix} ? \quad (5.39)$$

Three cases are of interest:

Case 1: When  $C_1=0$ , the equality holds. This is seen from the relationships of Section 2.2.2

Case 2: The equality holds for proportional damping, where  $C_1 K_1 = K_1 C_1$ .

Case 3: The equality does not hold when the increment  $d\Lambda = \gamma \Lambda$ . The four quarters of the  $dA$  matrix are

$$U_u d\Lambda V_u^T = -dC_1 \quad U_l d\Lambda V_l^T = -dK_1 \quad (5.40a)$$

$$U_l d\Lambda V_u^T = dI \quad U_u d\Lambda V_l^T = 0 \quad (5.40b)$$

So for this special case, the products will be

$$U_u d\Lambda V_u^T = -\gamma C_1 \quad U_l d\Lambda V_u^T = \gamma I \quad (5.41a)$$

$$U_u d\Lambda V_l^T = -\gamma K_1 \quad U_l d\Lambda V_l^T = 0 \quad (5.41b)$$

A difficulty occurs here because  $U_l d\Lambda V_u^T = \gamma I$ , which means that the redundant equation in state space is not maintained.

The above becomes more clear by the following example.

#### Example 5.1 One-step design of the $[C+G]$ matrix using Method I.

For this example, the mass matrix  $M$ ,  $K$  and the state space matrices  $M^*$  and  $K^*$  are

$$M = \begin{bmatrix} 2 & 0 \\ 0 & 2 \end{bmatrix} \quad K = \begin{bmatrix} 300 & -50 \\ -50 & 400 \end{bmatrix}$$

$$M^* = \begin{bmatrix} 2 & 0 & 0 & 0 \\ 0 & 2 & 0 & 0 \\ 0 & 0 & -300 & 50 \\ 0 & 0 & 50 & -400 \end{bmatrix} \quad K^* = \begin{bmatrix} 0 & 0 & 300 & -50 \\ 0 & 0 & -50 & 400 \\ 300 & -50 & 0 & 0 \\ -50 & 400 & 0 & 0 \end{bmatrix}$$

The characteristic matrix  $A$ , the eigenvalues  $\Lambda$  and the right and left eigenvector matrices are

$$A = \begin{bmatrix} 0 & 0 & -150 & 25 \\ 0 & 0 & 25 & -200 \\ 1 & 0 & 0 & 0 \\ 0 & 1 & 0 & 0 \end{bmatrix} \quad \Lambda = \begin{bmatrix} (0 + 11.8171 i) & 0 & 0 & 0 \\ 0 & (0 - 11.8171 i) & 0 & 0 \\ 0 & 0 & (0 + 14.5036 i) & 0 \\ 0 & 0 & 0 & (0 - 14.5036 i) \end{bmatrix}$$

$$U = \begin{bmatrix} 7.7199 i & -7.7199 i & -3.9247 i & 3.9247 i \\ 3.1977 i & -3.1977 i & 9.4750 i & -9.4750 i \\ 0.6533 & 0.6533 & -0.2706 & -0.2706 \\ 0.2706 & 0.2706 & 0.6533 & 0.6533 \end{bmatrix} \quad V = \begin{bmatrix} -0.0553 i & 0.0553 i & 0.0187 i & -0.0187 i \\ -0.0229 i & 0.0229 i & -0.0450 i & 0.0450 i \\ 0.6533 & 0.6533 & -0.2706 & -0.2706 \\ 0.2706 & 0.2706 & 0.6533 & 0.6533 \end{bmatrix}$$

Because of the special choice of the mass matrix and the normalization procedure, it happens that  $V_l = U_l$ , but this is not usually true.

For later reference, the sensitivity matrices are also recorded here. The  $S_2 = \bar{S}_1$  and  $S_4 = \bar{S}_3$ .

$$S_1 = \begin{bmatrix} 0.4268 - 0.0000 i & 0.1768 + 0.0000 i & 0.0000 - 0.0361 i & 0.0000 - 0.0150 i \\ 0.1768 - 0.0000 i & 0.0732 + 0.0000 i & 0.0000 - 0.0150 i & 0.0000 - 0.0062 i \\ 0.0000 + 5.0433 i & 0.0000 + 2.0890 i & 0.4268 - 0.0000 i & 0.1768 + 0.0000 i \\ 0.0000 + 2.0890 i & 0.0000 + 0.8653 i & 0.1768 - 0.0000 i & 0.0732 + 0.0000 i \end{bmatrix}$$

$$S_3 = \begin{bmatrix} 0.0732 + 0.0000 i & -0.1768 + 0.0000 i & 0.0000 - 0.0050 i & 0.0000 + 0.0122 i \\ -0.1768 + 0.0000 i & 0.4268 - 0.0000 i & 0.0000 + 0.0122 i & 0.0000 - 0.0294 i \\ 0.0000 + 1.0620 i & 0.0000 - 2.5639 i & 0.0732 - 0.0000 i & -0.1768 - 0.0000 i \\ 0.0000 - 2.5639 i & 0.0000 + 6.1898 i & -0.1768 + 0.0000 i & 0.4268 - 0.0000 i \end{bmatrix}$$

The goal now is to determine the  $A + dA$  matrix which will produce the following specified changes  $d\Lambda$  in the eigenvalues:

$$d\Lambda = \begin{bmatrix} (-0.30 + 0.0 i) & 0 & 0 & 0 \\ 0 & (-0.30 + 0.0 i) & 0 & 0 \\ 0 & 0 & (-0.50 + 0.0 i) & 0 \\ 0 & 0 & 0 & (-0.50 + 0.0 i) \end{bmatrix}$$

Using Eq. (5.21), assuming temporarily that the changes in eigenvectors may be neglected,

$$U d\Lambda V^T = dA = \begin{bmatrix} -0.3293 & 0.0707 & 0 & 0 \\ 0.0707 & -0.4707 & 0 & 0 \\ 0 & 0 & -0.3293 & 0.0707 \\ 0 & 0 & 0.0707 & -0.4707 \end{bmatrix}$$

The problem is that the  $A + dA$  will not produce a correct characteristic equation, since the lower right corner of  $A + dA$  should be zero. However, the trace of  $A + dA$  will be the same if the lower corner is added to the upper corner and the lower corner is made zero. So the modified  $dA$  matrix will be designated  $dA_G$  and the matrix  $A_G = A + dA_G$ .

$$dA_G = \begin{bmatrix} -0.6586 & 0.1414 & 0 & 0 \\ 0.1414 & -0.9414 & 0 & 0 \\ 0 & 0 & 0 & 0 \\ 0 & 0 & 0 & 0 \end{bmatrix} \quad A_G = \begin{bmatrix} -0.6586 & 0.1414 & -150 & 25 \\ 0.1414 & -0.9414 & 25 & -200 \\ 1 & 0 & 0 & 0 \\ 0 & 1 & 0 & 0 \end{bmatrix}$$

The eigenvalues of  $A_G$  are

$$\Lambda_G = \begin{bmatrix} -0.3000 + i 11.8133 & 0 & 0 & 0 \\ 0 & -0.3000 - i 11.8133 & 0 & 0 \\ 0 & 0 & -0.5000 + i 14.4950 & 0 \\ 0 & 0 & 0 & -0.5000 - i 14.4950 \end{bmatrix}$$

The real parts of the eigenvalues are those desired and the natural frequencies,  $\omega_1 = 11.8171$  and  $\omega_3 = 14.5036$ , are the same as those of the undamped, unperturbed matrix  $A$ . The mode shapes, in  $U_i$ , are unchanged as indicated by the  $dU$  listed next, but the upper halves of the right eigenvector have changed.

$$dU = U_G - U = \begin{bmatrix} -0.1960 - 0.0025 i & -0.1960 + 0.0025 i & 0.1353 + 0.0023 i & 0.1353 - 0.0023 i \\ -0.0812 - 0.0010 i & -0.0812 + 0.0010 i & -0.3299 - 0.0056 i & -0.3299 + 0.0056 i \\ 0 & 0 & 0 & 0 \\ 0 & 0 & 0 & 0 \end{bmatrix}$$

$$U_G = \begin{bmatrix} -0.1960 + 7.7174 i & -0.1960 - 7.7174 i & 0.1353 - 3.9223 i & 0.1353 - 3.9223 i \\ -0.0812 + 3.1967 i & -0.0812 - 3.1967 i & -0.3266 + 9.4693 i & -0.3266 - 9.4693 i \\ 0.6533 & 0.6533 & -0.2706 & -0.2706 \\ 0.2706 & 0.2706 & 0.6533 & 0.6533 \end{bmatrix}$$

Again, for later reference, one of the sensitivity matrices is recorded.

$$S_{1G} = \begin{bmatrix} 0.4268 + i 0.0108 & 0.1768 + i 0.0045 & 0.0000 - i 0.0361 & 0.0000 - i 0.0150 \\ 0.1768 + i 0.0045 & 0.0732 + i 0.0019 & 0.0000 - i 0.0150 & 0.0000 - i 0.0062 \\ 0.0000 + i 5.0449 & 0.0000 + i 2.0897 & 0.4268 - i 0.0108 & 0.1768 - i 0.0045 \\ 0.0000 + i 2.0897 & 0.0000 + i 0.8656 & 0.1768 - i 0.0045 & 0.0732 - i 0.0019 \end{bmatrix}$$

### Example 5.2 Same example as 5.1, but with $N \times N$ matrices and natural control.

If the mode shapes do not change, then the same problem could be done by  $2 \times 2$  matrices.

$$M = \begin{bmatrix} 2 & 0 \\ 0 & 2 \end{bmatrix} \quad K = \begin{bmatrix} 300 & -50 \\ -50 & 400 \end{bmatrix}$$

The eigenvalue matrices for  $M^{-1}K$  are

$$W_2 = \begin{bmatrix} 139.6447 & 0 \\ 0 & 210.3553 \end{bmatrix} \quad \Phi = \begin{bmatrix} -0.6533 & -0.2706 \\ -0.2706 & 0.6533 \end{bmatrix}$$

where the  $\Phi$  have been normalized by

$$\Phi^T M \Phi = M^D = I.$$

If the modal control matrix  $[g]$  is specified, then the control matrix  $[G]$  in the original coordinate system is calculated with the results as follows

$$[g] = \begin{bmatrix} -0.3 & 0 \\ 0 & -0.5 \end{bmatrix} \quad G = \begin{bmatrix} -0.6586 & 0.1414 \\ 0.1414 & -0.9414 \end{bmatrix}$$

If this  $dA$  is added to  $A$ , the resulting eigenvalues are  $\Lambda + d\Lambda$ , as follows and the eigenvectors are unchanged.

$$\Lambda = \begin{bmatrix} (-0.3 + 11.8133 i) & 0 & 0 & 0 \\ 0 & (-0.3 - 11.8133 i) & 0 & 0 \\ 0 & 0 & (-0.5 + 14.4950 i) & 0 \\ 0 & 0 & 0 & (-0.5 - 14.950 i) \end{bmatrix}$$

### 5.1.3.2 Method II: Design of the entire $dA$ for initially damped or undamped systems.

Recall that, in general,  $U_u = U_l \Lambda$ , so taking variations,

$$U_u + dU_u = (U_l + dU_l) (\Lambda + d\Lambda) \quad (5.42)$$

$$dU_u = U_l d\Lambda + dU_l \Lambda + dU_l d\Lambda \quad (5.43)$$

The Eq. (5.43) gives a general relationship for the change in the upper right eigenvectors and shows that even if the mode shapes do not change and  $dU_l = 0$ ,  $dU_u = U_l d\Lambda \neq 0$  if the eigenvalues change. So, even if the mode shapes do not change, the eigenvectors in state space will change if the eigenvalues change, because the upper  $n \times 2n$  portion of the  $U$  matrix changes. Further, under the usual normalization, the fact that the lower right vectors do not change may go unrecognized unless a special normalization procedure is used. In this section, the right eigenvectors are normalized using the  $n \times n$  mass matrix  $M$  by, for the  $r$ th vector,

$$\begin{matrix} 1 \times n & n \times n & n \times 1 & 1 \times 1 \\ u_{rl}^T & M & u_{rl} & = I = 1 \end{matrix} \quad (5.44)$$

Then  $U_u$  is found from 
$$U_u = U_l \Lambda \quad (5.45)$$

and  $V$  from 
$$V^T = U^{-1} \quad (5.46)$$

While the eigenvector matrices are square, and are assumed to be invertible because the vectors are independent, their upper and lower portions are rectangular, of size  $n \times 2n$ , and are not invertible.

If the mode shapes do not change, then the following process may be used, which does not appear in the literature. Let  $A_G = A + dA$  and  $\Lambda_G = \Lambda + d\Lambda$ . Then, if the lower right vectors do not change,

$$U_G = \begin{bmatrix} U_l [\Lambda + d\Lambda] \\ U_l \end{bmatrix} \quad \text{and} \quad V_G^T = U_G^{-1} \quad (5.47)$$

and the corresponding state matrix for the closed loop system is

$$U_G [\Lambda_G] V_G^T = A_G \quad (5.48)$$

where  $d\Lambda$  is the desired shift in the eigenvalues and  $dA$  represents the required change in  $A$ . Since only  $M^{-1}C_G$  and  $M^{-1}K_G$  are needed, it is more efficient to use

$$-M^{-1}C_G = U_{Gu} \Lambda_G V_{Gu}^T \quad (5.49a)$$

$$-M^{-1}K_G = U_{Gl} \Lambda_G V_{Gl}^T \quad (5.49b)$$

An important point is that the essential form of the  $A$  matrix is maintained, which requires that

$$I = U_{Gl} \Lambda_G V_{Gu}^T \quad (5.50a)$$

$$0 = U_{Gl} \Lambda_G V_{Gl}^T \quad (5.50b)$$

The equations (5.50) are easily proved by multiplying (2.41a) and (2.41b) by  $U_l$  and taking advantage of Eq. (2.47).

### Example 5.3 Design of damping and control matrices using Method II.

For this example, the mass matrix  $M$ ,  $C$ , and  $K$  matrices are

$$M = \begin{bmatrix} 1 & 0 \\ 0 & 2 \end{bmatrix} \quad C = \begin{bmatrix} 8 & -4 \\ -4 & 3 \end{bmatrix} \quad K = \begin{bmatrix} 300 & -100 \\ -100 & 400 \end{bmatrix}$$

The characteristic matrix  $A$ , the eigenvalues  $\Lambda$  and the right and left eigenvector matrices of  $A$  are

$$A = \begin{bmatrix} -8 & 4 & -300 & 100 \\ 2 & -1.5 & 50 & -150 \\ 1 & 0 & 0 & 0 \\ 0 & 1 & 0 & 0 \end{bmatrix} \quad \Lambda = \begin{bmatrix} (-0.2656 + 12.8083 i) & 0 & 0 & 0 \\ 0 & (-0.2656 - 12.8083 i) & 0 & 0 \\ 0 & 0 & (-4.4844 + 17.7483 i) & 0 \\ 0 & 0 & 0 & (-4.4844 - 17.7483 i) \end{bmatrix}$$

$$U = \begin{bmatrix} -0.5288 - 5.5239 i & -4.6636 + 16.0712 i \\ 0.3861 - 8.1868 i \text{ (conj)} & 0.4283 - 5.4188 i \text{ (conj)} \\ -0.4302 + 0.0502 i & 0.9136 + 0.0319 i \\ -0.6395 - 0.0169 i & -0.2927 + 0.0498 i \end{bmatrix}$$

The second and fourth columns of  $U$  are the complex conjugates of the first and third columns, respectively, and are denoted by the symbol "(conj)".

$$V = \begin{bmatrix} 0.0020+0.0168 i & 0.0010-0.0257 i \\ -0.0012+0.0501 i \text{ (conj)} & 0.0028+0.0165 i \text{ (conj)} \\ -0.1978+0.0557 i & 0.4535-0.1059 i \\ -0.6511-0.0212 i & -0.3042+0.1024 i \end{bmatrix}$$

The desired eigenvalue matrix is

$$\Lambda_G = \begin{bmatrix} (-3.0000 + 12.8083 i) & 0 & 0 & 0 \\ 0 & (-3.0000 - 12.8083 i) & 0 & 0 \\ 0 & 0 & (-5.5000+17.7483i) & 0 \\ 0 & 0 & 0 & (-5.5000-17.7483i) \end{bmatrix}$$

The corrected U matrix, used in the computation of  $A_G$  is

$$U_G = \begin{bmatrix} 0.6477-5.6612 i & -6.6398+6.4644 i \\ 2.1349-8.1406 i \text{ (conj)} & 1.6878-2.4945 i \text{ (conj)} \\ -0.4302+0.0502 i & 0.9136+ 0.0319 i \\ -0.6395- 0.0169 i & -0.2927+ 0.0498 i \end{bmatrix}$$

and

$$A_G = U_G \Lambda_G V_G^T = \begin{bmatrix} -10.63 & 2.15 & -313.60 & 97.05 \\ 1.05 & -6.37 & 47.60 & -205.25 \\ 1 & 0 & 0 & 0 \\ 0 & 1 & 0 & 0 \end{bmatrix}$$

The resulting matrices are

$$-M C_1 = C + d [ C + G ] = \begin{bmatrix} 10.63 & -2.15 \\ -2.10 & 12.74 \end{bmatrix}$$

$$-M K_1 = K + d [ K + H ] = \begin{bmatrix} 313.60 & -97.05 \\ -95.20 & 410.50 \end{bmatrix}$$

### 5.1.3.3 Method III: Design of damping and control matrices to achieve desired eigenvalues and eigenvectors.

The state space equations with *output feedback* are

$$I \dot{\underline{\eta}}(t) - A_o \underline{\eta}(t) = B u(t) \quad (5.51)$$

where  $B$ , of size  $2n \times p$ , is the control matrix and  $u(t)$  is the  $p \times 1$  vector of timewise control inputs. It is often economical to have the dimension of  $u(t)$  much less than  $2n$ , to minimize the number of controllers needed. The output  $w(t)$ , with  $D$  the  $p \times 2n$  output matrix, is

$$w(t) = D \underline{\eta}(t) \quad (5.52)$$

If  $u(t) = w(t)$ , Eq. (5.51) becomes

$$\mathbf{I} \dot{\underline{\eta}}(t) - \mathbf{A}_0 \underline{\eta}(t) = \mathbf{B} \mathbf{D} \underline{\eta}(t) \quad (5.53)$$

The Eqs. (5.53) and (2.28) have a similar appearance, but there may be more freedom in choosing the elements of the two matrices  $\mathbf{B}$  and  $\mathbf{D}$  than the single matrix  $\mathbf{R}$ .

Moore [4] is given credit for being the first to show that state feedback provides freedom to choose not only eigenvalues, but eigenvectors. He derived necessary and sufficient conditions for the existence of a  $\mathbf{D}$  which yields prescribed eigenvalues and eigenvectors for the *closed loop system* and presented a procedure for computation of  $\mathbf{D}$ . The theorem states that:

Let  $\{\lambda_i, i = 1 \dots 2n\}$  be a self-conjugate set of distinct complex numbers. There exists a real  $2n \times m$  matrix  $\mathbf{D}$  such that

$$[\mathbf{A}_0 + \mathbf{B} \mathbf{D}] \mathbf{v}_i = \lambda_i \mathbf{v}_i \quad i = 1, 2, \dots, 2n \quad (5.54)$$

if, and only if, for each  $i$ ,

- (i)  $\mathbf{v}_i$  are a linear independent set of vectors in the space of complex  $2n$ -vectors.
- (ii)  $\mathbf{v}_i = \bar{\mathbf{v}}_i$  when  $\lambda_i = \bar{\lambda}_i$ .
- (iii)  $\mathbf{v}_i \in \text{span } \mathbf{N}_{\lambda_i}$

If  $\mathbf{D}$  exists and  $\mathbf{B}$  is of rank  $p$ , then  $\mathbf{D}$  is unique. The  $\mathbf{N}_{\lambda_i}$  is identified from the definitions

$$\mathbf{S}_\lambda = [\lambda \mathbf{I} - \mathbf{A}_0, \mathbf{B}] \text{ and } \mathbf{T}_\lambda = \begin{bmatrix} \mathbf{N}_\lambda \\ \mathbf{M}_\lambda \end{bmatrix} \quad (5.55)$$

where the columns of  $\mathbf{T}_\lambda$ , partitioned to be compatible with  $\mathbf{S}_\lambda$  for the product  $\mathbf{S}_\lambda \mathbf{T}_\lambda$ , furnish a basis for the nullspace of  $\mathbf{S}_\lambda$ .

The work of Srinathkumar [8] is also relative, because it was shown in [8] that for controllable systems, a maximum of  $2n \times p$  eigenvector entries can be arbitrarily specified and that no more than  $p$  entries in any one eigenvector can be chosen arbitrarily.

In the present paper, we choose  $p = 2n$ , with full state feed-back, which means all the eigenvalues and eigenvectors may be specified, but care must be taken to choose independent eigenvectors and the relationship between the upper and lower portions of the eigenvectors must be kept in mind.

In general, the mode shapes and eigenvalues may be chosen, with the restrictions as outlined above. In full state feedback, all the entries in  $\mathbf{U}_l$  may be chosen and we restrict upper  $\mathbf{U}_u$  so that  $\mathbf{U}_u = \mathbf{U}_l \Lambda$ . The operation is represented by Eqs. (5.48)-(5.50).

#### Example 5.4 Design of damping and control matrices using Method III.

For this example, the mass matrix  $\mathbf{M}$ ,  $\mathbf{C}$ , and  $\mathbf{K}$  matrices are

$$\mathbf{M} = \begin{bmatrix} 1 & 0 \\ 0 & 2 \end{bmatrix} \quad \mathbf{C} = \begin{bmatrix} 5 & -4 \\ -4 & 3 \end{bmatrix} \quad \mathbf{K} = \begin{bmatrix} 400 & -200 \\ -100 & 700 \end{bmatrix}$$

The characteristic matrix  $A$ , the eigenvalues  $\Lambda$  and the right and left eigenvector matrices of  $A$  are

$$A = \begin{bmatrix} -5 & 4 & -400 & 200 \\ 2 & -1.5 & 50 & -350 \\ 1 & 0 & 0 & 0 \\ 0 & 1 & 0 & 0 \end{bmatrix} \quad \Lambda = \begin{bmatrix} (-1.4004+18.6658 i) & 0 & 0 & 0 \\ 0 & (-1.4004-18.6658 i) & 0 & 0 \\ 0 & 0 & (-2.5996+27.1165 i) & 0 \\ 0 & 0 & 0 & (-2.5996-27.1165 i) \end{bmatrix}$$

$$U = \begin{bmatrix} -0.419+17.523 i & -0.419-17.523 i & 5.798-10.077 i & 5.798+10.077 i \\ -1.937+ 4.851 i & -1.937- 4.851 i & -0.332+18.177 i & -0.332-18.177 i \\ 0.935- 0.048 i & 0.935 + 0.048 i & -0.389- 0.177 i & -0.389+ 0.177 i \\ 0.266+ 0.084 i & 0.266- 0.084 i & 0.665- 0.052 i & 0.665+ 0.052 i \end{bmatrix}$$

The goal is to design the mode shapes so the normalized modal amplitudes are

$$U_{Dl} = \begin{bmatrix} 0.8165 & 0.8165 & -0.5774 & -0.5774 \\ 0.4082 & 0.4082 & 0.5774 & 0.5774 \end{bmatrix}$$

in order to make the amplitudes in the ratio of 2/1 for the first two modes and -1/1 for the last two. The desired  $\Lambda+d\Lambda$  is

$$\Lambda+d\Lambda = \begin{bmatrix} (-6.0000+18.6658 i) & 0 & 0 & 0 \\ 0 & (-6.0000-18.6658 i) & 0 & 0 \\ 0 & 0 & (-8.0000+27.1165 i) & 0 \\ 0 & 0 & 0 & (-8.0000-27.1165 i) \end{bmatrix}$$

The complete, designed,  $U_D$  matrix is then

$$U_D = \begin{bmatrix} -4.899+15.241 i & -4.899-15.241 i & 4.619-15.656 i & 4.619+15.656 i \\ -2.450+ 7.621 i & -2.450- 7.620 i & -4.619+15.656 i & -4.619-15.656 i \\ 0.8165 & 0.8165 & -0.5774 & -0.5774 \\ 0.4082 & 0.4082 & 0.5774 & 0.5774 \end{bmatrix}$$

and

$$A_G = U_G \Lambda_G V_G^T = \begin{bmatrix} -13.33 & 2.67 & -522.71 & 276.60 \\ 1.33 & -14.67 & 138.30 & -661.01 \\ 1 & 0 & 0 & 0 \\ 0 & 1 & 0 & 0 \end{bmatrix}$$

The resulting matrices are

$$-M C_l = C + d | C + G | = \begin{bmatrix} 13.33 & -2.67 \\ -2.67 & 14.67 \end{bmatrix}$$

$$-M K_l = K + d | K + H | = \begin{bmatrix} 522.71 & 276.60 \\ -276.60 & 1322.02 \end{bmatrix}$$

### 5.1.4 Shifting poles using eigenvalue sensitivities, symmetric and unsymmetric control.

#### Example 5.5 Design of symmetrical control matrix using sensitivities.

Suppose we start with an undamped system and then add a symmetrical C+G matrix.

$$A_o = \begin{bmatrix} 0 & 0 & -5 & 4 \\ 0 & 0 & 2 & -2 \\ 1 & 0 & 0 & 0 \\ 0 & 1 & 0 & 0 \end{bmatrix}$$

The eigenvalues are  $\lambda_{01}, \bar{\lambda}_{01} = \pm 0.5463i$  and  $\lambda_{02}, \bar{\lambda}_{02} = \pm 2.5887i$

The eigenvectors are

$$U_o = \begin{bmatrix} 0.2816i & -0.2816i & -2.2183i & 2.2183i \\ 0.3310i & -0.3310i & 0.9436i & -0.9436i \\ 0.5155 & 0.5155 & -0.8569 & -0.8569 \\ 0.6059 & 0.6059 & 0.3645 & 0.3645 \end{bmatrix}$$

The sensitivities  $S_{01}$  and  $S_{03}$  are given. Note that  $S_{02} = \bar{S}_{01}$  and  $S_{04} = \bar{S}_{03}$

$$S_{01} = \begin{bmatrix} 0.1329 & 0.1562 & -0.2432i & -0.2859i \\ 0.3123 & 0.3671 & 0.5718i & -0.6720i \\ 0.0726i & 0.0853i & 0.1329 & 0.1562 \\ 0.1706i & 0.2006i & 0.3123 & 0.3671 \end{bmatrix}$$

$$S_{03} = \begin{bmatrix} 0.3671 & -0.1562 & -0.1418i & 0.0603i \\ -0.3123 & 0.1329 & 0.1207i & -0.0513i \\ 0.9504i & -0.4043i & 0.3671 & -0.1562 \\ -0.8086i & 0.3440i & -0.3123 & 0.1329 \end{bmatrix}$$

Now, the eigenvalues desired are

$$\lambda_{01}, \bar{\lambda}_{01} = -0.0820 \pm 0.5399i \text{ and } \lambda_{02}, \bar{\lambda}_{02} = -0.1680 \pm 2.5842i$$

The changes in eigenvalues are

$$\Delta\lambda_{01}, \Delta\bar{\lambda}_{01} = -0.0820 \mp 0.0064i \text{ and } \Delta\lambda_{02}, \Delta\bar{\lambda}_{02} = -0.1680 \mp 0.0045i$$

The complex conjugates provide no additional information with regard to choice of changes in the plant matrices. So there are four knowns, the real and imaginary parts of the changes in two eigenvalues. The question is, which four matrix elements in the plant matrices should be chosen. We choose C(1,1), C(2,2), K(1,1) and K(2,2). The equations are

$$\begin{aligned} \Delta\lambda_{01} &= S_{01}(1,1) \Delta A(1,1) + S_{01}(2,2) \Delta A(2,2) + S_{01}(1,3) \Delta A(1,3) + S_{01}(2,4) \Delta A(2,4) \\ \Delta\lambda_{03} &= S_{03}(1,1) \Delta A(1,1) + S_{03}(2,2) \Delta A(2,2) + S_{03}(1,3) \Delta A(1,3) + S_{03}(2,4) \Delta A(2,4) \end{aligned}$$

$$\begin{Bmatrix} \Delta\lambda_{01} \\ \Delta\lambda_{02} \\ \Delta\lambda_{03} \\ \Delta\lambda_{04} \end{Bmatrix} = \begin{bmatrix} 0.1329 & 0.3671 & -0.2432 i & -0.6720 i \\ 0.1329 & 0.3671 & 0.2432 i & 0.6720 i \\ 0.3671 & 0.1329 & -0.1418 i & -0.0513 i \\ 0.3671 & 0.1329 & 0.1418 i & 0.0513 i \end{bmatrix} \begin{Bmatrix} \Delta A(1,1) \\ \Delta A(2,2) \\ \Delta A(1,3) \\ \Delta A(2,4) \end{Bmatrix}$$

$$\begin{Bmatrix} \Delta A(1,1) \\ \Delta A(2,2) \\ \Delta A(1,3) \\ \Delta A(2,4) \end{Bmatrix} = \begin{Bmatrix} -0.4336 \\ -0.0664 \\ 0.0326 \\ -0.0023 \end{Bmatrix}$$

The resulting A matrix is

$$A_1 = \begin{bmatrix} -0.4336 & 0 & -4.9674 & 4 \\ 0 & -0.0664 & 2 & -2.0023 \\ 1 & 0 & 0 & 0 \\ 0 & 1 & 0 & 0 \end{bmatrix}$$

$$\lambda_{01}, \bar{\lambda}_{01} = -0.0827 \pm 0.5346i \text{ and } \lambda_{02}, \bar{\lambda}_{02} = -0.1673 \pm 2.5734i$$

The eigenvectors are

$$U_1 = \begin{bmatrix} -0.0367+0.2786i & 0.2317-2.2014i \\ -0.0527+0.3227i \text{ (conj)} & 0.0418+0.9502i \text{ (conj)} \\ 0.5193-0.0117i & -0.8577-0.0343i \\ 0.6044+0.0050i & 0.3666-0.0401i \end{bmatrix}$$

The sensitivities  $S_{11}$  and  $S_{13}$  are given. Note that  $S_{12} = \bar{S}_{11}$  and  $S_{14} = \bar{S}_{13}$

$$S_{11} = \begin{bmatrix} 0.1363+0.0148i & 0.1579+0.0221i & -0.0114-0.2531i & -0.0042-0.2948i \\ 0.3159+0.0443i & 0.3658+0.0628i & -0.0084-0.5896i & 0.0114-0.6861i \\ 0.0399+0.0780i & 0.0436+0.0922i & 0.1313-0.0949i & 0.1561-0.1057i \\ -0.0288+0.1682i & -0.0395+0.1946i & 0.3153+0.0051i & 0.3666+0.0173i \end{bmatrix}$$

$$S_{13} = \begin{bmatrix} 0.3637+0.0531i & -0.1579+0.0006i & 0.0114-0.1421i & 0.0042+0.0611i \\ -0.3159+0.0012i & 0.1342-0.0206i & 0.0084+0.1222i & -0.0114-0.0514i \\ -0.0399+0.9502i & -0.0436-0.4063i & 0.3687-0.0085i & -0.1561+0.0271i \\ 0.0288-0.8131i & 0.0395+0.3473i & -0.3153+0.0093i & 0.1334-0.0240i \end{bmatrix}$$

**Example 5.6 Design of an unsymmetrical control matrix using sensitivities.**

Given the Example 5.1 above, suppose it is desired to increase the damping in eigenvalues 1 and 2 and decrease it in eigenvalues 3 and 4, so  $\Delta\lambda_1 = -0.1$  and  $\Delta\lambda_3 = 0.1$ . The starting matrix  $A_G$  is that of Example 5.1 and the sensitivities used in the first trial are those of the undamped system. The only element to be changed in  $A$  is  $A_{12}$ . From the sensitivity matrix  $S_1$  in Example 5.1, the corresponding sensitivity is 0.1768. To find  $\Delta A_{12}$ , use  $(0.1768)\Delta A_{12} = -0.1$ . The result is  $\Delta A_{12} = -0.5656$ . Make this change in the matrix  $A$  and call the resulting matrix  $A_1$ .

$$A_1 = \begin{bmatrix} -0.6586 & -0.4242 & -150 & 25 \\ 0.1414 & -0.9414 & 25 & -200 \\ 1 & 0 & 0 & 0 \\ 0 & 1 & 0 & 0 \end{bmatrix}$$

The resulting eigenvalues are

$$\lambda_1, \bar{\lambda}_1 = -0.3998 \pm i 11.8070 \quad \lambda_2, \bar{\lambda}_2 = -0.4002 \pm i 14.5022$$

which have real parts very close to those desired. If an iteration process is used, the next step would be to update the sensitivities. The new  $S_{11}$  matrix is

$$S_{11} = \begin{bmatrix} 0.4253 + i 0.0262 & 0.1755 + i 0.0177 & 0.0010 - i 0.0361 & 0.0010 - i 0.0149 \\ 0.1787 - i 0.0293 & 0.0744 - i 0.0092 & -0.0030 - i 0.0150 & -0.0010 - i 0.0063 \\ -0.2241 + i 5.0330 & -0.1741 + i 2.0779 & 0.4264 + i 0.0045 & 0.1763 + i 0.0088 \\ 0.6236 + i 2.1048 & 0.2238 + i 0.8806 & 0.1763 - i 0.0588 & 0.0739 - i 0.0215 \end{bmatrix}$$

which shows that the sensitivities are now complex numbers, so a corresponding change in the imaginary part should be demanded. The damping is not proportional and a change in mode shape is expected. The new right eigenvectors are:

$$U_1 = \begin{bmatrix} -0.2171 + i 7.7170 & -0.2171 - i 7.7170 & -0.8304 - i 3.9956 & -0.8304 + i 3.9956 \\ -0.2147 + i 3.12881 & -0.2147 - i 3.1881 & -0.6548 + i 9.4990 & -0.6548 - i 9.4990 \\ 0.6535 - i 0.0037 & 0.6535 + i 0.0037 & -0.2737 + i 0.0648 & -0.2737 - i 0.0648 \\ 0.2703 + i 0.0090 & 0.2703 - i 0.0090 & 0.6557 + i 0.0271 & 0.6557 - i 0.0271 \end{bmatrix}$$

and 
$$dU = U_1^{-1} \cdot U_G = \begin{bmatrix} -0.0212 - i 0.0004 & -0.9567 - i 0.0733 \\ -0.1335 - i 0.0086 & \text{(conj)} & -0.3282 + i 0.0296 & \text{(conj)} \\ 0.0002 - i 0.0037 & & -0.0031 + i 0.0648 & \\ -0.0003 + i 0.0090 & & 0.0025 + i 0.0271 & \end{bmatrix}$$

**Example 5.7 Same problem as Example 5.6, but using a variation of Method I.**

For this example, which is the same problem as done in Example 5.6, the idea of Method I is used, but the eigenvectors used are  $U_G$  and  $V_G$  of the damped system of Example 5.1. The desired eigenvalues are those given in  $\Lambda_G$ , namely

$$\Lambda_G = \begin{bmatrix} -0.4 + i 11.8133 & 0 & 0 & 0 \\ 0 & -0.4 - i 11.8133 & 0 & 0 \\ 0 & 0 & -0.4 + i 14.4950 & 0 \\ 0 & 0 & 0 & -0.4 - i 14.4950 \end{bmatrix}$$

$$AG_1 = U_G * \Lambda_G * V_G^T = \begin{bmatrix} -0.7293 & 0.0707 & -150.00 & 25.00 \\ 0.0707 & -0.8707 & 25.00 & -200.00 \\ 1.0000 & 0.0000 & -0.0707 & -0.0707 \\ 0.0001 & 1.0000 & -0.0707 & 0.0707 \end{bmatrix}$$

The  $2 \times 2$  matrix in the lower right corner of  $AG_1$  is non-zero and not equal to the  $2 \times 2$  matrix in the upper left corner. Thus, in the spirit of Method I, we add it to the upper left corner and zero the lower right corner, producing the modified characteristic matrix.

$$\text{Modified } AG_1 = \begin{bmatrix} -0.8000 & 0.0000 & -150.00 & 25.00 \\ 0.0000 & -0.8000 & 25.00 & -200.00 \\ 1.0000 & 0.0000 & 0.0000 & 0.0000 \\ 0.0000 & 1.0000 & 0.0000 & 0.0000 \end{bmatrix}$$

**5.1.5 Nonsymmetric control matrices, forced vibration problem.**

To do a forced vibration problem with symmetric, or unsymmetric, control matrices  $G$  and  $H$ , the closed-loop matrix equations are

$$\begin{bmatrix} M & 0 \\ 0 & -K \end{bmatrix} \begin{Bmatrix} \ddot{z}(t) \\ \dot{z}(t) \end{Bmatrix} + \begin{bmatrix} [C+G] & [K+H] \\ K & 0 \end{bmatrix} \begin{Bmatrix} \dot{z}(t) \\ z(t) \end{Bmatrix} = \begin{Bmatrix} f(t) \\ 0 \end{Bmatrix}. \quad (5.56)$$

The shorthand form of Eq. (5.56) is

$$M^* \dot{\eta} + K^* \eta = F(t) \quad (5.57)$$

or 
$$\dot{\eta} - A \eta = [M^*]^{-1} F(t) \quad (5.58)$$

where  $A$  is the characteristic matrix for the closed-loop system and  $U$ ,  $V$ , and  $\Lambda$  are,

respectively, the right eigenvector, left eigenvector and eigenvalue matrices of the closed-loop system.

The equations are decoupled by substituting

$$\underline{\eta}(t) = \mathbf{U} \mathbf{q}(t) \quad (5.59)$$

into Eq. (5.58) and pre-multiplying by  $\mathbf{V}^T$ .

$$\dot{\underline{\mathbf{q}}}(t) + \Lambda \underline{\mathbf{q}}(t) = \mathbf{V}^T [\mathbf{M}^*]^{-1} \mathbf{F}(t) \quad (5.60)$$

## 5.2 Optimum damping and control by way of performance index and the Riccati equation.

### 5.2.1 Performance index and optimal control

An often-used form of a quadratic performance index for a controllable system is

$$J = \frac{1}{2} \int_0^{t_f} [z^T(t) Q(t) z(t) + z(t) R(t) z(t)] dt \quad (5.61)$$

where  $Q$  is real, symmetric and positive semidefinite while  $R$  is real, symmetric and positive definite. Finding the optimal solution involves solving the nonlinear Riccati equation, but which can be transformed to a linear form. The behavior is a function of time, but at  $t=t_f$  the Riccati matrix approaches a steady-state value. An numerical example of an optimal timewise solution is presented on page 199 in reference [M4].

### 5.2.2 The Riccati equation and modal control.

If the system is undamped and the control is such that the  $r$ th modal equation is independent of the other modal equations, the performance index may be written for each mode and the total performance index is obtained by summing the modal performance indices. For the  $r$ th mode, the performance index is given by

$$J_r = \int_0^{\infty} [u_r^T(t) Q_r u_r(t) + u_r^T(t) R_r u_r(t)] dt \quad (5.62)$$

and the total performance index  $J$  is the sum of the modal performance indices.

$$J = \sum_{r=1}^n J_r \quad (5.63)$$

The  $Q_r$  can be chosen so the first term in Eq. (1) is the sum of the modal kinetic and potential energies of the plant. Again, the state space differential equations are

$$M^* \dot{\underline{\eta}} + K^* \underline{\eta} = F(t) = G^* \dot{\underline{\eta}} + H^* \underline{\eta} \quad (5.64)$$

Assume the eigenvalues  $\Lambda$  and the right and left eigenvectors  $U$  and  $V$  for the  $M^{-1} K$  matrix are available. Hence we substitute (5.65) and pre-multiply (5.64) by  $M^{*-1}$

$$\underline{\eta}(t) = U q(t) \quad (5.65)$$

with the result

$$U q(t) + M^{*-1} K^* U q(t) = M^{*-1} F(t) \quad (5.66)$$

To decouple the equations, pre-multiply by  $V^T$  and take advantage of the usual orthogonality relationships.

$$\dot{q}(t) - \Lambda q(t) = V^T M^{*-1} F(t) = V^T M^{*-1} G U \dot{q} + V^T M^{*-1} H U q \quad (5.67)$$

$$\dot{q}(t) - \Lambda q(t) = Q(t) = V^T M^{*-1} F(t) = [g] \dot{q}(t) + [h] q(t) \quad (5.68)$$

In general, the  $[g]$  and  $[h]$  matrices will not be diagonal. If they are diagonal, the modal control is natural. The real and imaginary parts of the modal control force  $Q(t)$  are designated  $X(t)$  and  $Y(t)$ , written as

$$Q(t) = X(t) + i Y(t) = V^T M^{*-1} F(t) = [g] \dot{q}(t) + [h] q(t) \quad (5.69)$$

To return to the system coordinates, substitute from (5.65) for  $q(t)$

$$V^T M^{*-1} F(t) = [g] U^{-1} \dot{\eta} + [h] U^{-1} \eta \quad (5.70)$$

which gives 
$$F(t) = M^* V^{-T} [ [g] U^{-1} \dot{\eta} + [h] U^{-1} \eta ] \quad (5.71)$$

or alternatively 
$$F(t) = M^* V^{-T} [ X(t) + i Y(t) ] \quad (5.72)$$

The Example 5.8 is done next, to show how the optimum timewise modal control forces and associated closed loop poles, found from a solution of the Riccati equation are converted to control forces in the system coordinate system. In Example 5.9, the results are checked by the natural modal control approach, given the desired closed loop eigenvalues. In example 5.10, the same results are gotten by using Method II.

### Example 5.8 Conversion of modal control forces to system control forces.

The purpose of this example is to show how the optimum solution obtained from the Riccati equation for a specific problem by Meirovitch [M4] related to the present discussion. The plant matrices are

$$M = \begin{bmatrix} 1 & 0 \\ 0 & 2 \end{bmatrix} \text{ and } K = \begin{bmatrix} 5 & -4 \\ -4 & 4 \end{bmatrix}$$

and the eigenvalues are  $\lambda_1, \lambda_2 = \pm i 0.5463$  and  $\lambda_3, \lambda_4 = \pm i 2.5887$ . In [M4] special coordinates are introduced so that all the matrices will contain real numbers, rather than imaginary numbers. The  $Q$  and  $R$  matrices used in the special form of the performance index are taken as the unit matrix. The real part of the control forces  $X(t) = 0$  and the imaginary part is of the form

$$Y(t) = \begin{bmatrix} a_{11} & a_{12} & 0 & 0 \\ 0 & 0 & a_{34} & a_{44} \end{bmatrix} \begin{Bmatrix} \xi_1(t) \\ \eta_1(t) \\ \xi_2(t) \\ \eta_2(t) \end{Bmatrix}$$

Having the control forces, the closed loop eigenvalues can be determined. An alternate approach to that used in [M4] is to convert the timewise control forces in modal coordinates to system

coordinates. Then the **G** and **H** control matrices can be identified directly. The  $\xi_r(t)$  and  $\eta_r(t)$  are related to  $q(t)$  by

$$q_r(t) = \xi_r(t) + i \eta_r(t) \text{ and } \bar{q}_r = \xi_r(t) - i \eta_r(t)$$

To convert back to complex system coordinates, the complex conjugates come into play. The conversions are written in matrix form, like

$$\begin{Bmatrix} q_r \\ \bar{q}_r \end{Bmatrix} = \begin{bmatrix} 1 & i \\ 1 & -i \end{bmatrix} \begin{Bmatrix} \xi_r \\ \eta_r \end{Bmatrix} \text{ with the inverse } \begin{Bmatrix} \xi_r \\ \eta_r \end{Bmatrix} = \begin{bmatrix} 0.5 & 0.5 \\ -0.5i & -0.5i \end{bmatrix} \begin{Bmatrix} q_r \\ \bar{q}_r \end{Bmatrix}$$

The control forces in system coordinates are

$$Q(t) = \begin{bmatrix} -0.4404 & 0.0990 & -1.3705 & 0.0738 \\ 0.0991 & -0.7323 & 0.0738 & -2.6304 \end{bmatrix} \begin{Bmatrix} \dot{z}_1(t) \\ \dot{z}_2(t) \\ z_1(t) \\ z_2(t) \end{Bmatrix}$$

and the **G** and **H** control matrices are identified as

$$G = \begin{bmatrix} 0.4404 & -0.0990 \\ -0.0991 & 0.7323 \end{bmatrix} \text{ and } H = \begin{bmatrix} 1.3705 & -0.0738 \\ -0.0738 & 2.6304 \end{bmatrix}$$

From this, the new **A** matrix is formed and the closed loop eigenvalues calculated.

The closed loop eigenvalues are

$$\lambda_1, \lambda_2 = -0.6419 \pm i 0.4588 \text{ and } \lambda_3, \lambda_4 = -0.7009 \pm i 2.5870$$

so

$$\omega_1 = 0.5463 \text{ and } \omega_2 = 2.5887$$

The changes in the eigenvalues are

$$d\lambda_1 = -0.6419 - i 0.0875 \text{ and } d\lambda_2 = -0.6419 + i 0.0875$$

$$d\lambda_3 = -0.7009 - i 0.0017 \text{ and } d\lambda_4 = -0.7009 + i 0.0017$$

**Example 5.9 Same problem as 5.8, but using pole shifting by natural control method.**

The goal of this example is to determine the required control matrices using the method of natural modal control with  $n \times n$  matrices, rather than in state space. The form of the polynomial in  $\lambda$  is

$$\lambda_r^2 + g_r \lambda_r + (h_r + \omega_r^2) = 0$$

and the given roots are

$$\lambda_r, \bar{\lambda}_r = \alpha_r \pm i \beta_r$$

or

$$\lambda_r, \bar{\lambda}_r = -\frac{g_r}{2} \pm i \left[ (h_r + \omega_r^2) - \left(\frac{g_r}{2}\right)^2 \right]^{0.5}$$

so

$$g_r = -2 \alpha_r$$

and

$$h_r = \beta_r^2 - \omega_r^2 + \left(\frac{g_r}{2}\right)^2$$

The individual eigenvectors will be designated as  $\phi_r$  and the  $n \times n$  eigenvector matrix as  $\Phi$ .

$$\Phi = \begin{bmatrix} 0.5155 & 0.8569 \\ 0.6059 & -0.3645 \end{bmatrix}$$

The required diagonal modal control matrices are

$$g = \begin{bmatrix} 1.2838 & 0 \\ 0 & 1.4018 \end{bmatrix}$$

and

$$h = \begin{bmatrix} 0.3241 & 0 \\ 0 & 0.4825 \end{bmatrix}$$

The corresponding control matrices in the original coordinates are

$$\mathbf{H} = \begin{bmatrix} 1.3704 & -0.0737 \\ -0.0737 & 2.6304 \end{bmatrix} \text{ and } \mathbf{G} = \begin{bmatrix} 0.4404 & -0.0990 \\ -0.0990 & 0.7324 \end{bmatrix}$$

so the  $\mathbf{K}+\mathbf{H}$  matrix is

$$\mathbf{K}+\mathbf{H} = \begin{bmatrix} 5.4404 & -4.0990 \\ -2.0495 & 2.3662 \end{bmatrix}$$

**Example 5.10 Same as 5.8, but using Method II.**

Suppose we start with an undamped system and then add a symmetrical C+G matrix.

$$A_0 = \begin{bmatrix} 0 & 0 & -5 & 4 \\ 0 & 0 & 2 & -2 \\ 1 & 0 & 0 & 0 \\ 0 & 1 & 0 & 0 \end{bmatrix}$$

The eigenvalues are  $\lambda_{01}, \bar{\lambda}_{01} = \pm 0.5463i$  and  $\lambda_{02}, \bar{\lambda}_{02} = \pm 2.5887i$

The eigenvectors are

$$U = \begin{bmatrix} 0.2816i & -0.2816i & -2.2183i & 2.2183i \\ 0.3310i & -0.3310i & 0.9436i & -0.9436i \\ 0.5155 & 0.5155 & -0.8569 & -0.8569 \\ 0.6059 & 0.6059 & 0.3645 & 0.3645 \end{bmatrix}$$

The desired change in  $\Lambda$  is

$$d\Lambda = \begin{bmatrix} -0.6419 - 0.0875i & 0 & 0 & 0 \\ 0 & -0.6419 + 0.0875i & 0 & 0 \\ 0 & 0 & -0.7009 - i0.0017 & 0 \\ 0 & 0 & 0 & -0.7009 + i0.0017 \end{bmatrix}$$

$$U_G = \begin{bmatrix} U_1 & [\Lambda + d\Lambda] \\ & U_1 \end{bmatrix}$$

$$U_G = \begin{bmatrix} -0.3309 + 0.2365i & -0.6006 + 2.2168i \\ -0.3889 + 0.2780i \text{ (conj.)} & 0.2555 - 0.09430i \text{ (conj.)} \\ 0.5155 & -0.8569 \\ 0.6059 & 0.3645 \end{bmatrix}$$

$$V_G = \begin{bmatrix} -0.5618i & -0.1656i \\ -1.3207i & 0.1409i \text{ (conj.)} \\ 0.2577 - 0.3606i & 0.4284 - 0.1161i \\ 0.6059 - 0.8477i & -0.3645 + 0.0988i \end{bmatrix}$$

$$A_G = U_G | \Lambda + d\Lambda | V_G^T$$

$$A_G = \begin{bmatrix} -1.3704 & 0.0737 & -5.4404 & 4.0989 \\ 0.0369 & -1.3152 & 2.0495 & -2.3662 \\ 1 & 0 & 0 & 0 \\ 0 & 1 & 0 & 0 \end{bmatrix}$$

### 5.3 Summary and conclusions.

The present study has covered a range of problems related to the efficient representation and design of damping and control forces for discrete systems. Some conclusions are given at appropriate locations in the preceding portions of the report. A summary is given here in the form of suggestions for further study, as follows:

1. Some forms of passive and active damping are achieved by devices representable by viscous forces. However, viscoelastic damping is widely used and more work is needed to develop more efficient analytical and computational techniques. The mini-oscillator approach is readily adapted to present modal analysis methods and computer programs, but a considerable increase in size of matrices is required. The fractional calculus approach may be more efficient, but is not as easy to use. Complex numbers are readily handled in present computer programs and the use of a complex Young's modulus is efficient in some instances, especially if the modulus is fairly constant over the frequency range involved.
2. Eigenvalue and eigenvector sensitivities may be used for constrained optimization problems. Their use to achieve certain eigenvalues through design of dissipative damping and control matrices has been demonstrated in the present study. They can also be used to design eigenvectors, but eigenvectors tend to change rapidly with changes in parameters and more study is needed in this area.
3. Direct design of damping and control matrices through eigenvector as well as eigenvalue assignment is very promising, as indicated by the methods and examples outlined in Chapter 5. The literature on the inverse eigenstructure problem is relative and is increasing rapidly. Eigenvector sensitivities can be useful in choosing the eigenvector matrices and is an area worth further development.
4. Practical realization of the system and control matrices, while not a major topic of the present report, has been mentioned in some of the papers published by the writer and in many other papers. Maintaining data bases of properties of viscoelastic materials in forms that are readily useful in computer programs for structural analysis is an ongoing task. Graphical representation is helpful, but a listing of the parameters involved in curve-fitting, as described in Chapter 3, would be directly useful to the analyst.

## REFERENCES

- A1. Andry, A. N., Jr., E. Y. Shapiro and J. C. Chung, "Eigenstructure Assignment for Linear Systems," *IEEE Transactions on Aerospace and Electronic Systems*, AES-19, no. 5, pp. 713-729, 1983.
- B1. Bagley, D. L. and Torvik, P. J., "Fractional Calculus-A Different Approach to the Analysis of Viscoelastically Damped Structures," *AIAA Jnl.*, v. 21, n. 5, pp. 741-748, 1983.
- C1. Carabetta, Christopher J., "Damping Analysis of Axial Elements Treated with Constrained, Sectional, Viscoelastic Layers," Senior Honors Thesis, The Pennsylvania State University, May, 1991
- C2. Caughey, T. K. and O'Kelly, M.M.J., "Classical Normal Modes of Damped Linear Dynamic Systems," *J. of Appl. Mech.*, ASME, Vol. 32, pp. 583-588, 1965.
- C3. Christensen, R. M., *Theory of Viscoelasticity: An Introduction*, 2nd Edition, Academic Press, New York, 1982.
- F1. von Flotow, A. H. and D.W. Vos, "The Need for Passive Damping in Feedback Controlled Flexible Structures," *Proceedings of Damping '91*, (Flight Dynamics Laboratory of the Air Force Wright Aeronautical Laboratories 1991) pp. GBB-1 to GBB-12.
- G1. Gilheany, J. J., "Optimal Selection of Dampers for Freely Vibrating Multidegree of Freedom Systems," In *Proceedings of Damping '89* (Flight Dynamics Laboratory of the Air Force Wright Aeronautical Laboratories 1989) pp. FCC-1 to FCC-18.
- I1. Inman, D. J. and A. N. Andry, Jr., "A Procedure for Designing Overdamped Lumped Parameter Systems," *Shock and Vibration Bulletin*, 54(5), 49-53 (1980).
- I2. Inman, D. J. and Andreyi, A. N. Jr., "Some Results on the Nature of Eigenvalues of Discrete Damped Linear Systems," *Jnl. of Applied Mechanics*, ASME, 47, no.4, pp. 927-930, 1980.
- I3. Inman, D., *Vibration Control, Measurement and Stability*, Prentice-Hall, Englewood Cliffs, NJ, 1989.
- J1. Juang, J., Lim, K. B., and Junkins, John L., 1989, "Robust Eigensystem Assignment for Flexible Structures," *AIAA Journal of Guidance, Control and Dynamics*, Vol. 12, No. 3, pp. 381-387.
- L1. Liang, Z., Tong, M., and Lee, G. C., "A Strong Criterion for Testing Proportionally Damped Systems," *Proceedings of Damping '91*, San Diego, Wright-Patterson Air Force Base WL-TR-91-3078, paper ECD, August 1991.
- M1. McLoughlin, F. A., *Integrated Structural Damping and Control System Design for High-Order Flexible Systems*. Ph.D. Dissertation (Stanford University, 1991)
- M2. McTavish, D. J. and Hughes, P. C., "Finite Element Modeling of Linear Viscoelastic Structures," in Rogers, L. and Simonis, J. C., Editors, *The Role of Damping in Vibration and Noise Control*, ASME DE-Vol. 4, Sept., 1987.
- M3. Meirovitch, L., *Introduction to Dynamics and Control*, John Wiley & Sons, New York, 1985.

- M4. Meirovitch, L., *Dynamics and Control of Structures*, Wiley, New York, 1990.
- M5. Meirovitch, L., *Computational Methods in Structural Dynamics*, Sijthoff & Nordhoff, Rockville, Maryland, 1980.
- M6. Moore, B. C., "On the Flexibility Offered by State Feedback in Multivariable Systems Beyond Closed Loop Eigenvalue Assignment," *IEEE Transactions on Automatic Control*, AC-21, pp. 689-692, 1976.
- N1. Nashif, A.D., et al, *Vibration Damping*, John Wiley & Sons, New York, 1985.
- N2. Nelson, R. B., "Simplified Calculation of Eigenvector Derivatives," *AIAA Jnl.*, v. 14, n.9, pp. 1201-1205, Sept. 1976.
- N3. Neubert, V. H., *Mechanical Impdance, Modelling/Analysis of Structures*, Jostens Printing Company, State College, PA, 1987.
- N4. Neubert, Vernon H., "Optimization of Energy Dissipation Rate in Structures," *Proceedings DAMPING 89*, Flight Dynamics Laboratory of the Air Force Wright Aeronautical Laboratories, 1989, pp. FCD-1 to FCD-24.
- N5. Neubert, Vernon H., "Optimization of Location and Amount of Viscous Damping to Minimize Random Vibrations," Oral presentation at Acoustical Society of America Semi-Annual Meeting, May 1990.
- N6. Neubert, Vernon H., "Optimization of Location and Amount of Viscous Damping to Minimize Random Vibrations," *JASA*, v. 93, n. 5, pp. 2707-2715, May 1993.
- N7. Neubert, Vernon H., "Fitting Curves to Data for Complex Moduli of Viscoelastic Materials, Technical Report, Applied Research Laboratory, The Pennsylvania State University, (In preparation from a completed internal memorandum.)
- N8. Neubert, Vernon H., "Optimum Design of Constrained Layer Viscoelastic Damping for Structures," Technical Report, Applied Research Laboratory, The Pennsylvania State University, (In preparation from a completed internal memorandum.)
- N9. Neubert, Vernon H., "Sensitivity of Modal Parameters to Nonsymmetrical, Dissipative Control Matrices," *Proceedings of the 63rd Shock and Vibration Symposium*, October, 1992, Las Cruces, New Mexico, v. 1, pp. 161-171.
- N10. Neubert, Vernon H., "Sensitivity of Eigenvalues to Nonsymmetrical, Dissipative Control Matrices," *Journal of Shock and Vibration*, v. 1, n. 2, Dec., 1993
- N11. Neubert, Vernon H., "Design of Control Matrices in the Presence of Viscous Damping," *Proceedings of the 64th Shock and Vibration Symposium*, Oct., 1993, Ft. Walton Beach, Fla., v. 1, pp. 515-524.
- N12. Neubert, Vernon H., "Design of Damping and Control Matrices by Modification of Eigenvalues and Eigenvectors," accepted for publication in *Journal of Shock and Vibration*, submitted Oct., 1993.
- P1. Porter, B. and R. Crossley, *Modal Control*, Barnes and Noble Books, New York, 1972.

- R1. Rogers, L. C., "Derivatives of Eigenvalues and Eigenvectors," *AIAA Journal*, **8**, 943-944, (1970).
- S1. Silverberg, L., "Uniform Damping Control of Spacecraft," *J. Guidance, Control, Dynamics*, **9**(2), 221-227 (1986).
- S2. Simoniam, S. S., "Synthesis of Discrete Passive Vibration Dampers," *Society of Automotive Engineers*, Paper 851935, Warrendale, PA. 1986.
- S3. Smith, David, "Optimization of Damping in a 3-Layered Beam Using the Finite Element Method," Senior Honors Thesis, The Pennsylvania State University, May, 1991.
- S4. Srinathkumar, S., "Eigenvalue/Eigenvector Assignment Using Output Feedback," *IEEE Transactions on Automatic Control*, **AC-23**, no1, pp. 79-81, 1978.
- S5. Starek, L., and Inman, D. J., 1991, "On Inverse Problems with Rigid Body Modes," *ASME Journal of Applied Mechanics*, Vol. 50, pp. 1101-1104.
- S6. Starek, L., Inman, D. J., and Kress, A., 1992, "A Symmetric Inverse Vibration Problem," *ASME Journal of Vibration and Acoustics*, Vol. 114, pp. 564-568.
- V1. Venkayya, V. B., and V. A. Tischler, "Frequency Control and Its Effect on the Dynamic Response of Flexible Structures," *AIAA Journal*, **23**(11), 1768-1774 (1985).
- W1. Wittrick, W. H. "Rates of Change of Eigenvalues, with Reference to Buckling and Vibration Problems," *Proceedings of the Royal Society*, **66**, 590-591 (Sept. 1962).